TU

Technische Universität Wien

DISSERTATION

New Chemical and Biological Insights into the Chemistry of Highly Reactive Oxygen Species

ausgeführt zum Zwecke der Erlangung des akademischen Grades eines
Doktors der Technischen Wissenschaften unter der Leitung von

a.o. Univ. Prof. Wolfgang Linert

am Institut für Angewandte Synthesechemie E163
eingereicht an der Technischen Universität Wien
Fakultät für Technische Chemie

von

Dipl. Ing. Wolfhardt Freinbichler
Matr. Nr. 9225752
Richtergasse 9-2-12
1070 Wien

Wien, im Oktober 2007

Thanks to …..

I want to thank my supervisor Prof. Dr. Wolfgang Linert for providing me with such an exciting and interesting topic, and for the academic freedom which I could enjoy during all my stay in his lab.

Further on I want to thank my second supervisor Prof. Laura Della Corte (University of Florence) for escorting me on my interesting journey into biology, for her enthusiastic engagement into our work and for her great hospitality.

Our working group in Vienna, above all Dr. Peter Weinberger, and the group in Florence, especially Dr. Maria − Alessandra Colivichi, I want to thank for a fantastic atmosphere, interesting discussions and for their great support.

Without the help of my family this work never would have been written, so I want to express here my thanks to their patience and for supporting me also during more difficult times.

Last but not least I want to thank the Fushikaden Dojo Vienna, above all Ing. Arnold Stiehl, for a good training, nights on end discussions about science, philosophy and reality and for giving me a bigger picture (Gairon) of this world. Same is to the Sommerland community, above all Mag. Tanja Kozak for passionate debates and fantastic gatherings, stimulating not only my scientific creativity.

Dedicated to the love of my life Barbara Janu

and our daughter Maya

Table of contents

Zusammenfassung

Der Schwerpunkt der vorliegenden Arbeit ist einerseits die Entwicklung einer neuen zuverlässigen Methode, um hoch reaktive Sauerstoffverbindungen direkt im Gehirn mittels Mikrodialysesonden messen zu können, und andererseits die chemisch-mechanistische Untersuchung der Fenton Reaktion unter physiologische Bedingungen, da diese höchstwahrscheinlich den Grund für die Bildung dieser Verbindungen im Gehirn darstellt. Des Weiteren werden die Entwicklung und *in vivo* Anwendung von zwei weiteren Methoden beschrieben, wobei eine zur Bestimmung von reaktivem Eisen (II) sowie freigesetztem Eisen (III) und die andere zur Messung von Wasserstoffperoxid herangezogen werden kann.

Hochreaktive Sauerstoffverbindungen (hROS), die im Allgemeinen entweder als Hydroxylradikale oder Eisen(IV) Verbindungen auftreten, wird eine entscheidende Rolle bei der Entstehung von neurodegenerativen Krankheiten und beim Alterungsprozess zugeschrieben. Aufgrund ihrer sehr hohen Reaktivität ist eine direkte Messung derzeit unmöglich, und es muss auf indirekte Methoden, die meist auf der Hydroxylierung von Aromtaten basieren, zurückgegriffen werden. Die am häufigsten benutzte Methode zu ihrer Messung greift auf die Hydroxylierung von Salicylsäure zurück. Da diese jedoch einerseits biologisch aktiv ist, und andererseits ihre, je nach chemischer Umgebung unterschiedlichen, Hydroxylierungsprodukte keine einwandfreie Quantifizierung erlauben, wurden immer wieder andere Substanzen als Alternative vorgeschlagen. In dieser Arbeit wurde die Hydroxylierung von Terephthalsäure (TA), deren Produkt die äußerst gut fluoreszierende 2-Hydroxy-Terephthalsäure (OH-TA) ist, sowohl nach chemischen als auch nach biologischen Kriterien untersucht. Es konnte festgestellt werden, dass TA weder die Neurotransmitter Glutamat, Aspartat, γ-Aminobuttersäure und Taurin im Striatum der Ratte beeinflusst, noch chemische Artefakte einer genauen Quantifizierung von hROS im Wege stehen. Die *in vivo* Stimulierung des Striatums mit drei unterschiedlichen Konzentrationen des Neurotoxins Kainsäure ergab eine Dosis abhängige Bildung von hROS, womit das Funktionieren der Methode bestätigt werden konnte. Auf der anderen Seite konnte gezeigt werden, dass neuroprotektive Substanzen die hROS Bildung unterdrückten. Von praktischem Vorteil ist weiters, dass OH-TA gemeinsam mit o-Phthaldialdehyd derivatisierten Aminosäuren

mittels HPLC gemessen werden kann, und so keine zusätzlichen Probemengen gebraucht werden.

Wird die hROS Bildung durch die Fenton Reaktion in einer der extrazellulären Flüssigkeit nachempfundenen Salzlösung beobachtet, so ist die Menge vom gebildeten OH-TA unabhängig von der TA Konzentration. Diese Beobachtung kann nicht mit der Bildung von freien Hydroxylradikalen in Übereinstimmung gebracht werden, sondern ausschließlich mit einem „krypto" Radikal oder einer Eisen(IV) Verbindung erklärt werden. Diese Annahme konnte mit Experimenten in Kaliumacetetat Puffer mit Hilfe eines durch kinetische Messungen unterstützen Reaktionsschemas bestätigt werden.

Um die Fenton Reaktion auch *in vivo* messen zu können war es notwendig mit kleinsten Probemengen eine Eisen -und Wasserstoffperoxidbestimmung durchführen zu können. Die bereits bekannte, aber für Mikrodialyseexperimente nicht brauchbare, photometrischen Eisenbestimmung mit Hilfe von Bathophenanthrolin wurde modifiziert, um Eisenmengen im nano-molaren Bereich unter Verwendung der nicht selektiven UV-Bande bei 385 nm mittels HPLC messen zu können. Zusätzlich wurde Wasserstoffperoxid mit Hilfe von TA und Fe(II)EDTA bestimmt. Es konnte gezeigt werden, dass die *in vivo* Stimulierung mit 6-Hydroxy-dopamin, das als einfaches Tiermodell für die Parkinson`sche Krankeit gilt, zu einer massiven Eisen- und Wasserstoffperoxidfreisetzung führt, wobei für die hROS Bildung ausschließlich die Menge an aktivem Eisen (II) entscheidend ist.

Abstract

The main emphasis of this work was to develop and test a new reliable method to detect *in vivo* highly reactive oxygen species (hROS) directly in the rat's striatum using microdialysis and to analyse a Fenton system in a chemical environment approximated to the extra cellular fluid utilising kinetic measurements. Beside that, two new methods to detect iron and H_2O_2 in the nano-molar range with sample volumes of few micro-litres via HPLC are introduced. Finally the results of *in vivo* experiments using a simple model of Parkinson's disease, combing all methods developed in this work are presented.

Sodium terephthalate was validated as a new robust and sensitive chemical trap for highly reactive oxygen species (hROS), lacking the drawbacks of the salicylic acid method. Reaction of the almost non-fluorescent terephthalate (TA^{2-}) with hydroxyl radicals or ferryl-oxo species resulted in the stoichiometric formation of the brilliant fluorophor 2-hydroxyterephthalate (OH-TA). Neither hydrogen peroxide nor superoxide reacts in this system. This procedure was validated for determining hROS formation during microdialysis under *in vivo* conditions, accompanied by chemical *in vitro* investigations. Derivatisation with *o*-phthalaldehyde, for amino acid detection, had no effect on OH-TA fluorescence, which could easily be resolved from the amino acid derivatives by HPLC, allowing determination in a single chromatogram, with a detection limit of 0.5 femtomol/μl of OH-TA in microdialysis samples. In microdialysis experiments the neurotoxin kainate was shown to evoke hROS formation in a dose-dependent manner. The presence of TA^{2-} in the perfusion fluid did not affect basal or evoked release of aspartate, glutamate, taurine and GABA. Assessment of cell death '*ex vivo*' showed TA^{2-} to be non-toxic at concentrations up to $1.0*10^{-3}$ mol/L .

The *in vitro* results based on kinetical measurements indicate a mechanism in the Fenton system (Fe^{2+} + H_2O_2) without the involvement of a free hydroxyl radicals, whereby TA^{2-} forms a primary complex with Fe^{2+} followed by an intramolecular hydroxylation accompanied by intramolecular electron transfer.

To measure all relevant compounds involved in the Fenton reaction also *in vivo*, two new methods, based on known procedures, to measure iron and H_2O_2 were developed. Iron was detected by HPLC using the non selective UV band at 285 nm of the Fe(II)-bathophenanthroline complex, whereas H_2O_2 was measured by utilising Fe(II)EDTA and TA. In the end of this work the *in vivo* results regarding hROS, active and released iron and H_2O_2 using the stimulation with 6-hydroxy-dopamine (6-OHDA) which can be considered a simple model of PD, are presented. It is shown that the massive formation of hROS after stimulation is mainly caused by active Fe(II) and not by total iron or H_2O_2.

Part I

1 Introduction

1.1 General

The main aim of this work was to investigate Fenton chemistry in a simple animal model of Parkinson's disease *in vivo* using 6-hydroxy dopamine (6-OHDA) stimulation. Based on the *in vitro* work done in our group in the past decades [1-12] it should be searched for evidence whether or not similar mechanisms could also play a role *in vivo*. Beside that, the nature of the oxidizing species in the Fenton reaction should be examined in a physiological relevant system. As there is no possibility to perform any *in vivo* experiments at the Vienna University of Technology, all animal experiments were performed at university of Florence (Italy) in the laboratories of Prof. Laura Della Corte.

To achieve this goal several theoretical and practical problems had to be resolved. Among others the probably most important task was to develop and test a reliable method to monitor Fenton activity *in vivo*, as it turned out that common used techniques had fundamental problems.

As many different experimental techniques and protocols were used in this work, only a general overview about the methods used will be presented in a closed part, whereas exact experimental conditions will be described together with the corresponding results. The general disposition of this work leads from a detailed introduction into the state of art and problem definition (Part I) over a general overview about the *in vitro* and *in vivo* methods used (Part II) to the development and testing of the terephthalate method (Part III) and finally to its practical application for monitoring Fenton activity *in vitro* and in vivo (Part IV and Part V).

1.2   Oxidative stress and Fenton chemistry

Oxidative stress is defined as an imbalance between the production of reactive oxygen species (ROS) and a biological system's ability to readily detoxify the reactive intermediates and/or easily repair the resulting damage. The term ROS covers several substances, ranging from the rather unreactive H_2O_2 through O_2^- and singlet O_2 to the highly reactive oxygen species (hROS), which may exist as free hydroxyl radicals (OH•), as bound ("crypto") radicals or as Fe(IV)-oxo species[13-15]. The occurrence of oxidative stress correlates with numerous pathologies including neurodegenerative diseases, ischemic or traumatic brain injuries, cancer, diabetes liver injury and AIDS [16-18] Moreover, the possibility that oxidative stress plays an important role in the ageing process is under discussion [19-21]. However, it has been difficult to distinguish whether oxidative stress causes the pathologies or is itself a consequence of them. The problematic nature of investigating this question may be illustrated by taking the example of ageing. There is no doubt that if an organism gets older its ability to repair DNA and protein damage decreases, whereas the concentration of ROS increases. This observation led to the formulation of the "radical theory of aging", which predicts that increasing the concentrations of antioxidants or blocking ROS generation should result in increased lifespan. Although there have been several reports, mostly with invertebrates, that an enhanced production of antioxidants by genetic manipulation significantly increases lifespan [22-24], the results of similar studies with mice have been largely disappointing, and did not show a significant correlation between an enhanced production of ROS and ageing [25-28]. Similarly, unclear results can also be found in research reports on the possible relation between oxidative stress and neurodegenerative diseases, such as Alzheimer's and Parkinson's diseases.

Although some ROS species are believed to have specific biological roles, many studies have been based on the extrapolation of superoxide or H_2O_2 data to hROS behaviour. This may have led to contradictory results.

As ROS, such as hydrogen peroxide and the superoxide anion, have low toxicity, and only a chemical or biological transformation e.g. a reaction with transition metal complexes may lead to the formation hROS [29], it might well be, that hROS formation does not go along with an increase of other ROS. One possible way of the transformation of ROS to hROS is the Fenton reaction (see equation 1a-1-c).

(1a) $Fe^{2+} + H_2O_2 \rightarrow Fe^{3+} + OH\bullet + OH^-$

(1b) $Fe^{2+} + H_2O_2 \rightarrow Fe^{3+}\text{-}OH\bullet + OH^-$

(1c) $Fe^{2+} + H_2O_2 \rightarrow FeO^{2+} + H_2O$
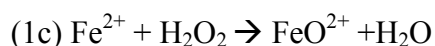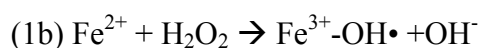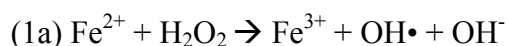
As already mentioned above, there has been an ongoing debate in the past decades, whether the product of the Fenton reaction or a Fenton like process is the free hydroxyl radical, a bound "crypto" radical or a Fe(IV)-oxo species. [13-15]. A broad line of evidence indicate that the nature of hROS produced via a Fenton system strongly depends on the chemical environment, like the pH, the ligand(s) of the Fe(II)complex or the presence or absence of O_2. [13,30-32]. The uncertainty of this matter is mainly based on the difficulties to distinguish between this species. Although in some cases it seems to be possible by using ESR-spectroscopy together with the spin trapping technique to distinguish between these species, even this technique does not provide a clear answer to this question for all cases. [14,30,33]]

As for free hydroxyl radicals as well as Fe(IV)-oxo species the redox potential is higher than 1.6 V [34], both species will comparably hydroxylate chemical compounds, thus leading to similar or identical results when indirect methods are used for hROS detection. However, when the potential of hROS to oxidise a chemical trap is defined as Fenton activity, it is evident that its dependency on chemical conditions like pH, ionic strength, etc. should differ from one hROS species to another

From a biological viewpoint, the two most important questions related to hROS are (1) to gain information about their direct damaging potential and (2) to examine their role as possible signalling substances under pathological and non pathological conditions. For (1) the question on the nature of the redox active species is irrelevant, and any hydroxylation reaction which can compete successfully with other biological substances for hROS should give, under the assumption of only one hydroxylation product, a reliable representation of the direct damaging potential.

For (2) the question on the redox active species becomes important, as a free hydroxyl radical solely reacts unspecific whereas a crypto radical and a ferryl species can react more specific due to their charge. As it seems very unlikely that a biological pathway,

e.g. for apoptosis can be triggered by a non specific chemical agent, the possibility for a signalling role of hROS stays and falls with the evidence that not only free hydroxyl radicals are present in a Fenton system under physiological like conditions.

However, this issue will be discussed in more detail in Part IV whereas for a better description of the problem definition the next chapter will focus on the state of the art of commonly used *in vivo* hROS detection methods, followed by a short statement on the detection of iron and H_2O_2 in microdialysis samples.

1.3   Methods for hROS detection

As hROS posses an extreme reactivity and a very short lifetime around 1 ns, there exist only one direct method of detecting hROS, namely electron spin resonance spectroscopy (ESR), including the spin trapping technique. However, its application to *in vivo* experiments, in particular in freely moving animals, is impracticable because of technical difficulties, which include high disturbing noise levels and low sensitivity [35]. All the common methods used for *in vivo* experiments are indirect and based on the hydroxylation of aromatic compounds. The necessity of such methods led to the development of several chemical traps to facilitate hROS detection and quantitation [36]. This account presents a brief overview of the most common and also some newer methods and their advantages and disadvantages.

1.3.1   Salicylate

The most commonly used procedure is based on the hydroxylation of salicylic acid, which is based on the chemical reaction shown in Scheme 1.1.
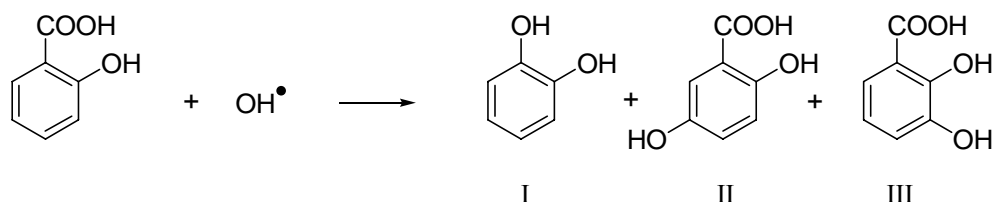
Scheme 1.1 *The Hydroxylation of Salicylic acid.*

By measuring all three hydroxylation products the assay may allow a simple and accurate quantitative detection of hROS by either electrochemical or photometric methods. As species I is formed only in small amounts, only species II and III are normally used for determining the amount of hROS. However, several problems arise under *in vivo* conditions. Species II is also produced enzymatically [37-38], leaving only species III available for detection as a simple hROS product. A constant product ratio is essential for determinations based on only one of the derivatives to be reliable. However, as shown in Tables 1.1 and 1.2, this requirement is far from being fulfilled [39-41]. The product ratio shows time dependence and there is also a strong influence of the chemical environment. As the ratio between species III and species II varies from 5:1 to 1:1, the resulting quantitation error is far from being negligible. Species (III) is also quite unstable and, in common with the other species, is quickly metabolised [39,42].

9

Table 1.1. Yields of 2,3-DHBA and 2,5-DHBA, and ratios of 2,3-DHBA:2,5-DHBA reported for different conditions of hROS generation.

Method	2,3-DHBA (μM)	2,5-DHBA (μM)	Ratio	Ref.[#]
Radiolysis[+]	105	20	5.25	[22]
Radiolysis[+] (1mM Fe(III)EDTA added)	100	75	1.33	[22]
Fenton system[*]	22	4	5.5	[22]
Fenton system [*] (100 μM Fe(III)EDTA added)	25	9.5	2.6	[22]
Fenton system[*] (1.3 mM Fe(III)EDTA added)	52	44	1.2	[22]
Photochemical reduction of Fe(III) in O_2 sat. solution[++] (0.3mM $K_2C_2O_4$)			1	[20]
Photochemical reduction of Fe(III) in O_2 sat. solution[++] (3mM $K_2C_2O_4$)			1.7	[20]

[+] *The yields were measured after a radiation dose of 600 Gy, buffered with 5 mM phosphate, pH 7.5, under N_2O; initial concentration of salicylic acid = 1 mM.*

[*] De-aerated solutions of 200 μM Fe(II)EDTA were mixed with 200 μM H_2O_2, buffered at pH 7.5 with 5 mM phosphate; initial concentration of salicylic acid = 1 mM.

[++] initial concentrations: 0.8 mM salicylic acid; 0.06 mM; Fe(III)

Table 1.2. Dependence of the ratio of 2,3-DHBA:2,5-DHBA on the reaction time during the photo-hydroxylation of salicylic acid [21][*].

Reaction time (min)	60	120	240	300
2,3-DHBA/2,5-DHBA	1.08	1.38	1.58	1.59

[*]*Photohydroxylation of salicylic acid (initial concentration = 0.7 mM) with hydrogen peroxide (initial concentration = 10 mM) sensitised with methylene blue (initial concentration = 0.01 mM) and photocatalysed by Fe(acac)$_3$.*

Furthermore, salicylic acid inhibits cyclooxygenase (EC 1.14.99.1), a key enzyme in the pathway of prostaglandin synthesis. Products of this pathway have many physiological functions in both normal and disease conditions [43-44] and are known to influence inflammatory processes associated with oxidative stress [45-47]. Thus the biochemical actions of salicylate itself may perturb the hROS results. All these considerations raise serious questions about the validity of *in vivo* results obtained using this method [35-38].

1.3.2   Phenylalanine

The hydroxylation reaction of phenylalanine has been proposed as an alternative to salicylate, mainly because the administration of phenylalanine has fewer identified side effects [38,48]. The disadvantage of multiple hydroxylation products remains, since reaction of phenylalanine with hROS yields a mixture of the 2-, 3- and 4-hydroxylated products (*o*-, *m*- and *p*-tyrosine). However, *p*-tyrosine is an endogenous compound, which is formed from L-phenylalanine by the enzyme phenylalanine hydroxylase (EC 1.14.16.1) and, therefore, cannot be used for quantitation of hROS. Since D-phenylalanine is not a substrate for this enzymatic hydroxylation, it has been proposed as a more suitable compound for hROS detection [49], although *p*-tyrosine still cannot be used for hROS determination unless a detection procedure that can distinguish between the D- and L-enantiomers is used. An additional potential problem is that D-

phenylalanine is a substrate for D-amino acid oxidase (EC 1.4.3.3), which is present in brain [50] and produces H_2O_2 as a product.

Chemokinetic studies have shown hydroxylation of phenylalanine to be rather slow [38, 48], and the amount of hROS required to overcome the detection limit, about 50 nM [38, 51], is rarely present in tissues, even in abnormal conditions. Furthermore, one, or more, unknown compound(s) were reported to coelute with *m*-tyrosine in ischemia-reperfusion experiments that used HPLC analysis with electrochemical detection [48, 52]. This yields an apparently greater increase of *m*-tyrosine, in comparison to *o*-tyrosine, which has also been reported by others, with e.g. 6-OHDA as hROS generator [53]. Since similar results were obtained by using different experimental procedures and detection methods (electrochemical and photometric), it seems unlikely that a coeluted unknown compound was the sole explanation for these results. An alternative explanation would be that, as in the case of salicylic acid, there is a change in the ratio of hydroxylated products due to a change in the chemical environment, which favours *m*-tyrosine formation in comparison to *o*-tyrosine. Since *p*-tyrosine cannot be considered for hROS detection and the above considerations suggest that it is doubtful whether if the sum of *o*- and *m*-tyrosine can be taken for an artefact-free hROS quantitation *in vivo* [see 48,52-43], results obtained with this procedure should be treated with caution. Nevertheless, this method has the potential advantage that nitration can be detected simultaneously, allowing concurrent monitoring of peroxynitrite formation [53].

1.3.3   4-Hydroxybenzoic acid (4-HBA)

Detection of hROS with 4-hydroxybenzoic acid (4-HBA) is less complicated, because only one hydroxylation product, 3,4-dihydroxybenzoic acid (3,4-DHBA), is formed in significant amounts. Thus, from a chemical viewpoint, this method should provide a much more reliable possibility for hROS quantitation *in vitro*. It has been used in microdialysis experiments, using HPLC separation with electrochemical detection [54-56]. Although 4-HBA can be hydroxylated by monooxygenases from some microorganisms, this apparently does not occur in mammals, suggesting its suitability as chemical trap for hROS determination *in vivo*. As 4-HBA is an endogenous compound that shows little or no apparent toxicity, it has been claimed that it could be also used for

human studies [55]. However, it is necessary to use high (mM range) concentrations of 4-HBA and further work is necessary to assess whether any biochemical processes are affected by 4-HBA, or its metabolites, at such levels.

1.3.4   2-[6-(4'-hydroxy)phenoxy-3H-xanthen-3-on-9-yl]benzoic acid (HPF) and 2-[6-(4-amino)phenoxy-3H-xanthen-3-on-9-yl]benzoic acid (APF)

Another approach using fluorescence detection should be reported here, because it describes for the first time the possibility to distinguish between different species of ROS, although up to now it has not been tested *in vivo*. Recently the group of Ken-ichi Setsukinai has produced 2-[6-(4'-hydroxy)phenoxy-3H-xanthen-3-on-9-yl]benzoic acid (HPF) and 2-[6-(4-amino)phenoxy-3H-xanthen-3-on-9-yl]benzoic acid (APF). If both substances are used together, they can selectively detect OH radicals and OCl$^-$. In this case the radical oxidation breaks the phenolic ether bond leading to one highly fluorescent product (see also scheme 1.2) [57]. The method has been tested *in vitro*, including cell cultures. However, the further development of this indicator seems to be limited by its difficult preparation and high cost.
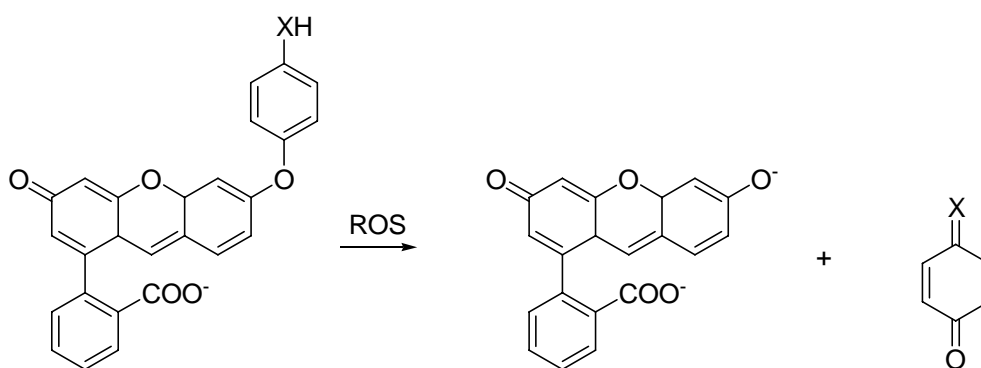
Scheme 1.2. *Reaction of HPF (X = O) and APF (X = NH) with ROS.*

1.3.5   Conclusion

As a conclusion it can be said that several trapping compounds have been developed for determining hROS production *in vivo*. These have sometimes been used with insufficient experimental validation. Both chemical and biochemical considerations indicate that neither salicylate nor the phenylalanine can provide an artefact-free quantitation of hROS. The two newer methods, which use either 4-DHBA or APF and HPF, do not have many of these drawbacks; however, they were not tested sufficiently *in vivo* to draw final conclusions about their validity.

1.4   Detection of Iron and H_2O_2

For a complete understanding of Fenton chemistry *in vivo*, beside the detection of hROS also Fe(II), Fe(III) and H_2O_2 must be monitored.

Although numerous methods for the *ex vivo* detection of Fe(II), Fe(III) and H_2O_2 are described the literature, none of these was practicable for our purpose. This was on one hand due to the small volume of microdialysis sample (ca. 10 µl) which was available for analysis and on the other hand due to instrumental restrictions in our labs. This led in the case of iron to the necessity to entirely modify an already known procedure based on the complexation of Fe(II) with bathophenanthroline and in the case of H_2O_2 to design a new method on the basis of the TA^{2-} assay.

1.5   Summary of the problem definition

On the way to a practicable *in vivo* protocol to monitor simultaneously all relevant compounds involved in Fenton chemistry together with the neurotransmitter behaviour numerous *in vitro* and *in vivo* tasks had to be solved. First of all a new substance working as a reliable hROS indicator had to be found and tested in terms of possible chemical or biological artefacts. Secondly kinetic experiment had to be performed to get information about the possible reaction mechanism of the substance with hROS to estimate its chemical behaviour during a typical *in vivo* stimulation.

Thirdly methods for iron and H_2O_2 detection had to be adapted and tested together with hROS and neurotransmitter monitoring. After solving these problems the question on the involvement of Fenton chemistry in the brain during 6-OHDA stimulation could be addressed.

Part II

2 General overview of the experimental methods used

2.1 Kinetic measurements

2.1.1 Principle

The basic data of kinetic measurements are the concentration of the reactants at different time points. The concentration is calculated from a standard curve linking the measured property (e.g. absorbance or fluorescence) with the known concentration of a standard sample.

These data are then fitted with a mathematical expression representing the solution of a differential equation, the so called rate law of the reaction.
As in this work all measured reactions are second order reactions, only the mathematical derivative of second order rate equations will be presented here. For a systematic introduction into this matter the author refers to the literature [58].

2.1.2 Second order rate law and rate constants

The measured rate (v) of a second order reaction is proportional to the concentrations of the reactants A and B. The proportionality constant k is then called the rate constant.

$$v=k*[A]*[B] \tag{2.1}$$

An experimentally determined equation of this kind is called the rate law of the reaction, and expresses the rate of the reaction v as a function of all species present, including the products. The theoretical application of a rate law is one guide to the

mechanism of a reaction, and any proposed mechanism must be consistent with the observed rate law.

The determination of a second order rate law is simplified by the isolation method in which the concentration of one reactant is kept in large excess, and therefore stays practically constant during the reaction. Via this way equation (2.1) simplifies to a first order rate law.

$$v=k'*[A] \quad \text{where } k'=k*[B]_0 \tag{2.2}$$

Since the true rate law has been forced into first-order form, it is called a pseudo first order rate law.

Writing equation (2.2) with differential quotients leads to

$$-dA/dt=k'*[A] \tag{2.3}$$

The solution of this differential equation gives

$$[A] = [A]_o \exp(-k'*t) \tag{2.4}$$

If the reversing of the isolation by keeping substance A constant, also leads to a first order rate law, the reaction obeys a second order rate law. In a system of sequential reaction only reactions before the so called rate determining step can be observed. The rate determining step is the slowest reaction in the system.

2.1.3 The stopped flow technique

The stopped flow technique allows a monitoring of fast reactions in the low ms range. The name of this method comes from its principle, which is presented in 2.1, to initiate a flow of two or more reactants into a mixing chamber which is stopped after a few milliseconds.
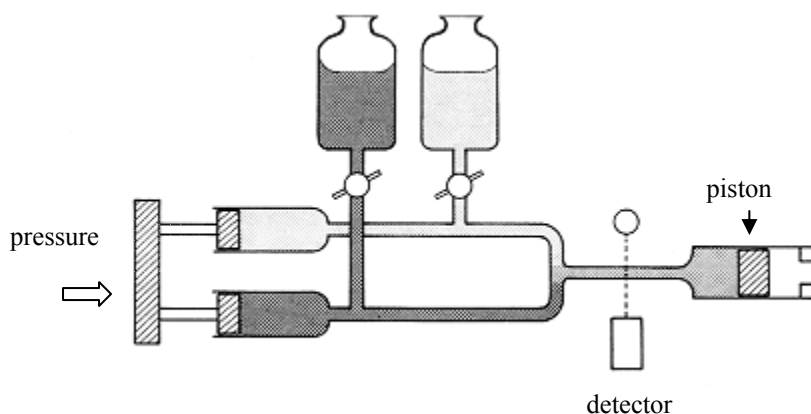
Figure 2.1. *Schematic scheme of the principle of stopped flow technique*

More detailed the reaction is initiated by quickly mixing the solutions, which is reached by injecting them into the reaction chamber under high pressure. The chamber is shut by a piston, which firstly is pushed backwards by the incoming fluid until it reaches the stop bar. The reaction can be monitored e.g. by different methods of spectroscopy. As this technique only needs small amounts of sample (some ml), it is also suitable for biochemical investigations such as enzyme kinetics. The methods of analysis are usually restricted to UV/VIS or fluorescence spectroscopy and conductivity measurements.

2.2 High performance liquid chromatography [59]

2.2.1 General

HPLC is used to separate components of a mixture by using a variety of chemical interactions between the substance being analyzed (analyte) and the chromatography column. The basic operating principle of HPLC is to force the analyte through a column of the stationary phase (usually a tube packed with small round particles with a certain surface chemistry) by pumping a liquid (mobile phase) at high pressure through the column. The sample to be analyzed is introduced in small volume to the stream of mobile phase and is retarded by specific chemical or physical interactions with the stationary phase as it traverses the length of the column. The amount of retardation

depends on the nature of the analyte, stationary phase and mobile phase composition. The time at which a specific analyte elutes is called the retention time and is considered a reasonably unique identifying characteristic of a given analyte. The use of pressure increases the linear velocity giving the components less time to diffuse within the column, leading to improved resolution in the resulting chromatogram. Common solvents used include any miscible combinations of water or various organic liquids (the most common are methanol and acetonitrile). Water may contain buffers or salts to assist in the separation of the analyte components, or compounds such as Trifluoroacetic acid which acts as an ion pairing agent.

Especially for complex separations, a technique, called gradient elution, is widely used. The name comes from the practise of varying the mobile phase composition during the analysis. The gradient separates the analyte mixtures as a function of the affinity of the analyte for the current mobile phase composition relative to the stationary phase. On the contrary to that keeping a constant composition of the mobile phase during the whole analysis is called.isochratic elution.

2.2.2 Reversed phase chromatography

Reversed phase HPLC consists of a non-polar stationary phase and an aqueous, moderately polar mobile phase. One common stationary phase is a silica which has been treated with RMe2SiCl, where R is a straight chain alkyl group such as $C_{18}H_{37}$ (C-18) or C_8H_{17} (C-8). As in this work only a C-18 reverse phase column was used, the following general description will be based on this example. Due to the apolar surface of the stationary phase, the retention time is longer for molecules which are more non-polar in nature, allowing polar molecules to elute more readily. Retention time is increased by the addition of polar solvent to the mobile phase and decreased by the addition of more hydrophobic solvent. Reverse phase chromatography (RPC) operates on the principle of hydrophobic interactions, which result from repulsive forces between a polar eluent, the relatively non-polar analyte, and the non-polar stationary phase. The binding of the analyte to the stationary phase is proportional to the contact surface area around the non-polar segment of the analyte molecule upon association with the ligand (the C-18 chain) and indirect proportional to the solubility of the analyte in the aqueous eluent.

This solvophobic effect is dominated by the force of water for "cavity-reduction" around the analyte and the C-18 chain versus the complex of both. The energy released in this process is proportional to the surface tension of the eluent and to the hydrophobic surface of the analyte and the ligand, respectively. The retention can be decreased by adding less-polar solvent into the mobile phase to reduce the surface tension of water. Gradient elution uses this effect by automatically changing the polarity of the mobile phase during the course of the analysis.

Structural properties of the analyte molecule play an important role in its retention characteristics. In general, an analyte with a larger hydrophobic surface area (C-H, C-C, and generally nonpolar atomic bonds, such as S-S and others) results in a longer retention time because it increases the molecule's nonpolar surface area, which is non-interacting with the water structure. On the other hand, polar groups, such as -OH, -NH_2, COO^- or -NH_3^+ are reducing retention as they are well integrated into water. Very large molecules, however, can result in an incomplete interaction between the large analyte surface and the ligands alkyl chains and can have problems entering the pores of the stationary phase.

Retention time increases with hydrophobic - nonpolar - surface area. Branched chain compounds elute more rapidly than their corresponding linear isomers because the overall surface area is decreased. For example, similarly organic compounds with single C-C-bonds elute later than the ones with a C=C or C-C-triple bond, as the double or triple bond is shorter than a single C-C-bond.

Aside from mobile phase surface tension (organizational strength in eluent structure), other mobile phase modifiers can affect analyte retention. For example, the addition of inorganic salts causes a moderate linear increase in the surface tension of aqueous solutions, and because the entropy of the analyte-solvent interface is controlled by surface tension, the addition of salts tends to increase the retention time. Another important component is the influence of the pH since this can change the hydrophobicity of the analyte. For this reason most methods use a buffering agent, such as sodium phosphate, to control the pH. Besides controlling the pH buffers also neutralize the charge on any residual exposed silica on the stationary phase and act as

ion pairing agents to neutralize charge on the analyte. The effect varies depending on use but generally improves the chromatography.

2.3   Microdialysis

2.3.1   Principle

Microdialysis is a technique used to determine the chemical components of the fluid in the extracellular space of tissues. It uses the principle of dialysis (Greek: separate), in which a membrane (microdialysis probe), permeable to water and small solutes typically up to 25 kDA, is introduced into the tissue. The membrane is perfused with a liquid (perfusate) which equilibrates with the fluid outside the membrane by diffusion in both directions. Osmotic pressure is the driving force.

In brain microdialysis the probe is implanted under anaesthesia into a specific area of the brain stereotactically, and fixed with cement. After recovery, the animal is allowed to move freely and behave normally while the experiment is performed. The inlet of the probe is connected via polyethylene tubing to a micro infusion with flow rates of 1-3 µl/min, whereas the outlet is connected to the sample collector. After equilibration time the perfusate reflects the extracellular fluid of the chosen brain area, allowing a real time monitoring of changes in the neurochemistry of the animal (see figure 2.2 a-f). Moreover, local chemical stimulation can be performed applying substances through the perfusion fluid [60-62].

Figure 2.2a. *The brain coordinates of the interested area of the brain is located stereotactically*
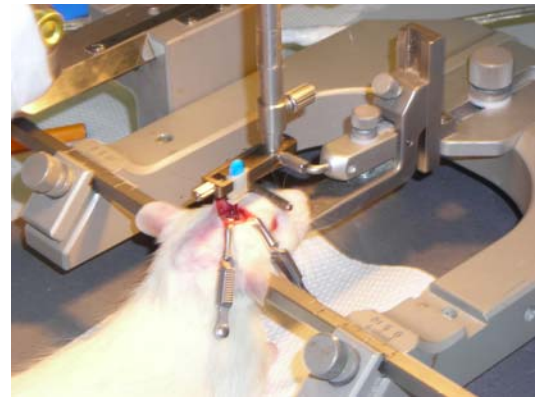
Figure 2.2b. *A tiny hole is drilled into the skull, and the probe is placed in the specified area*

Figure 2.2c. *The probe is fixed with cement, and the rat allowed to recover.*

Figure 2.2d. *After 24 h the experiment is conducted in the freely moving and normal behaving animal*

Figure 2.2f. *The perfusate is pumped with a micro infusion pump into the probe. Usual flow rates are between 1-3 µl*
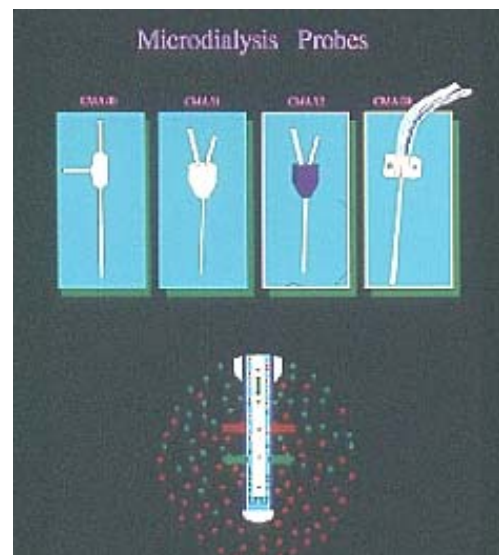
Figure 2.2e. *Several types of probes are commonly used depending on the specific problem definition. Local chemical stimulation can be achieved via perfusing the stimulus through the probe.*

22

Part III

3 Developing and Testing the Terephthalate Method

3.1   Introduction

As already described above, due to the problems with the commonly used methods for detecting hROS *in vivo*, numerous substances have been tested for this purpose.

Very recently interest has turned to terephthalic acid. This has long been used as a dosimeter in radiolysis experiments [37, 63-66] because of its ease of use, as detection is easily achieved by fluorescence spectroscopy. Terephthalic acid (H_2TA) as well as the terephthalate dianion (TA^{2-}) react selectively with hROS to OH-terephthalic acid (OH-H_2TA) or OH-terephthalate (OH-TA), both showing fluorescence with an excitation between 309 - 326 nm and an emission between 412 and 435 nm dependent on the chemical conditions [35, 37, 38, 63-71]. Detailed emission spectra have only been reported for an excitation wavelength of 315 nm and 326 nm for the dianion at a pH of 10 and 7.5, respectively [35, 38]. As the pK values of H_2TA are 2.60 and 4.35 [72] under physiological conditions, however, only the properties of the dianion were of interest.

The hydroxylation reaction (Scheme 3.1) is quite specific, as it requires redox potentials of OH-radicals or ferryl species (>1.6 V) [34] and does not take place with other reactive oxygen species such as the superoxide radical or H_2O_2 [22, 26, 29-30].
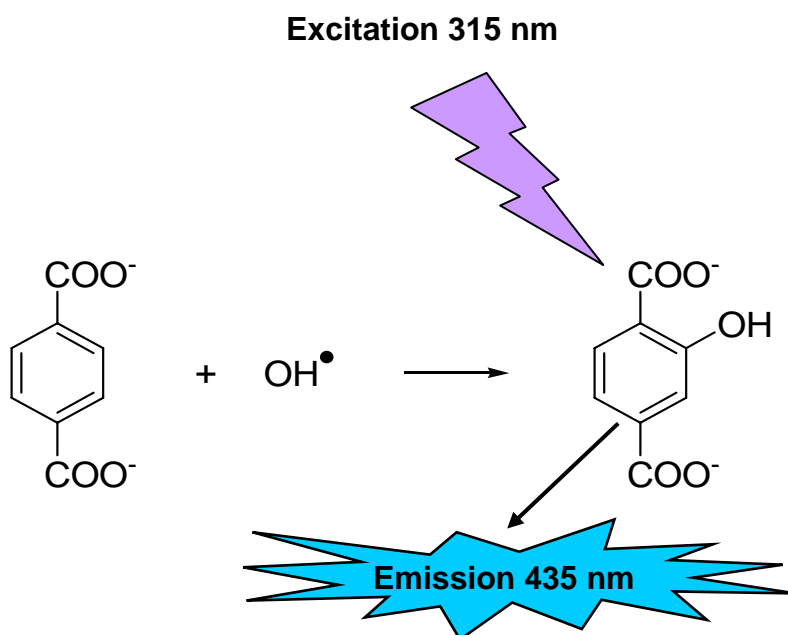
Scheme 3.1. *The hydroxylation of terephthalic acid due to radical oxidation.*

A big advantage of this system is that, apart from some minor fragmentation products, which occur in all aromatic hydroxylation processes, the symmetry of the molecule leads to only one hydroxylated product and this shows, in contrast to the (quasi) non fluorescent TA^{2-}, a brilliant fluorescence.

An overview of the conditions used in the literature to detect OH-radicals or hROS formed by radiolysis [63-64, 66, 70], ultrasound [64, 67, 73] or Fenton (type) reactions [35, 38, 64] with TA^{2-} is given in Table 3.1.

Table 3.1. Conditions used for the hydroxylation of terephthalate or terephthalic acid.

Methods used to produce hydroxyl radicals	pH	Conc. of buffer TA^{2-}	
Radiolysis (12 Gy/min) in N$_2$, air and O$_2$ sat. solution [26]	5.0 – 8.0	20 – 400 µM	Phosphate buffer
Radiolysis in N$_2$O sat. Sol. (0.14 Gy/s) [27]	5.0; 10.0	1 mM	no
Modified Fenton system: H$_2$O$_2$ is produced via O$_2$ and Fe(II)EDTA without the addition of H$_2$O$_2$ [28]	7.4	10 µM	potassium phosphate
Liver microsomal enzymes; addition of Fe(III)EDTA (0.1, mM 1.0mM NADPH) [16]	7.4	1 mM	potassium phosphate (20 mM)
Mohr's salt (Fe(II)) 50µM; 10 – 60 µM H$_2$O$_2$ [19]	3.15 – 10;	4.25 mM	phosphate buffer + 2% KCl
Methods used to produce hydroxyl radicals	**pH**	**Conc. of TA^{2-}**	**buffer**
Fenton system Fe(II)SO$_4$•7H$_2$O, H$_2$O$_2$ (1 – 30 µM, equimolar) [17]	7.4	5mM	0.05 M NaH$_2$PO$_4$/ Na$_2$PO$_4$ buffer
Steady state γ-irradiation; (30 Gy/min) radiolysis; (1 – 5 GY/pulse); in N$_2$O sat. Solution [32]	7.4	5mM	10 mM phosphate buffer
Radiolysis: γ-irradiated aqueous Sol. [30]	10.0	0.1 – 10 mM	No

Table 3.2. Composition of the artificial cerebrospinal fluid (aCSF)

Salt	Concentration
NaCl	140 mM
KCl	3 mM
$CaCl_2$	1.2 mM
$MgCl_2$	1 mM
Na_2HPO_4	1.2 mM
NaH_2PO_4	0.21 mM

It can be concluded from table 3.1 that on the way to a practicable *in vivo* standard a lot more details on the reaction system had to be clarified. By comparing table 3.1 with table 3.2, which shows the ingredients of the artificial cerebrospinal fluid (aCSF) used in the microdialysis experiments as its composition fits as close as possible the one of the extra cellular fluid, it can be seen that no literature existed covering the details of a Fenton system under these conditions using TA^{2-} as hROS indicator. As all used ions (Na^+, Ca^{2+}, Mg^{2+}, halides, phosphate anions) are well known to quench or enhance the fluorescence in a given system, first of all, it was necessary to investigate their systematic influence on the TA^{2-} system, also because in many *in vivo* experiments the rise of the concentration of one or more salts given in table 2 is taken as a stimulus. Moreover, a systematic work on the time dependence and the hydroxylation yield including the question of a linear dependence of TA^{2-} hydroxylation on the hROS concentration in a Fenton type system, under conditions close to the extra cellular fluid, was still missing. In conclusion it can be said that before going to the *in vivo* experiments a set of *in vitro* work had to be done to close the remaining gaps of knowledge.

3.2   *In vitro* validation of TA^{2-} as a trapping system for hROS

3.2.1   Experimental

3.2.1.1   Chemicals and solutions

All chemicals used for the preparation of artificial cerebrospinal fluid (aCSF) and buffer solutions were of analytical grade, obtained from Sigma-Aldrich (Milan, Italy), and were used without further purification. The aCSF used for the *in vitro* experiments was glucose-free, prepared by dissolving 8.17 g (140 mmol) NaCl, 0,2237 g (3 mmol) KCl, 203 mg (1 mmol) MgCl$_2$, 213 mg (1.2 mmol) Na$_2$HPO$_4$ and 37.4 mg (0.27 mmol) NaH$_2$PO$_4$ in 1 l double distilled water (resistance: $\geq$ 18.2 MΩ). To investigate the use of potentially complexing anions as the mobile phase for HPLC, acetate buffer (100 mM) was prepared by dissolving potassium acetate in double distilled water and adjusting the pH with glacial acetic acid to 5.48.

Mohr´s salt (NH$_4$)$_2$Fe(II)(SO$_4$)$_2$ (6 H$_2$O) (p.A.) was obtained from Merck (Vienna, Austria). Stock solutions of 0.9 mM Fe(II) were always freshly prepared, by dissolving the Mohr´s salt in water and diluting to the final concentrations with aCSF or buffer. Stock solutions of 90 mM H$_2$O$_2$ were prepared from a 30% hydrogen peroxide solution (Sigma-Aldrich, Vienna, Austria) and titrated with KMnO$_4$ before used. They were diluted to the appropriate final concentration, either with aCSF or buffer. Sodium terephthalate (96%) was obtained from Sigma-Aldrich (Vienna, Austria) and stock solutions (3 mM) were prepared in aCSF or buffer and were either used directly or after further dilution.

For preparing standard curves and for the quenching experiments 1 mM (18.2 mg) OH-TA was dissolved with ca. 20 ml of 10 % (w/v) NaOH and adjusted to 100 ml with double distilled water. It was not desirable to use an ultrasonic bath to aid dissolution, since ultrasound, in itself, produces hydroxyl radicals. The OH-TA stock solution was then diluted, with aCSF or buffer, to which TA^{2-} was added to the final desired

concentration. The fluorescence measurements were obtained by subtracting the auto-fluorescence value of TA^{2-}. For the quenching experiments, the standard solution was diluted 1:1, either with H_2O or with the potential quencher dissolved in water, and directly injected into the fluorimeter.

3.2.1.2   Fenton reaction

Fenton reagent was prepared by mixing Fe(II) and TA^{2-} solutions. The reaction was initiated by adding H_2O_2 to this solution, followed by intensive shaking, either by hand or, when Eppendorf tubes were used, with a Labinco L46 vibrations mixer (Breda, The Netherlands). After 15 min, the mixture was either injected into an HPLC coupled to a fluorescence detector or directly into a fluorimeter cell. In all cases the data were corrected for the auto-fluorescence of TA^{2-}. When not otherwise stated, the fluorescence of a blank sample, containing the same concentrations of Fe(II) and TA^{2-} but no H_2O_2, was subtracted from the fluorescence of the sample to eliminate also any contribution from the auto-oxidation of Fe(II). The experiments with a microdialysis probe were done in a magnetically stirrer beaker containing aCSF. To simulate *in vivo* conditions, the same solution as used for the *in vivo* experiments (aCSF with added TA^{2-}) was pumped through the probe at a flow rate of 3 μl/min. After 20 min equilibration, a 20 min sample was taken as the blank and the reaction was initiated by adding, successively, Fe^{2+} and H_2O_2, as under these conditions no significant auto-oxidation of Fe^{2+} occurred. To check the response linearity with respect to the reactant concentrations, the reaction was stopped after 6 min, by adding about 1000 U of catalase (Sigma-Aldrich, Vienna, Austria).

3.2.1.3   Equipment

When measurements were performed without an HPLC system, samples were directly injected into an HP 1096A fluorescence detector (Agilent Technology, Vienna, Austria), using an excitation wavelength of 306 nm and an emission wavelength of 432 nm.

28

HPLC analysis was carried out using a reverse-phase Shimadzu (Shimadzu Italia S.r.l., Milan, Italy) HPLC system, consisting of LC-10A$_{VP}$ pumps, SIL-10AD$_{VP}$ refrigerated autoinjector, RF-551 fluorescence detector or Perkin Elmer CC90 (Pelkin Elmer Milan, Italy) UV/VIS detector and a Class-VP^{TM} 7.2.1 SP1 unit. The manufacturer's software was used for controlling the system and for chromatographic peak recording and integration.

3.2.1.4   Synthesis of the standard 2-hydroxyterephthalic acid

All chemicals used were of analytical grade (if not otherwise stated) and were purchased from Sigma-Aldrich (Vienna, Austria). The product was synthesised by a modification of the previously published procedures (38, 74-75). In general, 2.465 g (10.0 mmol) of *ortho*-bromoterephthalic acid (95%, Sigma-Aldrich) and 0.91 g NaOH (20.1 mmol) were dissolved in 57 ml of water. For surface activation, 5 g of copper powder was treated with concentrated HCl, filtered and washed neutral with H_2O; 12.9 mg (0.20 mmol) of the activated copper powder, together with 1.826 g (22.1 mmol) sodium acetate, were added to the solution. After the addition of some drops of phenolphthalein the colour of the solution turned purple. The mixture was then heated to reflux and stirred with a magnetic stirrer for 25 hours. During the reaction the colour quickly turned to yellow. At intervals, 10% (w/v) KOH was added, to keep the reaction mixture at a pH of ca. 8, since precipitation occurred if the solution became acidic. The solution was then allowed to cool to room temperature and filtered. The filtrate was acidified (pH of ca. 3) with 2 M HCl to precipitate the product. The mixture was then kept at 4 °C in a refrigerator overnight to complete the crystallization.The cream coloured product was filtered (frit pore size 3), dried in vacuo and stored in a desiccator above phosphorous pentoxide. It was characterised by ^{1}H NMR. The final yield was 1.42 g (78%).

3.2.2 Results

A reliable *in vivo* standard procedure for hROS detection must stringently fulfil the following conditions *in vitro*: (1) The fluorescence (or any other detectable property) must be a linear function of the substance concentration; (2) The concentration of the hydroxylated product must show a linear dependence on the amount of hROS; (3) The behaviour of the fluorescence (or any other detected property) must not be influenced by any change of the chemical environment, unless it directly affects the hROS formation. Firstly, the behaviour of the terephthalate system was evaluated in terms of each of the above criteria *in vitro*.
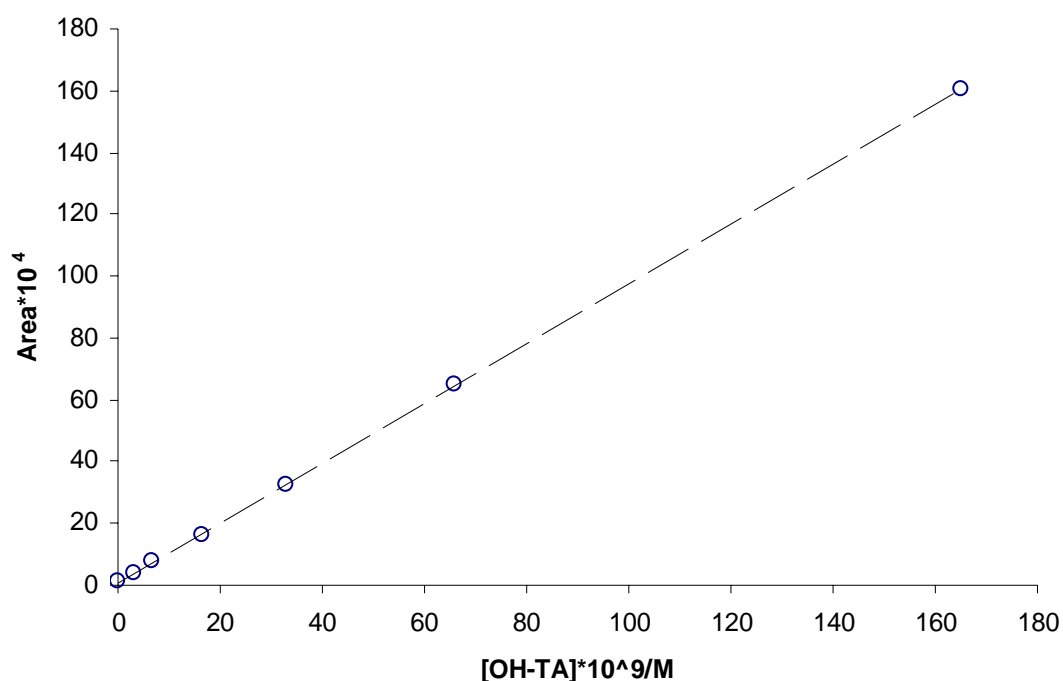
Figure 3.1. *Peak areas of relative fluorescence (retention time 3,29 min; flow 1 ml/min) as a function of [OH-TA]. $R^2 = 0.99996$;*

To test condition (1), different concentrations of OH-TA were dissolved in aCSF containing 250 μM, 500 μM or 1 mM TA^{2-} and the fluorescence was measured with a fluorescence detector following HPLC separation. The fluorescence was linearly dependent on the fluorophor concentration in the range 0.5 – 1,000 nM (see figure 3.1.). The detection limit was estimated to be equivalent to 0.5 nM OH-TA, with the equipment used. To verify conditions (2) and (3) a Fenton system under conditions approximating to physiological, was chosen as a model reaction for biological systems. Non-chelated Fe(II) shows only a small Fenton activity at physiological pH values [76-78]. Nevertheless, the OH-TA formed could be detected without any problems. To check if linearity is maintained with higher Fenton activities, the reaction was also
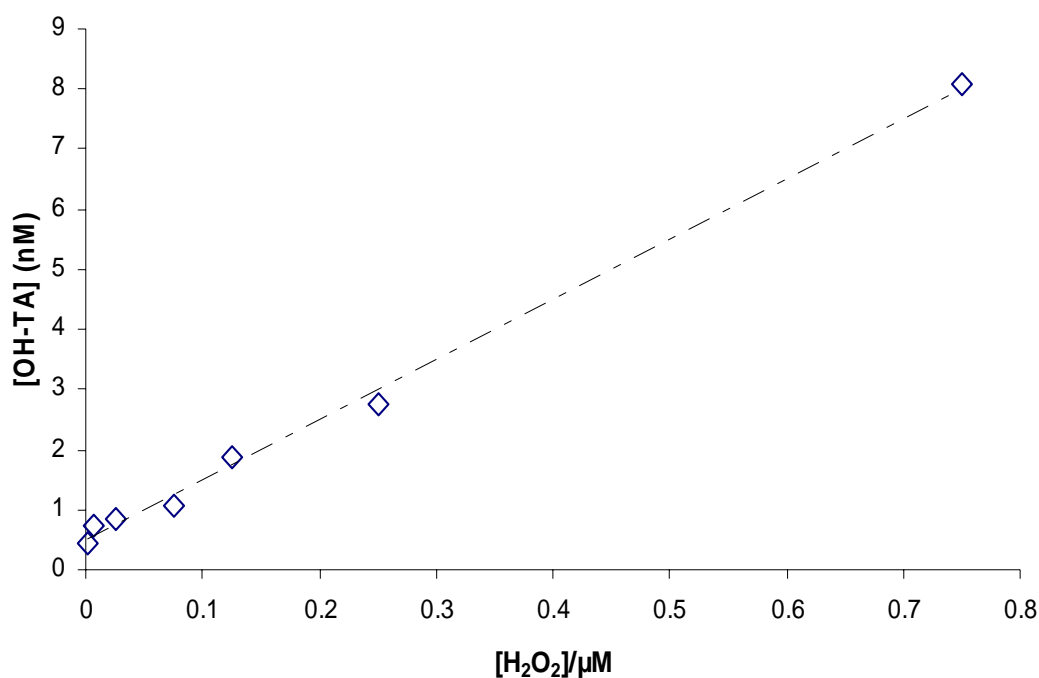
Figure 3.2. Dependence of OH-TA concentration on the amount of hROS.
Concentration of OH-TA formed as a function of H_2O_2, at concentration of TA^{2-} of 250 μM. Linear regression analysis was performed after subtraction of the blank value. The Fe(II) concentration was 30 μM. Reactions were carried out in aCSF (pH

carried out at lower pH values. As shown figures 3.2 and 3.3, the concentration of the fluorophor was linearly dependent on the amount of H_2O_2, which is directly

proportional to the amount of hROS formed over a wide concentration range. In the experiments carried out in aCSF, the concentration of OH-TA was independent on the amount of TA^{2-}. This point will be discussed in more detail in Part (IV) of this work.
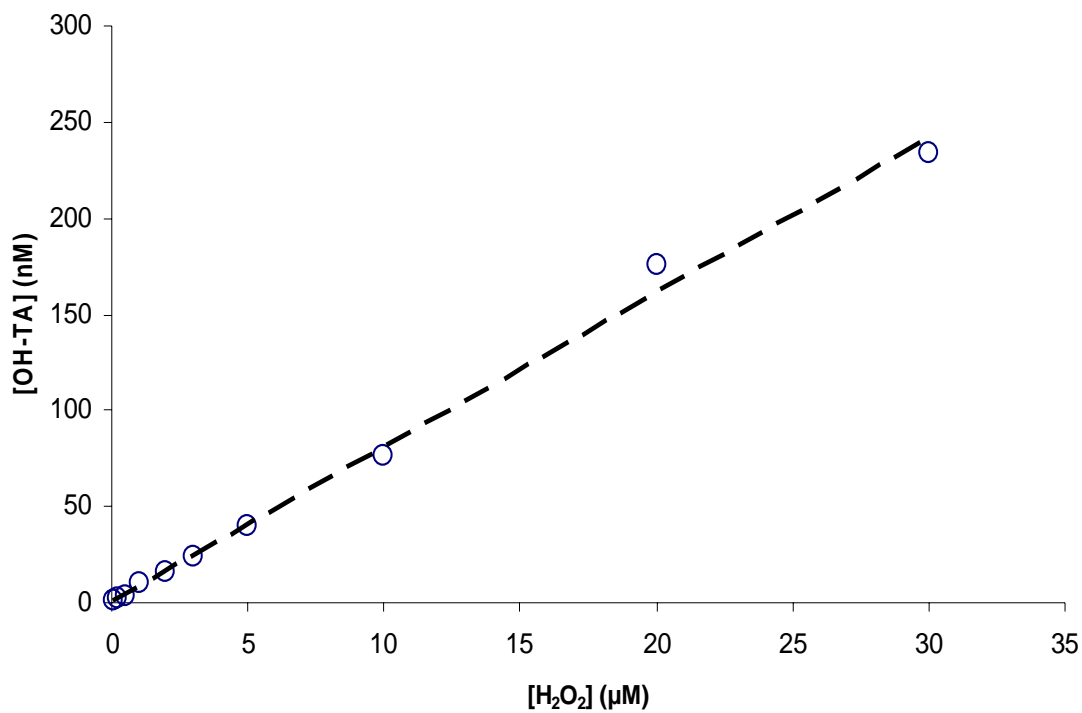
Figure 3.3. Dependence of OH-TA concentration on the amount of hROS.
Concentration of OH-TA formed as a function of H_2O_2, at concentration of TA^{2-} of 250 μM. Linear regression analysis was performed after subtraction of the blank value. The Fe(II) concentration was 30 μM. Reactions were carried out in 100 mM potassium acetate buffer (pH 5.48). r = 0.997; slope = 8.06; n = 2;

The most likely source of artefacts, in measuring time courses of hROS formation *in vivo* using TA^{2-}, is the possible quenching of the fluorescence of OH-TA by either halogenides or metal cations, which are present in high concentrations in a physiological medium. However, no quenching could be observed, either with each of the individual components of the perfusion fluid (140 mM NaCl, 3 mM KCl, 1 mM $MgCl_2$, 1.2 mM $CaCl_2$, 0.27 mM NaH_2PO_4, 1.2 mM Na_2HPO_4) or with 100 mM KCl, used in experiments to evoke neurotransmitter release. There was also no quenching due

to TA^{2-} up to 5mM, or by any of the compounds involved in the Fenton process (0.3 mM $(NH_4)_2Fe(II)(SO_4)_2$, 0.3 mM $Fe(III)(NO_3)_3$). A quenching could only be observed when 100nM OH-TA were dissolved together with 200 $Fe(III)(NO_3)$ in water without the presence of TA^{2-} . However, already the addition of 250 μM TA^{2-} as well as adding an equal amount (related to H_2O) of aCSF or 100mM acetate buffer (pH 5.48) led to a complete disappearance of the quenching.

For testing the possible influence of Fe(III) on the hydroxylation yield, an equimolar amount (related to Fe(II)) of Fe(III) was added to a Fenton system, consisting of aCSF, 50 μM H_2O_2 , 200μM Fe(II) and 1mM TA^{2-} prior to the initiation of the reaction. In this case as well as in the case of saturating the solution with argon before initiating the reaction, no difference of the fluorescence could be observed in comparison to a Fenton system in aCSF under aerobic conditions.

In order to address the issue of artefactual problems, we examined the possibility that non-linear permeability of the probe membrane with respect to TA^{2-} or OH-TA concentration, as well as release of iron from the metal part of the probe, might be a possible source of artefacts in microdialysis experiments. Thus, experiments with a microdialysis probe were done in a magnetically stirred beaker containing aCSF. To simulate *in vivo* conditions, the same solution and flow rate as applied in the *in vivo* experiments (aCSF with added TA^{2-}) was used. However, as shown in Fig. 3.4, the concentration-dependence with respect to the amount of hROS formed, and its independence from TA^{2-} concentration, was maintained. Moreover, the fluorescence of the blank was identical to that of the standard solution containing the same concentration of TA^{2-}, before it was perfused through the probe.
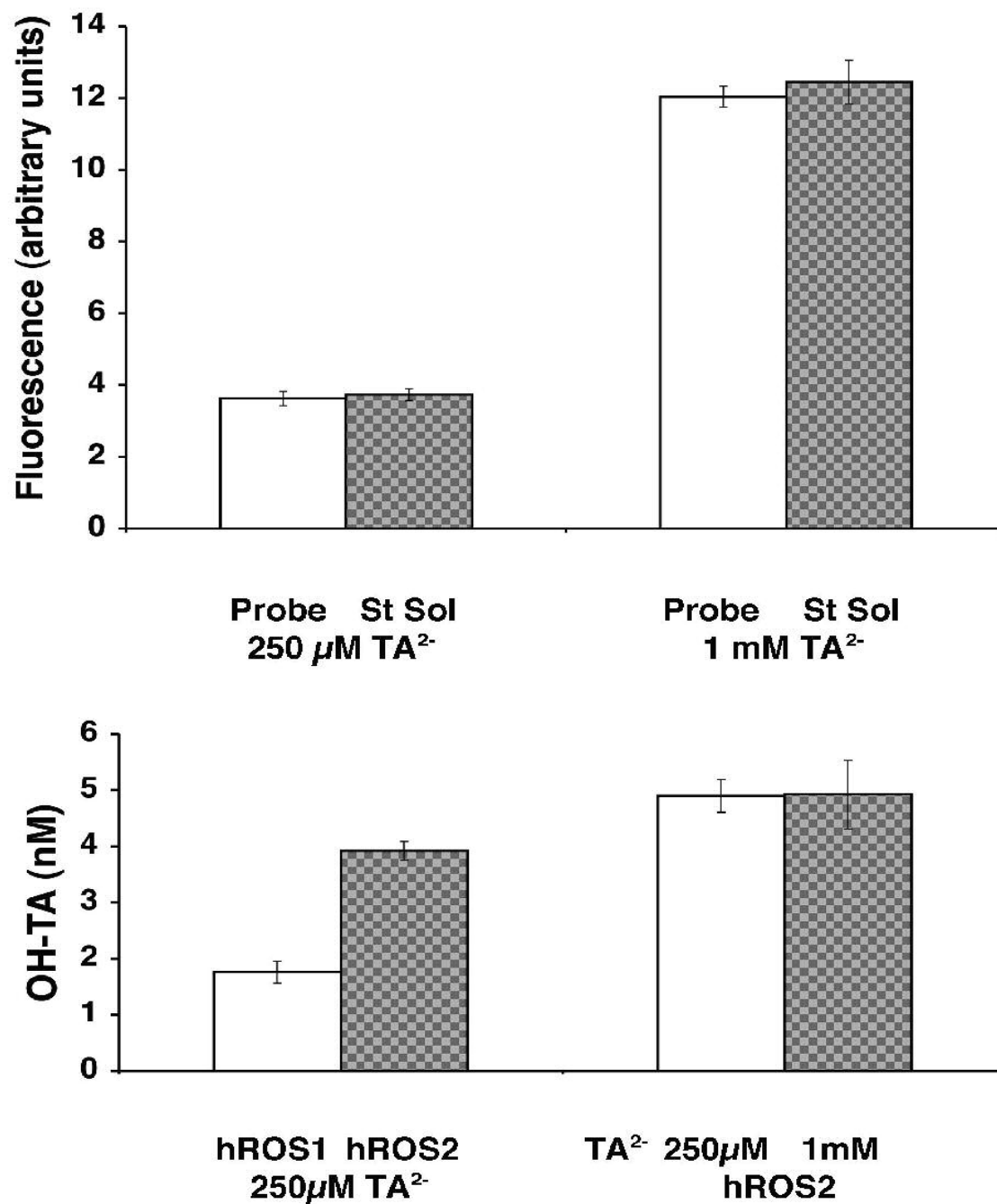
.**Figure 3.4. OH-TA formation during in vitro microdialysis experiments.**

The microdialysis probe placed in a magnetically stirred beaker containing aCSF, was perfused (3 μl/min) with a standard solution (St Sol) of aCSF containing TA^{2-}. After 20 min equilibration, a first 20 min fraction (Fraction 1) was collected to estimate the fluorescence of TA^{2-}, as a blank (upper panel). When collection of the second 20 min fraction (Fraction 2) started, the reaction was initiated by adding, successively, Fe^{2+}

and H_2O_2 (bottom panel). Each column represents the mean ± SEM derived from 4 experiments.

Upper Panel - Fluorescence due to TA^{2-}, *detected either in fraction 1* (**Probe**), *before starting the reaction, or directly in the **St Sol**, containing 250 μM (right columns) or 1 mM (left columns) TA^{2-}.* ***Bottom Panel*** *– Columns represent the fluorescence detected in fraction 2, after subtraction of the fluorescence of fraction 1 taken as the blank. Fluorescence values were transformed into OH-TA concentration by inverse prediction from a standard calibration curve.* ***The effects of increasing hROS*** *(left columns): The TA^{2-} concentration in aCSF was 250 μM, the Fenton reaction was stopped after 6 min.* ***hROS1 -*** *Fe^{2+} and H_2O_2 concentrations were 30 μM and 0.75 μM, respectively;* ***hROS2 -*** *Fe^{2+} and H_2O_2 concentrations were 60 μM and 1.5 μM, respectively.* ***The effects of increasing TA^{2-}*** *(right columns): the reaction was performed under* ***hROS2*** *conditions; TA^{2-} concentration was 250 μM (white column) and 1mM (dark column).*

3.2.3   Discussion

From a chemical point of view numerous sources of artefacts for *in vivo* microdialysis as well as for stopped flow kinetic experiments could be excluded. For the quenching experiments the iron and acetate concentration were chosen far above the levels observed even under damaging conditions, whereby acetate was chosen as model substance for carboxylic acids. It should be pointed out here that in the extra cellular fluid under damaging condition the total iron, carboxylic and amino acid concentrations are in the low (1 to 40) μM range. Since it was observed that neither substances mainly present in the extracellular fluid nor high millimolar concentration of acetate nor non-physiological high concentration of Fe(II) and Fe(III) influence the fluorescence, it is very unlikely that a change in the chemical environment, which does not affect the hROS formation, causes an artefactual increase or decrease of the fluorescence. On the contrary to the salicylic acid assay, where the formation or addition of Fe(III) causes a change of the ratio of the hydroxylation products (see introduction), which could lead to a quantitation error of hROS, no such influence could be observed using TA^{2-}. This excludes at least for a simple Fenton system an artefactual time dependence of the fluorescence, caused by an increase of Fe(III)

concentration during the reaction. This allows an application of TA^{2-} in stopped flow kinetic experiments.

Concerning the dependence of the hydroxylation yield on the oxygenation, contradictionary results obtained in radiolysis experiments are found in the literature. [63, 64]. However, under the conditions used here, this influence could not be replicated, maybe because the chemistry of hROS in a Fenton system in aCSF differs from the one in radiolysis experiments under the described conditions (see also Tab. 3.1 and Chapter 1.2)

The experiments with microdialysis probes (Fig. 3.4) demonstrate that the probes do not lead to a non linear distortion of a linear hROS signal, proving that the permeability of the membrane is linear for OH-TA as well as for TA^{2-}. Furthermore, the results do not indicate any hROS formation caused by the microdialysis equipment, thus showing the inertness of the probes in terms of an artefactual hROS background.

As a conclusion it can be said, that according to the presented results, the application of TA^{2-} *in vivo* for microdialysis and *in vitro* for stopped flow kinetic experiments should provide, from a chemical viewpoint, a reliable and robust method for hROS detection.

3.3   *In vivo* testing of the method

3.3.1   Introduction

Already some time ago the known *in vitro* properties of TA^{2-} led to the suggestion that it can be used *in vivo* [63] and based on the known properties Yan et al. [38] have applied this method to the microdialysis of sheep. This study, however, has several fundamental problems. Firstly, the perfusion medium contains an extremely high (non-physiological) concentration of phosphate (required to solubilise the free acid form of terephthalate), which in our own experiments resulted in the death of one laboratory rat and extreme oxidative stress in another. Secondly, they did not clearly and unequivocally

demonstrate that the increase in fluorescence observed was not due to other factors including changes in medium. Finally, they did not show a dose dependence of hROS formation under *in vivo* conditions. Despite these problems, this work inspired us to develop the terephthalate method for use in microdialysis experiments and resolve the remaining questions about its validity in a physiologically relevant system.

As there was no work performed examining the possible influence of TA^{2-} on the biochemistry of the brain our first target was to systematically investigate this matter.
As TA^{2-} was reported to be non endogenous, non toxic and non accumulative [79-80] we saw a realistic chance that it does not show any bioactivity. As a second step we conducted experiments to validate a dose dependent formation of OH-TA related to a neurotoxic stimulus to complete the evaluation of the method.

3.3.2   Experimental

3.3.2.1   Animal housing and surgery.

All animal experiments were performed according to the Italian Guidelines for Animal Care (D.L. 116/92) and the European Communities Council Directives (86/609/ECC), with all efforts to minimise animal sufferings and the number of animals necessary to collect reliable scientific data. Male Wistar rats (200-220 g) were anaesthetised with chloral hydrate (400 mg/kg i.p.) and placed in a stereotaxic frame. One microdialysis cannula (concentric design) was implanted vertically in the right neostriatum (4 mm probe tip). Stereotaxic co-ordinates for the neostriatum, relative to the Bregma, were AP 0.7, L 3.2, DV 5.5 mm [81]. The microdialysis experiments were performed on freely-moving rats about 24 h later.

3.3.2.2 Microdialysis setup

Under non stimulation conditions artificial cerebrospinal fluid (aCSF) comprising 140 mM NaCl, 3 mM KCl, 1.2 mM CaCl$_2$, 1.0 mM MgCl$_2$, 1.2 mM Na$_2$HPO$_4$, 0.27 mM NaH$_2$PO$_4$ and 7.2 mM glucose (pH 7.4) in the presence or absence of various concentrations of TA^{2-} was used as the perfusate. For stimulation the stimulus was dissolved in the same perfusate and perfused through the probe. The dialysis probes were perfused at the flow-rate of 3 µl/min via polyethylene tubing (i.d. 0.38 mm) connected to a 1 ml syringe mounted on a micro-infusion pump (CMA/100, CMA/Microdialysis AB, Stockholm, Sweden). After a 60 min stabilization period, the dialysate samples were collected every 20 min, giving a sample volume of 60 µl. The samples were analyzed by HPLC as described in the experimental part of the *in vitro* section. (3.1.2.3)

3.3.2.3   The kainate protocol

After equilibration at least 3 samples were collected to measure the basal extracellular concentrations of GABA, taurine, glutamate, aspartate and, if TA^{2-} was present, the concentration of OH-TA under resting conditions. This was followed by the local application of 50 mM KCl for one fraction (20 min). After collecting 3 more fractions, the rats were anaesthetised (chloral hydrate 400 mg/kg i.p.) just before an excitotoxic concentration (250 µM to 1 mM) of the non-NMDA glutamate receptor agonist, kainate(KA), was applied to the neostriatum for 20 min (1 fraction) through the dialysis probe. The dialysate samples were then collected every 20 min for the next 3 h. In some experiments, following this, 50 mM KCl was again administered to the neostriatum for one fraction (20 min) and 3 more fractions collected. For the neuroprotection experiments the potential neuroprotector JAKD was given i..p. 10 mg/kg 40 min before KA stimulation and Tauropyrone was given intra peritoneal (i.p.) 0.5 mg/kg 1 h before KA administration, respectively.

3.3.2.4 Measurements of amino acids and OH-TA

The content of GABA, taurine, glutamate and aspartate in the microdialysis perfusates was measured by HPLC with fluorimetric detection using an excitation wavelength of 340 nm and an emission wavelength of 455 nm. As the detailed procedure is described in the literature [82] only a short summary is given here. The amino acids were derivatised with mercaptoethanol and *o*-phthalaldehyde (OPA) using l-cysteic acid as internal standard. The OPA derivatives were then separated on a 5 μm reverse-phase Nucleosil C18 column (250 x 4 mm; Machery-Nagel, Duren, Germany) kept at room temperature, using a mobile phase consisting of methanol and potassium acetate (0.1 M, pH adjusted to 5.48 with glacial acetic acid) at a flow rate of 0.9 ml/min in a 3 linear step gradient (from 25% to 90% methanol). The dialysate samples were either analysed immediately or frozen, after which they could be stored at -20°C for up to 6 months before analysis [82].

OH-TA was analysed either together with the amino acids or by using an isocratic mobile phase containing 25% methanol and 75% buffer. In both cases an excitation wavelength of 315 nm and an emission wavelength of 435 nm were used.

3.3.2.5 Brain histology.

At the end of the microdialysis experiment, the animal was sacrificed by decapitation, the brain removed and the isolated neostriatum fixed in 4% formaldehyde in phosphate buffer solution for 72 h. Following paraffin inclusion, coronal slices (50μm thick) were cut at a cryostat (Leica CM800) and examined by light microscopy (Leits, Dialva 20EB) to verify the correct probe placement. Tunel immunohistochemistry, using the Klenow fragEL[MT] DNA Fragmentation Detection Kit (Inalco, Milano, Italia) was applied to determine apoptotic nuclei. Quantitative image analysis was performed using the public domain software Scion Image (Scion Corporation, USA). Apoptotic, pre-apoptotic and healthy nuclei were expressed as percentage of the total number of nuclei.

3.3.3 Results

In addition to the already mentioned *in vitro* criteria (1)-(3) (see 3.2.2) a reliable *in vivo* standard procedure for hROS detection must stringently fulfil the following criteria *in vivo*: (4) The reagent and the hydroxylation product must be inert in biological systems and not cause any oxidative stress themselves. (5) The chemical trap must respond *in vivo* to a stimulus causing oxidative stress in a dose dependent manner. The *in vivo* behaviour of the terephthalate system was evaluated in terms of these criteria.

3.3.3.1 Analysis of OH-TA together with the OPA-derivatised amino-acids

As the amount of sample obtained in a microdialysis experiment is only a few microliters, it is a key factor to minimize its quantity required for analysis. If possible, the easiest way to achieve that is to combine the measurements of two or more classes of substances to one analysis method. Therefore, a series of experiments was performed to develop a suitable protocol for detecting hROS using the same HPLC and fluorescence detection conditions used for the determination of extracellular amino acid concentrations in microdialysis experiments. In order to test the feasibility of measuring OH-TA together with the OPA-derivatives of the amino acids under the same HPLC
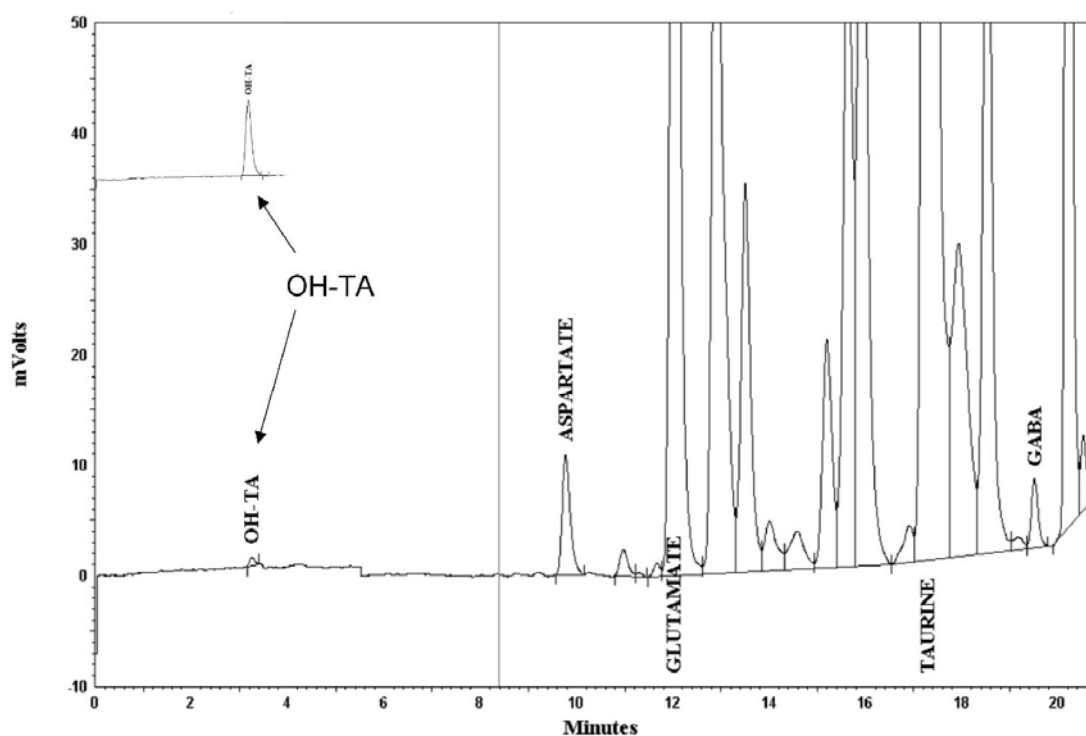
Figure 3.5. *A typical chromatogram showing the peak of OH-TA detected at λ_{ex} = 315 nm and λ_{em} = 435 nm (expanded scale indicated by the upper arrow), followed by OPA-derivatised amino acids detected at λ_{ex} = 340 nm and λ_{em} = 455 nm.*

conditions, a sample of 100 nM OH-TA was put through the system in the presence and absence of the OPA reagent used for pre-column amino-acid derivatization. The internal standard, cysteic acid, was also added. Under the elution conditions used for the amino acid analysis, the area and retention time of the fluorescence peak corresponding to OH-TA were not different from a standard of OH-TA that had not been exposed to OPA. As at the pH of the mobile phase OH-TA bears two negative charges its retention time (approx. 3.2 min) is significantly lower than those of the derivatised amino acids. This allows OH-TA to be determined, at λ_{ex} = 315 nm and λ_{em} = 435 nm), with no interference with the subsequent detection of amino acids (retention times > 5 min), which is achieved by simply switching to λ_{ex} = 340 nm and λ_{em} = 455 nm. A typical chromatogram showing the OH-TA peak, as well as the peaks of the OPA-derivatised amino acids, is shown in Fig. 3.5. Data on the accuracy and precision of the method and parameters of linear regression analysis of standard curves are presented in Tables 3.3

and 3.4. All data are related to the concentration in the microdialysis sample, before the derivatization procedure.

Table 3.3. Precision and Accuracy

	Precision			Accuracy CV (%)	Minimum detectable concentration [nM] (99% CI)
	OH-TA concentration [nM]				
	Nominal	Found	Difference (%)		
Intraday	0.5	0.53	+0.03 (6.0)	7.2	0.535 ± 0.015 (0.481-0589)
	2.5	2.76	+0.26 (5.2)	5.2	
	25	24.2	-0.80 (-3.2)	8.1	
	250	251.2	+1.2 (0.48)	0.8	
Interday	0.5	0.56	+0.06 (12.0)	11.0	
	2.5	2.38	-0.12 (-4.8)	7.4	
	25	24.9	-0.10 (-0.4)	9.3	
	250	247.1	-2.90 (-1.2)	3.1	

Table 3.4. Parameters of linear regression analysis

Concentration range [nM]	Slope * 10^3			r
	N	Mean	Average SD	
0.5-250	7	3.71	0.29	>0.999

3.3.3.2   Microdialysis experiments

3.3.3.2.1   *Effect of TA^{2-} on apoptotic damage.*

To validate conditions (4) and (5) a series of microdialysis experiments were performed, using 3 different concentrations of TA^{2-} in the absence of any stimulation. At the end of each experiment the neostriatal tissue around the probe was processed to evaluate apoptotic damage. A significant degree of apoptosis was observed when a TA^{2-} concentration of 5 mM was used (data not shown). However, no significant apoptosis could be detected when the TA^{2-} concentration was reduced to 1 mM as compared to tissue not exposed to TA^{2-} (Fig. 3.6). TA^{2-} concentrations of 1mM or below were used in all subsequent experiments, with 250 μM being used routinely.
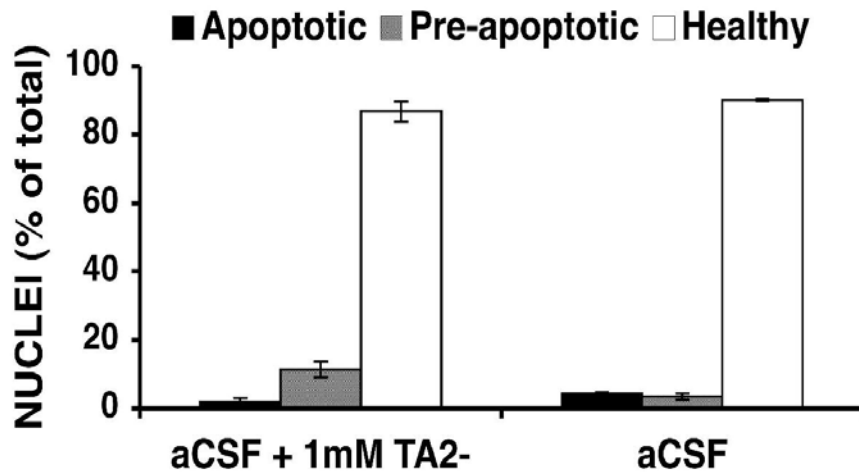
Figure 3.6. Apoptotic signal of neostriatal tissue observed 48 h after microdialysis. *Number of apoptotic (black columns), pre-apoptotic (grey columns) and healthy nuclei (white columns), expressed as percentage of total counts. Column represent mean values ± SEM bars. Results obtained perfusing aCSF + 1 mM TA^{2-} (left columns) as compared with aCSF alone (right columns).*

3.3.3.2.2 Effects of TA^{2-} on extracellular amino acid levels.

The basal and K$^+$- and KA- evoked extracellular levels of the amino acids, aspartate, glutamate, taurine and GABA, were compared in the presence and absence of TA^{2-}. As
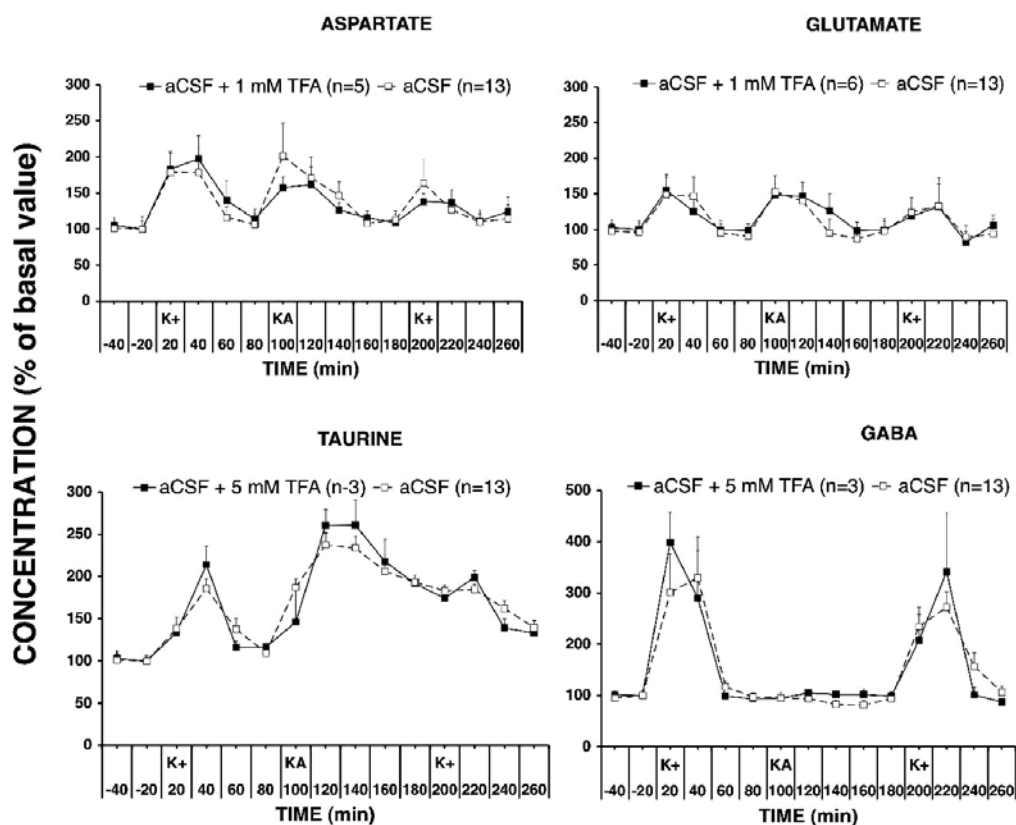
Figure 3.7. Time course of the evoked release of aspartate, glutamate, taurine and GABA in the presence and absence of TA^{2-}. *The extracellular concentrations of aspartate (upper left panel), glutamate (upper right panel), taurine (lower left panel) and GABA (lower right panel), expressed as % of their respective basal values (mean ± SEM), are plotted against time. Each time point corresponds to one 20 min microdialysis fraction. Fractions collected at -40 and -20 min represent basal values. The perfusion fluid was aCSF, either alone (open squares) or with the addition of TA^{2-} (closed squares), 1 mM (aspartate and glutamate) or 5 mM (taurine and GABA). Three stimulations were locally applied, each for 20 min (1 fraction), 50 mM K$^+$ at 20 min and 200 min and 1 mM KA at 100 min. Basal values (mean ± SEM) in the presence and absence of TA^{2-}, respectively, were (nM) 277 ±34 and 258 ± 36 for aspartate, 758 ±71 and 858 ± 142 for glutamate, 1,307 ± 220 and 1460 ±94 for taurine, 23 ±6 and 21 ± 3 for GABA.*

shown in Fig. 3.7, the extracellular concentrations of the four amino acids, basal and evoked by 50 mM K^+ or stimulation with the non-NMDA glutamatergic agonist, KA, were not affected by the presence of TA^{2-} in the aCSF, at concentrations up to 1 mM, for aspartate and glutamate, and up to 5 mM, for taurine and GABA. The time course of OH-TA formation, which reflects the production of hROS, during microdialysis experiments performed with aCSF containing 3 different concentrations of KA, is shown in Fig. 3.9. (right panel). Basal levels of OH-TA could be detected in all animals, their mean value ± s.e.m. was 5.01 + 0.38 nM (n=15). The infusion of 50 mM K^+ induced a short lasting increase in OH-TA concentration. (see Fig. 3.8) However, following the subsequent administration of an excitotoxic concentration of KA, the evoked increase of OH-TA concentration was much higher and long-lasting and appeared to be related to KA concentrations. When the area under the concentration peak (AUC), evoked by the 3 different concentrations of KA, was plotted against KA concentration, a statistically significant linear dependence of OH-TA, and thus of hROS production, on stimulus strength was obtained (Fig 3.9 right panel).
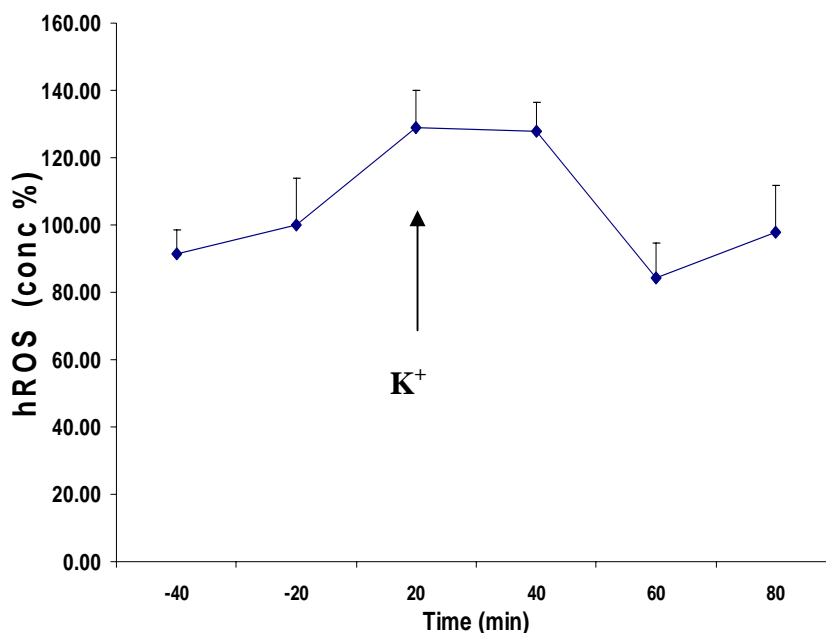
Figure 3.8 OH-TA formation due to K^+ stimulation.

The extracellular concentration of OH-TA, expressed as % of their respective basal values (mean ± SEM), is plotted against time. Each time point corresponds to one 20 min microdialysis fraction. Fractions collected at -40 and -20 min represent basal values. During collection of the subsequent fraction (20 min) K^+ was locally applied.
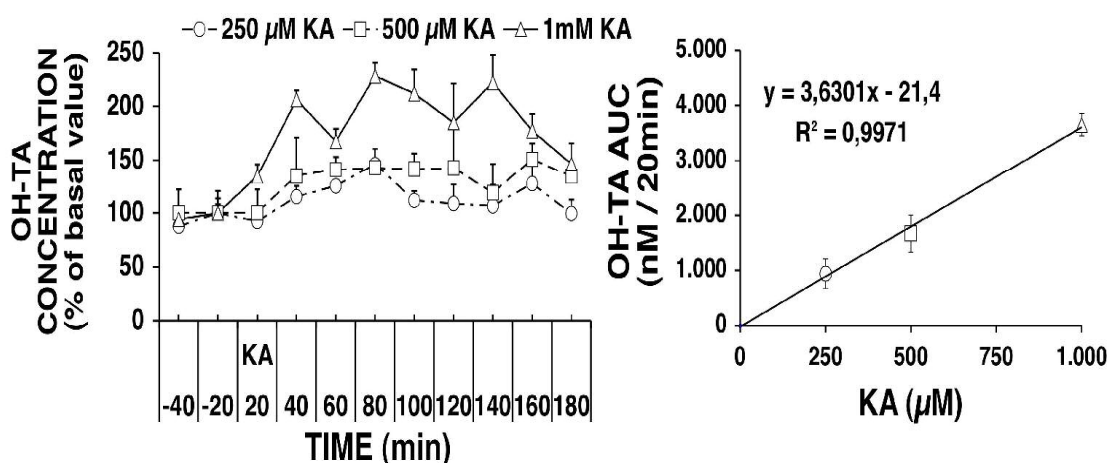
Figure 3.9. Dependence of OH-TA formation on KA concentration.

*Left panel. The extracellular concentration of OH-TA, expressed as % of their respective basal values (mean ± SEM), is plotted against time. Each time point corresponds to one 20 min microdialysis fraction. Fractions collected at -40 and -20 min represent basal values. During collection of the subsequent fraction (20 min) KA was locally applied at three different concentrations: 250 μM (open circles), 500 μM (open squares) and 1 mM (open triangles). **Right panel.** The areas under the KA-stimulated curves shown in the left panel (AUC, from -20 to 260 min), minus their respective area under the basal curve and standardized to one time interval of 20 min, are plotted against KA concentration. Parameters of the linear regression analysis are shown in the inset.*

3.3.3.2.3 *The effect of potential neuroprotectors on the hROS level*

To investigate the possible correlation between hROS formation, apoptotic damage and reduced apoptotic damage caused by the addition of (potential) neuroprotecting substances, JackD and the taurine analog tauropyrone (Fig. 3.10) was given i.p. 60 resp. 40 min prior to KA stimulation.

47
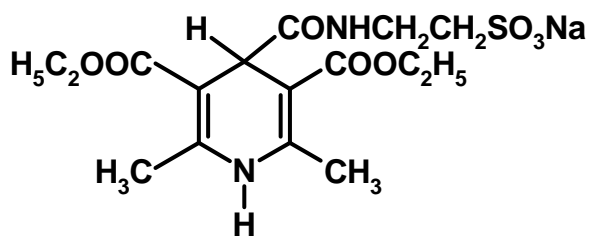
Fig. 3.10 *Structural formula of tauropyrone*

As JackD is still under development and going to be patented no chemical structure can be given here. However, it can be seen (Fig. 3.11 and Tab. 3.5) that both substances caused a significant reduction ($P<0.05$) of hROS formation, whereby tauropyrone was more effective. These findings correlate well with the apoptosis data (Fig. 3.11) which obviously show the same trend as the ones of hROS formation.
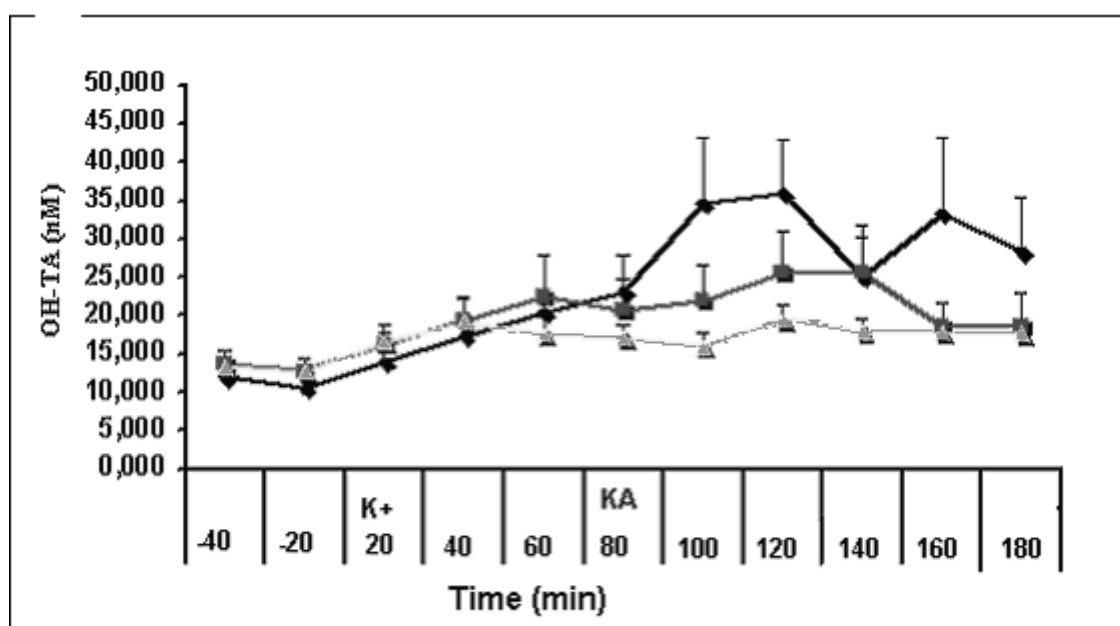
Fig. 3.10 Time course of hROS formation in the presence of neuroprotectors.
OH-*TA formation after stimulation with 1 mM KA was monitored without (upper curve) the addition of neuroprotectors and with JackD (middle curve) or tauropyrone (lower curve) added i.p. 60 resp. 40 min prior to KA stimulation.*

48

Tab. 3.5 AUC values of hROS peaks (taken from Fig. 3.11 from 80-180 min).

	AUC Basal	AUC Stimulated	Difference Stim. – bas.	
KA 1mM (n=4)	10.04 ± 2.09	20.365 ± 2.94	10.31 ± 1.92	
KA 1mM + JackD (n=5)	12.77 ± 1.70	18.604 ± 2.72	5.83 ±1.95	P<0.05
KA 1mM + Taurop. (n=4)	12.62 ± 0.46	16.91 ± 1.48	4.28 ± 1.48	P<0.05
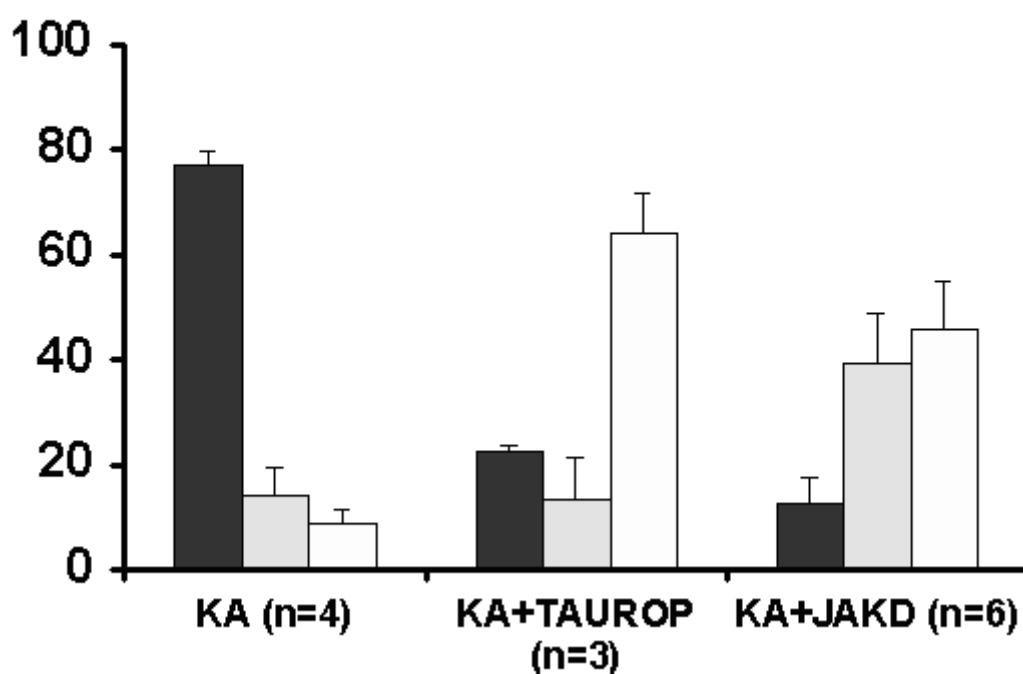
Fig 3.11 Reduction of apoptotic signal due to the addition of neuroprotectors. *Number of apoptotic (black columns), pre-apoptotic (grey columns) and healthy nuclei (white columns), expressed as percentage of total counts. Column represent mean values ± SEM bars. Results obtained stimulating with 1 mM KA (left columns) as compared with 1mM KA stimulation with tauropyrone (middle columns) and 1mM KA with JackD (right columns) added.*

3.3.4   Discussion

Several authors have questioned the, commonly used, salicylic acid hydroxylation procedure for the *in vivo* detection of hROS [35, 37-38)]. One aim of this work was to develop an alternative method, free from the drawbacks of the salicylic acid method, which would allow hROS to be detected simultaneously with the amino acids aspartate (ASP), glutamate (GLU), taurine (TAU) and GABA during brain microdialysis *in vivo*. The present results demonstrate the validity of the terephthalate method for this purpose.

The microdialysis approach allows changes in the extracellular concentration of neuroactive chemicals to be monitored in real time with simultaneous behavioural studies. This can then be followed by '*ex vivo*' assessment of tissue damage. The application of TA^{2-}, which has been reported to be non-toxic, not to be accumulated in the tissues and not to be metabolised [79-80], could further extend the capabilities of this approach. However, it was necessary to verify that two conditions were fulfilled: (1) that both, the reagent and the hydroxylation product were inert in biological systems and did not cause any oxidative stress themselves, and (2) that, the chemical trap responded in a dose-dependent manner to stimuli causing oxidative stress *in vivo*.

To verify the first condition, two parameters were taken into consideration: the degree of tissue apoptotic damage and the extracellular levels of amino acid neurotransmitters. Apoptotic damage is one of the common consequences of toxic insults mediated by oxidative stress. Although, high concentrations (5 mM) of TA^{2-} in the perfusion medium did induce a significant degree of apoptotic damage, as detected 48 h later, no such effects were seen at concentrations of 1 mM and below. The extracellular levels of neurotransmitter amino acids are affected by depolarising agents and many toxins, and were, therefore, used to determine whether TA^{2-} fulfils the important demand of physiological inactivity. The present results show that, during striatal microdialysis, the presence of TA^{2-} neither modifies the basal release, nor it affects the K^{+}- or KA-evoked release of the studied neurotransmitters. The sensitivity of the method is high enough (detection limit 0.5 nM OH-TA in the sample) for the quantitative detection of hROS formation *in vivo*.

Basal levels of extracellular hROS were detected in healthy and freely moving animals. Much higher levels have also been reported with the salicylate procedure (see [83-84] and in the study of Yan *et al.* using terephthalate [38] . Although it is possible that this might, at least in part, result from iron-catalysed hROS formation induced by the stainless-steel probes used in this work [85], no such background level was observed when these probes were used in the *in vitro* experiments. Furthermore, background hROS levels have also been observed with isolated cell preparations (see Mason *et al.*, 2000). The possibility that this hROS arises from cell damage resulting from probe insertion [86] cannot be excluded, but the alternative possibility that the formation and release of hROS under basal conditions is a normal physiological process, warrants further investigation.

The depolarizing K^+ stimulus, which did not cause any detectable tissue damage, caused a slight and sharp increase in extracellular hROS concentration. As KA induces excitotoxic cell damage and symptoms of neurological disorder [87] it was expected that different concentrations of KA applied to the striatum might induce hROS production. This was shown to be the case, with the hROS levels being dependent on KA concentration. The effective suppression of both hROS as well as apoptotic damage by tauropyrone and JackD, shows on one hand the effectivity of the substances and on the other hand demonstrates a direct relationship between hROS formation and the potency of a substance to prevent apoptotic damage providing evidence for a direct involvement of hROS in the cell's suicide program.

All together, these data confirm the value of using the terephthalate system as a reliable and sensitive method to monitor changes in hROS production *in vivo*. Furthermore, the ability to determine evoked amino acids release and hROS, simultaneously, considerably enhances the versatility of this procedure. The method could also be helpful for studying oxidative stress in cell cultures by detecting hROS release in real time without an HPLC separation. In conclusion, this experimental protocol provides a method to monitor damage induced by KA or other neurotoxins *in vivo*, not only in terms of release of the excitatory (aspartate and glutamate) and inhibitory (taurine and GABA) amino acids and of the degree of apoptotic damage, but also in terms of hROS release in the extracellular fluid.

Part IV

4   Mechanistic aspects of the Fenton reaction under conditions approximated to the extracellular fluid

4.1   Introduction

As already mentioned in Part I the question upon the nature of the reactive intermediate in Fenton (like) systems plays a crucial role in the discussion of a possible non pathological role of hROS chemistry and is therefore not only of academical interest. It has already been shown [88] that the hydroxylation of TA^{2-} is not selective for OH•, because in a H_2O_2 –free ferrous aqueous solution (Fe(II) auto-oxidation) the yield of hydroxylation strongly depends on the nature and concentration of the buffer. This indicates a different redox active intermediate than OH•, as a free OH radical demands no or only a minor influence of the nature and the concentration of the buffer on the hydroxylation yield. The results are well in agreement with the assumption of a bound radical or a Fe(IV) species, because in this case a significant dependence of the hydroxylation yield on Fe(II) coordination is expected. ESR-measurements confirmed these considerations, as a "translation" of the oxidation-signal by ethanol was required to monitor it, which contradicts the assumption of a free OH radical as this directly would oxidize the spin trap. Although other authors question the unambiguousness of such ESR results [14,30 ,89], taking all these arguments together the oxidation via a free radical seems to be very unlikely in this case. As it is known that during Fe(II) auto-oxidation also H_2O_2 is formed and therefore Fenton chemistry occurs also in this system, this observation could also be important for regular Fenton systems under similar conditions. However, there are no results in the literature discussing these points for a regular Fenton system under conditions close to ECF. This issue will be addressed in this part, and several lines of evidence will be presented showing that a free OH

radical is not the reactive intermediate also in a regular Fenton system under conditions close to ECF.

4.2 Experimental

4.2.1 Chemicals

All chemicals used were of analytical grade, obtained from Sigma-Aldrich (Vienna, Austria), and were used without further purification. For all experiments described here, deionised H_2O was used.

4.2.2 Preparation of solutions and Stopped Flow experiments

Details on preparation of the Fenton reagent for HPLC measurements using non chelated Fe(II) are described in 3.2.1.2. When Fe(II)EDTA was used Fe(II) and Na_2EDTA solutions were prepared separately, de-oxygenated with argon, and then mixed. Only this procedure could avoid quick oxidation to the deep yellow Fe(III)EDTA complex. For the stopped flow experiments Fe(II) and H_2O_2 stock solutions were prepared with H_2O as described above and in 3.2.1.2. To avoid oxidation the stock solutions were kept at -20 °C and saturated with argon before freezing. For conducting the experiments aliquots were taken as soon as enough amount of sample was defrosted. The stock solutions were diluted with argon saturated buffer solution or H_2O and an aqueous TA^{2-} solution containing 250μM to 1mM TA^{2-} to the desired concentration[*]. After measuring the pH the Fe(II) and H_2O_2 solutions were injected into the stopped flow machine and the formation of OH-TA was monitored by fluorescence detection. For the quenching experiments a solution containing 200μM Fe(III) or Fe(II) was prepared in water or in the desired buffer with and without the addition of an equimolar amount of EDTA. The solution was injected together with 1 μM OH-TA dissolved in the same solvent. Both solutions contained no, 250μM or 1 mM TA^{2-}. To

---

[*] All concentrations mentioned here refer to the detected final concentrations in the reaction chamber of the stopped flow apparatus

guarantee a good signal to noise ratio maximum excitation light intensity was used by opening the monochromator slits to 9 mm. Fluorescence time curves were background corrected by subtracting the constant emission of de-ionized water or the corresponding buffer and were analyzed using the internal software of the instrument.

4.2.3 Instrumental

All absorption spectra and kinetic data were collected on an Applied Photophysics SX.18V-R (Leatherhead, UK), apparatus. Absorption spectra were measured using diode array detection, whereas fluorescence was measured using the sensitive fluorescence option of the machine, which allows a definite excitation but counts all emitted photons above the wavelength of a cut-off filter. For the experiments with TA^{2-} a 380 nm cut off filter was chosen leading to an emission photon-count range from 380 to 800 nm. The temperature was kept at 25 ±0.2 °C using a Lauda RM6 (Lauda-Königshofen, D) thermostat. HPLC experiments were carried out using a HP-1090 HPLC system (Agilent Technology, Vienna) with built in diode array and external fluorescence (HP-1046A) detection. The details of HPLC instrumentation in Florence, which was used for the data presented in Fig. 4.7, were already described in Part III in the *in vitro* section (3.2.1.3).

4.3 Results

4.3.1 Stopped flow experiments

To check the sensitivity and the linearity of the fluorescence detector and stability of OH-TA during excitation with maximum light intensity several concentrations of OH-TA were injected into the machine and the fluorescence was monitored for 1000s. It can be seen in Fig. 4.1 that linearity was achieved over a wide concentration range, (the intercept reflects the stray light in water), whereby the detection limit was in the low nano-molar range. As additionally the fluorescence did not change during the maximum detection time of 1000s (data not shown), it can be concluded that detection of a certain fluorescence can be unequivocally related to a definite OH-TA concentration.
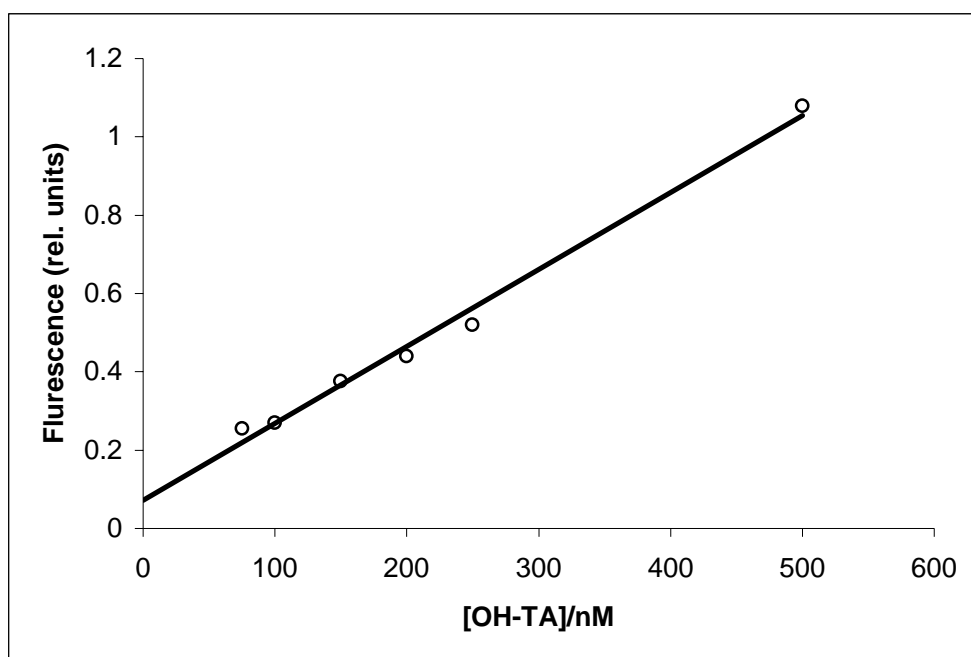
Figure 4.1. *Rel. fluorescence of different concentrations of OH-TA in aCSF. Linear regression analysis gave a slope (k) of 1.9 *10^{-3}, an intercept (d) of 7.22*10^{-2} and an R value of 0.994*

To test the possibility of an artefactual quenching of the fluorescence due to Fe(III) formation during the Fenton reaction, OH-TA was injected under several conditions together with Fe(III) solutions. As it can be seen in Fig. 4.2 (solid line) a significant quenching could indeed be observed when solely OH-TA and Fe(III) were present in H_2O. However, already the addition of 250 µM TA^{2-} causes an almost complete disappearing of quenching (dashed line) as did the chelation of Fe(III) with EDTA (data not shown). Moreover, neither in aCSF nor in 10mM KAC buffer any quenching could be observed (data not shown). As additionally to Fe(III) also Fe(II) is known as potential quencher the described experiments were also conducted with Fe (II). However, no quenching could be observed in any experiment. Therefore it can be concluded that no artefactual influence of Fe(III) or Fe(II) during hROS monitoring can be expected, in the case of Fe(III) because experiments are normally performed in buffer solutions and TA^{2-} is present in all experiments in large excess.
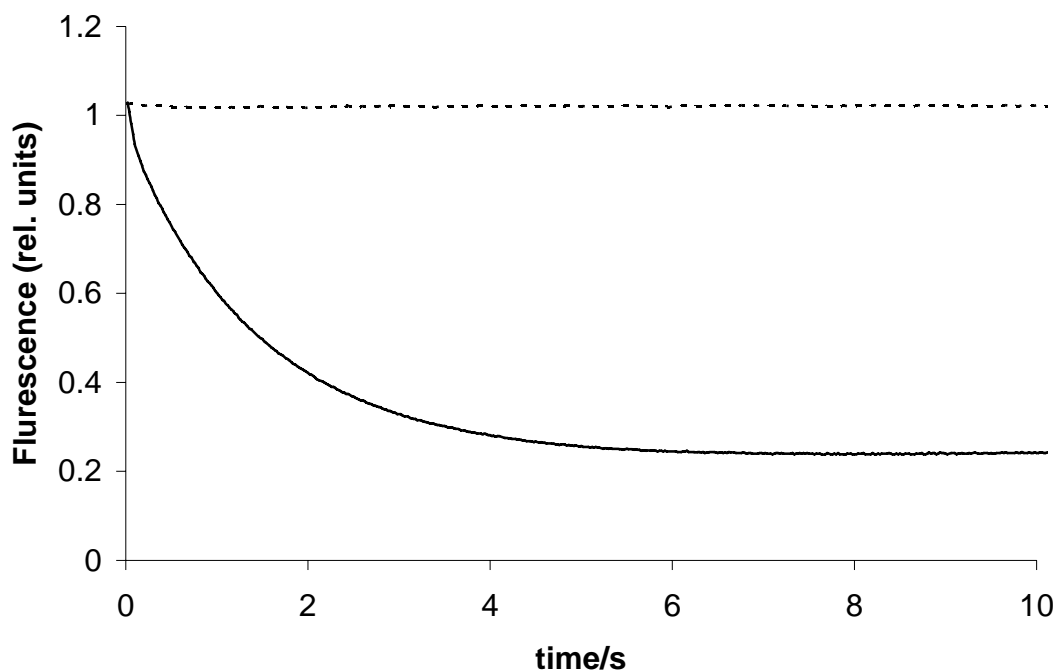
Figure 4.2. *Time plot of the rel. fluorescence of 100 nM OH-TA after reaction with 100 μM Fe(III)$_2$(SO$_4$)$_3$. The reaction was carried out in H$_2$O without (solid line) and with (dashed line) the addition of 250 μM TA^{2-}.*

After clarifying the question of possible fluorescence artefacts, a series of stopped flow experiments were performed monitoring the Fenton reaction under various conditions. As for these investigations a regeneration of Fe(II) via the reduction of formed Fe(III) with H$_2$O$_2$ should be avoided and pseudo first order conditions should be obtained, Fe(II) was used in markedly (at least 4:1)excess. A typical example of a kinetical (solid line) plot together with a simple first order fit (dashed line) is presented in Fig. 4.3. As described earlier the Fenton reaction under these conditions must result in a first order rate law, therefore the difference in the last bit of Fig. 4.3 between the plotted and the fitted curve must be explained by a parallel reaction, which obviously is the auto-oxidation of Fe(II). It should be stressed here, that saturating the solution with argon did not prevent the reaction and its rate rose significantly with the number of injections during the same experiment indicating a strong dependence of the reaction rate on oxygen leaking into the system, which is expected for the auto-oxidation of Fe(II). As the Fenton reaction was sufficiently fast in comparison to Fe(II) auto-oxidation both curves could be analyzed separately. However, a double exponential function always

56

perfectly fits the whole experimental curve which indicates two parallel (pseudo) first order reactions thus confirming the above given arguments.
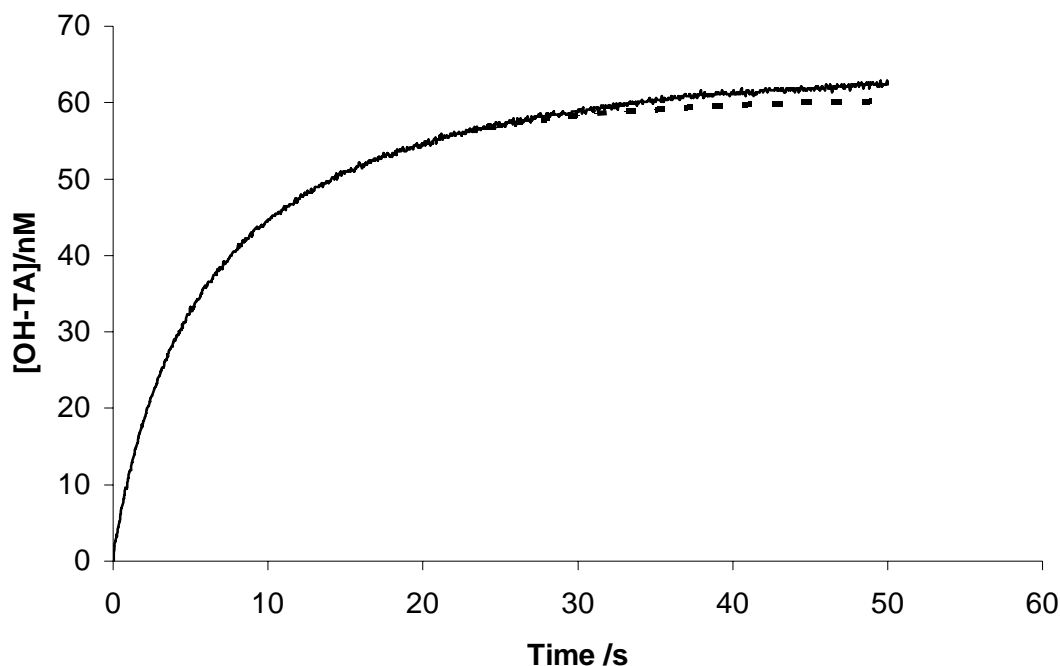
Figure 4.3. *OH-TA formation in a Fenton system (50μM (NH$_4$)$_2$Fe(II)(SO$_4$)$_2$ with 250 μM TA^{2-} in aCSF. The dashed line indicates the first order fit of the curve.*

Tab. 4.1 shows the second order rate constants ± SEM of the Fenton reaction under the investigated conditions. When iron was chelated with EDTA no significant difference between the reaction rates in aCSF and KAC buffer could be observed. The measured rate constants of 14,516 and 12,084 are somewhat 10 times higher than with unchelated iron which is in excellent agreement with the literature [90]. On the contrary to that, reducing the KAC buffer concentration from 100mM to 33mM led to a 3 fold increase of the rate constant, indicating a gradual ligand exchange from KAC to either H$_2$O or TA^{2-}. Furthermore, the rates in aCSF and H$_2$O were practical identical, whereas a change from KAC to aCSF caused an approx. 5 fold increase of the rate. This demonstrates on one hand the independence of the rate determining step upon a ligand exchange from H$_2$O to Cl$^-$, and on the other hand its dependence on the pH and/or on the stoichiometry of KAC to H$_2$O at the iron centre. Finally, under all conditions tested the reaction rate was not sensitive to the TA^{2-} concentration. As shown in Fig. 4.4 plotting k^{obs} against Fe(II) concentration resulted in a straight line through the origin, illustrating the expected first order dependence on Fe(II).

57

Table 4.1. Rates of OH-TA Formation

Conditions	Solvent/ buffer	Number of experiments	[Fe]/µM	k*M^{-1}*s^{-1}
pH=5.48 [H$_2$O$_2$]=15 µM [TA^{2-}] = 250µm	KAC 100mM	4	50	99.9 ±2.75
pH=5.48 [H$_2$O$_2$]=15 µM [TA^{2-}] = 250µm	KAC 100 mM	3	50	102.3±1.58
pH=5.48 [H$_2$O$_2$]=160 µM [TA^{2-}]= 3.33mM	KAC 33.33 mM	7	800, 1200, 2500, 3200	332.2±11.37
pH=7.38 [H$_2$O$_2$]=15 µM [TA^{2-}] = 250µM	aCSF	8	50	1,554.5±209.49
pH=7.42 H$_2$O$_2$=160 µM [TA]=3.33mM	aCSF	7	800, 1200, 2500, 3200	1,548.7±110.25
pH=6.43 [H$_2$O$_2$]=15 µM [TA^{2-}] = 250µM	H$_2$O	4	50	1,529.0±82.69
pH=7.00 H$_2$O$_2$=160 µM [TA]=3.33mM	HEPES 100mM	7	800, 1200, 2500, 3200	4,158.6±555.16
pH=5.48 [H$_2$O$_2$]=160 µM [TA^{2-}]= 3.33mM [EDTA]= 1.1*[Fe(II)]	aCSF	3	400, 800, 2000	14,516.6± 1169.16
pH=5.48 [H$_2$O$_2$]=160 µM [TA^{2-}]= 3.33mM [EDTA]= 1.1*[Fe(II)]	KAC 33.33 mM	3	1200, 1600	12,084.4±633.35
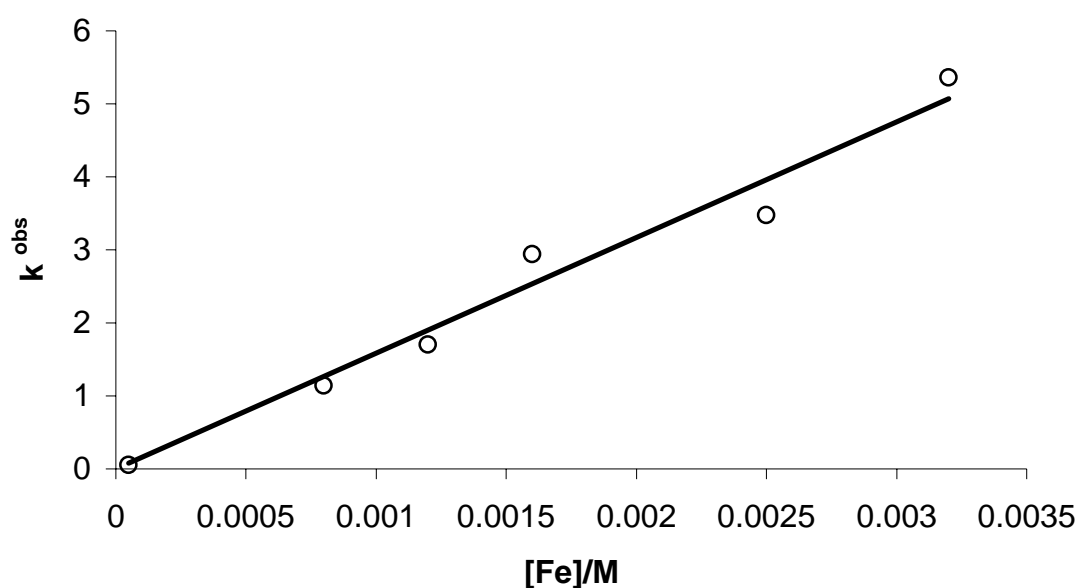
Figure 4.4: *The observed rate (k^{obs}) of the Fenton reaction in aCSF ([H_2O_2]=160 μM, lowest point: 15μM) plotted against different iron concentrations. Linear regression analysisyielded: k=1584; R=0.984.*

To investigate the possible formation of a Fe(II)TA complex, TA^{2-} dissolved in aCSF was injected with a 10 fold higher concentrated Fe(II) solution, and the resulting spectrum was compared with the spectrum of the pure ligand. It can be seen in Fig. 4.5 that these two were entirely different indicated by the appearance of well pronounced shoulder around 300 nm, which strongly suggests the assumption of a Fe(II)TA complex formation. However, even in the single wavelength mode a direct monitoring of the reaction was not possible, most probably due to a faster reaction time than the instrument can resolve (~ 2ms).
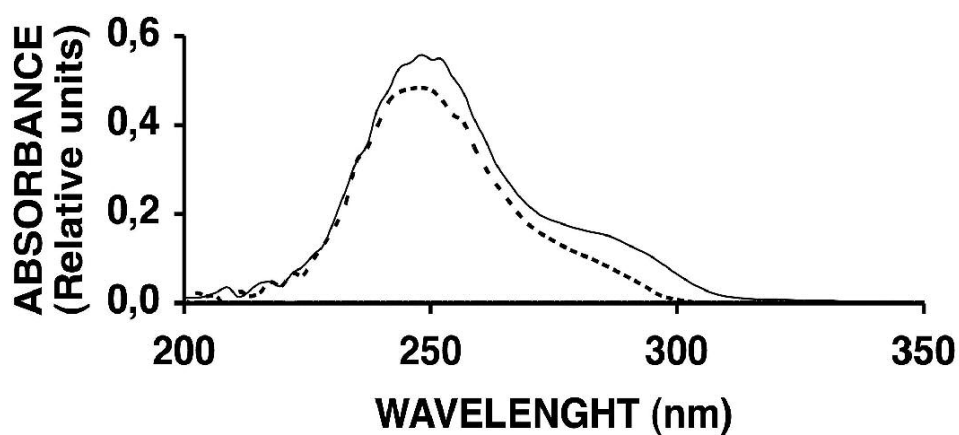
Figure 4.5. Absorbance spectra of TA2- and Fe-TA. *Absorbance spectrum of the Fe-TA complex, obtained in aCSF containing 0.5 mM TA^{2-} and 5 mM Fe(II) (——);* *Absorbance spectrum of TA^{2-}, obtained in aCSF containing 0.5 mM TA^{2-} (··············).* *Solutions were at pH=7.2, degassed and saturated with argon.*

4.3.2 HPLC analysis

To get an overview of the Fenton activity in various chemical environments, and data that can be compared with results in literature obtained by using different chemical traps, the Fenton reaction was carried out under the conditions presented in Tab.4.2, whereby the amount of formed OH-TA was analyzed by HPLC.

Table 4.2 Amount of OH-TA formed in various Fenton systems

Conditions	Solvent	[OH-TA]/nM
[Fe]=50µM [H$_2$O$_2$]=16 µM; TA=250 µM pH=5.48	100 mM KAC	87.24
[Fe]=50µM [H$_2$O$_2$]=16 µM; TA=250 µM pH=7.42	aCSF	76.79
[Fe]=50µM [H$_2$O$_2$]=16 µM; ; TA=250 µM pH=6.32	H$_2$O	15.86
[Fe]=50µM; [EDTA]=55µM [H$_2$O$_2$]=16 µM; TA=250 µM pH=5.48	100 mM KAC	172.52
[Fe]=50µM; [EDTA]=55µM [H$_2$O$_2$]=16 µM; TA=250 µM pH=7.42	aCSF	584.46
[Fe]=50µM; [EDTA]=55µM [H$_2$O$_2$]=16 µM; TA=250 µM pH=6.32	H$_2$O	247.33

It can be seen that the amount of OH-TA, which represents the Fenton activity, depends on both the solvent and the coordination sphere of Fe(II). Interestingly, as shown in Fig. 4.6 the Fenton activity increased when the buffer concentration was raised, whereas the data points suggest a saturation dependence on KAC, which would be expected if the stoichiometry of KAC to H$_2$O on the iron centre is the reason for this behaviour. However, it should be pointed out that the Fenton activity showed an inverse behaviour to the rate (see 4.3.1 for details).
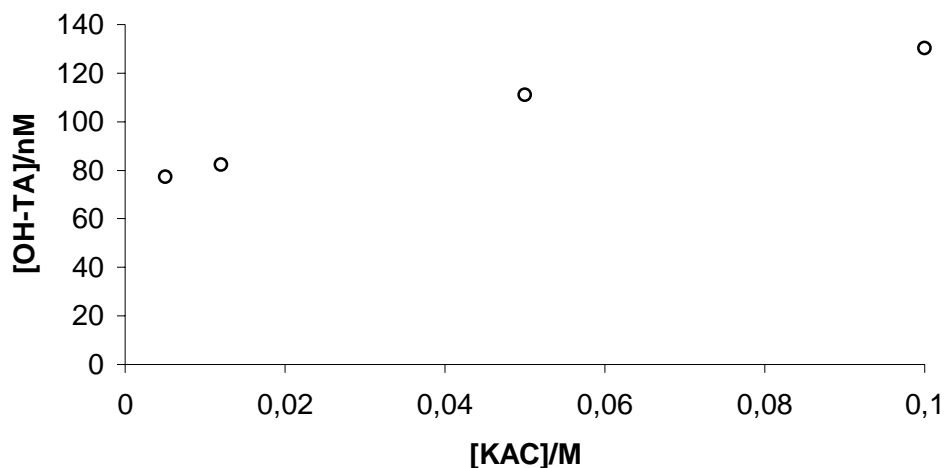
Figure 4.6 *The amount of OH-TA formed as a function of KAC concentration. Conditions of the Fenton reaction: $[Fe^{2+}]=50\mu M$; $H_2O_2=16 \mu M$; $TA=250\mu M$*

To minimize biological side affects in *in vivo* experiments it was aimed to find the minimum concentration of TA^{2-} which still leads to a linear response on the amount of formed hROS in a Fenton system. Interestingly, when aCSF was used as the reaction medium with 250 μM TA^{2-}, the quantity of OH-TA formed was not affected by further increases in the concentration of TA^{2-} (Fig. 4.7 upper panel) The same results were found, when the reaction was carried out in H_2O. However, following replacement of aCSF by 100 mM KAC buffer, pH 5.48, the concentration of OH-TA formed was influenced by the amount of TA^{2-} present (Fig. 4.7 bottom panel). The amounts of OH-TA produced in the presence of 500 and 1000 μM TA^{2-}, were found to be 180 and 300 %, respectively, of that formed using 250 μM TA^{2-}. Similar dependencies on the increase of TA^{2-} could be found when Fe(II) was chelated with EDTA. In this case the ratio of OH-TA concentrations obtained in experiments done with 250 μM TA^{2-} to those performed in the presence of 1mM TA^{2-} was found to be 1:2.25 in KAC buffer, 1:1.39 in aCSF and 1:1.78 in H_2O.
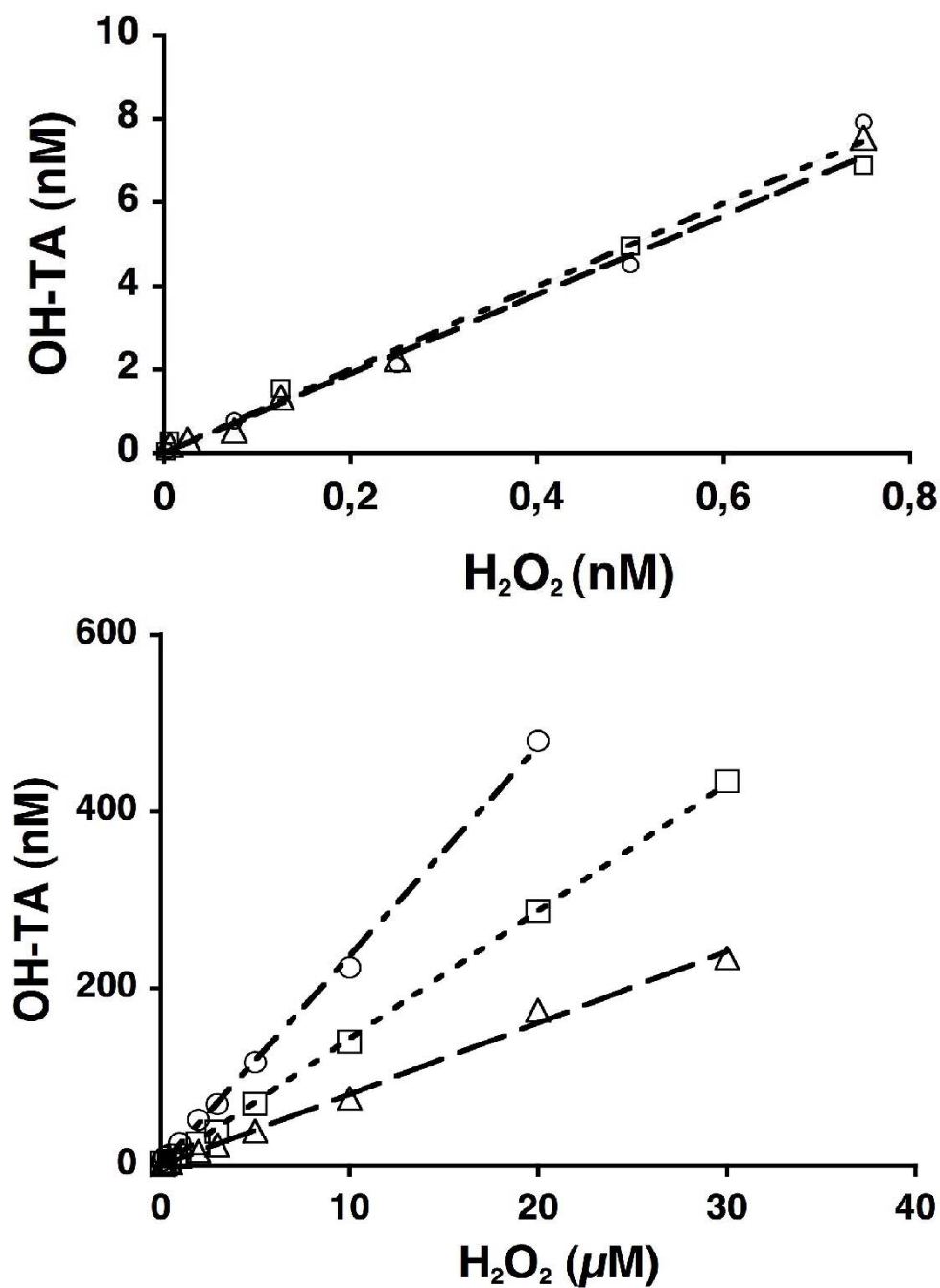
Figure 4.7 Dependence of OH-TA concentration on the amount of hROS. *Concentration of OH-TA formed as a function of H_2O_2, at 3 different concentrations of TA^{2-}. Linear regression analysis was performed after subtraction of the blank value. The Fe(II) concentration was 30 μM.*

Upper panel - Reactions were carried out in aCSF (pH 7.31). △ *250 M TA²⁻ (r = 0. 998; slope = 9.95; n = 2);* □ *500 μM TA²⁻ (r = 0.996; slope = 9.46; n = 2);* ○ *1mM TA²⁻ (r = 0.993; slope = 9.95; n = 2).* ***Bottom panel -*** *Reactions were carried out in 100.0 mM potassium acetate buffer (pH 5.48).* △ *250 μM TA²⁻ (r = 0.997; slope = 8.06; n = 2);* □ *500 M TA²⁻ (r= 0.999; slope =14.35; n = 2);* ○ *1 mM TA²⁻ (r = 0.999; slope = 23.67; n = 2).*

4.4   Discussion

As one of the targets of the stopped flow experiments was to test the validity of the TA^{2-} method the results obtained were compared to similar Fenton systems using different chemical traps. According to Isao Yamazaki and Lawrence H. Piette [90] the variability of the Fenton activity can be explained by assuming four reaction pathways for the Fenton reaction, whereby not all of them lead to hROS formation. For all pathways the rate determining step is the formation of the transient complex depicted in the middle (see Scheme 4.1). Reaction (I) in scheme 4.1 represents the classical Fenton pathway generating a free hydroxyl radical, whereas reaction (II) displays an alternative path via a ferryl species. As already mentioned earlier both pathways will lead to a reactive intermediate with a similar oxidation potential, and therefore monitoring hROS formation via aromatic hydroxylation will give the sum of hROS formed via these reaction paths. A key factor in understanding the variance of Fenton activity is pathway (III), as it does not lead to hROS formation, but represents a simple two electron oxidation of two moles of Fe(II). Pathways (IVa) and (IVb) are only of importance, if Fe(III) concentration reaches a comparable level to Fe(II). As in our experiments it was worked with a marked access of Fe(II) it is not evident that these paths played a significant role. It was demonstrated [90] that pathway (III) gains importance when Fe(II) is used in excess compared to H_2O_2 resulting in a lower overall Fenton activity. This effect can be overcome by iron chelation e.g. with EDTA and /or by changing the pH.

Fe (II) ---- O(H)—O--H $\longrightarrow$ Fe (III) + OH$^-$ + OH$^•$ (I)

Fe (II) ---- O(H)—O--H $\longrightarrow$ Fe(IV)=O + H$_2$O (II)

Fe (II) + H$_2$O$_2$

Fe(II)

Fe(III)

Fe (II) ⋯ O(H) ⋯ Fe(II) with O--H $\longrightarrow$ 2 Fe(III) + 2 OH$^-$ (III)

Fe (II) ⋯ O(H) ⋯ Fe(III) with O--- H $\nearrow$ 2 Fe(III) + OH$^-$ + OH$^•$ (IVa)
$\searrow$ Fe(IV)=O + Fe(III) + H$_2$O (IVb)
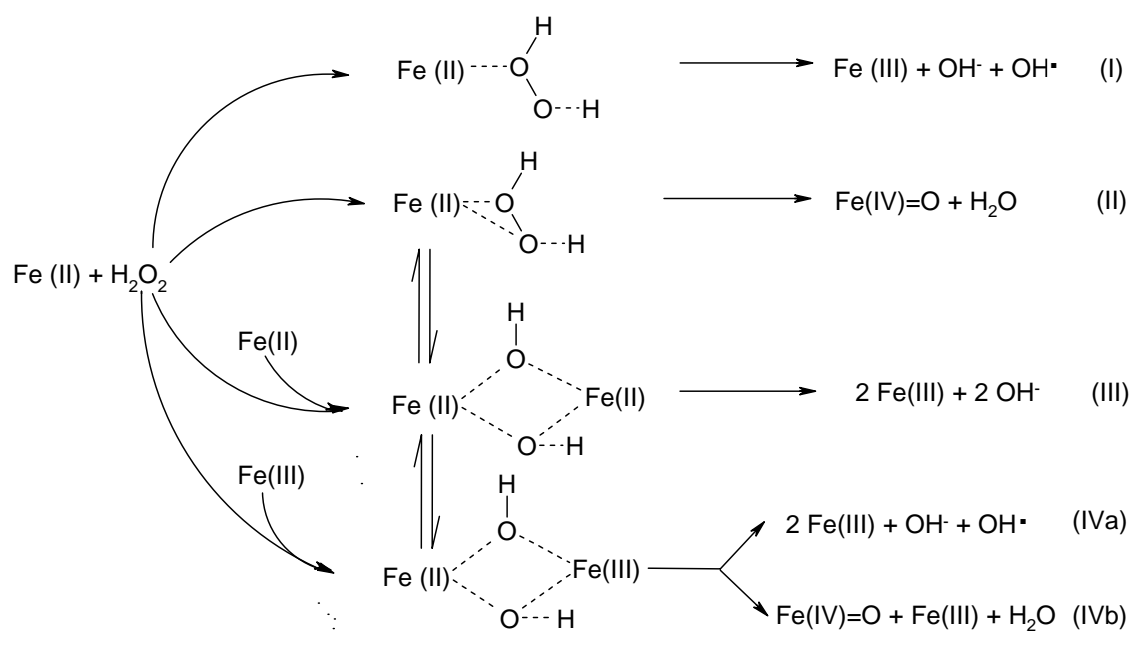
Scheme 4.1 *Possible pathways of the Fenton reaction*

There has been done exhaustive work on the change of the Fenton activity upon iron complexation. On the first sight it seems obvious that iron chelation should minimize the Fenton activity as the ligand shields the reactive centre. Based on this assumption it seemed to be likely to reduce oxidative stress *in vivo* by iron chelation. However, among others it was reported by John M. C. Gutterrid [91] that Fe(II)EDTA posses a higher Fenton activity than uncomplexed Fe(II), thus demonstrating that chelation can also enhance oxidative damage. The most likely explanation for that is a hindrance of Fe(II)$_2$H$_2$O$_2$ complex formation due to EDTA chelation, which diminishes the probability of pathway (III). The experimental findings of several authors could be replicated here in a quantitative manner [60, 90, 92], whereby the effect on the Fenton activity by EDTA chelation increases from KAC to H$_2$O to reach its maximum in aCSF. As in the concerned pH area the Fenton activity of Fe(II)EDTA is not sensitive to pH [41,89] it is likely that the reason for this observation are different complex species. It is assumed that in H$_2$O EDTA reacts as a hexadentate to form a Fe(II)EDTA complex [76], whereas in aCSF and KAC, when the salts are present in marked excess, it acts as a pentadentate leading to a Fe(II)EDTA-Cl$^-$ and Fe(II)EDTA-Ac$^-$ complex, respectively. Due to the high excess of KAC in the investigated concentration range it is evident that the rate is independent of the amount of KAC.

As already mentioned in the introduction, it was found by Saran et al. [88] that also Fe(II) auto-oxidation caused aromatic hydroxylation, whereby it was shown that the reactive intermediate was definitely not a free hydroxyl radical. One convincing argument used by the authors was the increasing of the hydroxylation yield upon an increase of the buffer concentration. As the same behaviour was also observed here in KAC buffer, using the same argument suggests a reactive intermediate different from a free hydroxyl radical. It is likely that the octahedral coordination sphere of Fe(II) is occupied partly by Ac$^-$ and partly by H_2O, whereby the exact stoichiometry depends on KAC buffer concentration. If one supposes that Ac$^-$ coordination increases the redox potential of the transient complex, the data can be well explained by the assumption of a crypto radical or a Fe (IV)-oxo species as the reactive intermediate. By contrast to that, the assumption of a free hydroxyl radical would demand a *decrease* of Fenton activity with an increase of the buffer concentration, because the probability of OH• to collide with TA^{2-} is decreasing with altering the amount of KAC. However, an alternative explanation would be a lower probability of pathway (III) in scheme 4.2 with increasing the amount of KAC, as it is possible that the formation of the Fe(II)$_2$H$_2$O$_2$ transient complex is hindered by KAC coordination. In this case the formation of a free hydroxyl radical cannot be excluded, nevertheless additional arguments, confirming the assumption of a different reactive intermediate than OH•, will be given below.

Just as the arguments stated above, the observation that the concentration of OH-TA detected is independent of the concentration of TA^{2-} (range 0.25 - 1 mM), in the experiments performed in aCSF, contradicts the assumption of a free hydroxyl radical, as it is consistent with a mechanism involving complex formation between Fe(II) and TA^{2-}, followed by an intra-molecular electron transfer accompanied by an intra-molecular hydroxylation. As long as TA^{2-} is used in sufficient excess, the yield of OH-TA depends only on the Fe(II) and H_2O_2 concentrations. The complex formation could be followed by spectrophotometry measuring the appearance of an absorption band (visible as a clearly pronounced shoulder) at 284 nm (Fig. 4.5). Furthermore, the formation of such a complex, involving TA^{2-} and both Fe(II) and Fe(III), has been also reported by others [93] under similar experimental conditions.

On the contrary, the experiments performed in acetate buffer, where acetate was present in marked excess (100 to 400 fold related to TA^{2-}), showed a significant dependence of the concentration of OH-TA on that of TA^{2-}. This is likely to be explained by complex

formation between acetate and the Fe(II) ions present in the medium, since also the rate inversely depends on KAC concentration. As acetate binds with a higher affinity to Fe(II) than H_2O a hindrance of transient complex formation by acetate and therefore a lower rate is expected when raising the stoichiometry of acetate at the iron centre. Since aliphatic carboxylic acids have lower complex stability constants (pK ~ 3) than their aromatic analogues (pK ~ 5) [94], addition of TA^{2-} at the concentrations used in the present work would result in a continuous replacement of acetate by TA^{2-} in the iron complex. Assuming that only an intra-molecular mechanism can generate OH-TA, leads to the condition that the found dependency of OH-TA on TA^{2-} is solely correlated to the concentration of the FeTA, complex, which means mathematically that it can be expressed as a linear function of FeTA concentration with a slope of one with an intercept at the origin.

This assumption can surprisingly well be demonstrated by simply assuming two competitive reactions (I) and (II).

$$Fe(II) + Ac^- \rightleftharpoons FeAc^+ \qquad K_1 = \frac{[FeAc+]}{[Fe]\,[Ac^-]} \qquad (I)$$

$$Fe(II) + TA^{2-} \rightleftharpoons FeTA \qquad K_2 = \frac{[FeTA]}{[Fe]\,[TA^{2-}]} \qquad (II)$$

When $FeAc^+$ is named y and FeTA x, equations (I) and (II) can be written as

$$y = K_1 \cdot ([Fe]_0 - y) \cdot ([Ac^-]_0 - y) \qquad (Ia)$$

$$x = K_2 \cdot ([Fe]_0 - x) \cdot ([TA^{2-}]_0 - x) \qquad (IIa)$$

The assumption that all Fe(II) is complexed leads to the boundary condition:

$$x + y = [Fe]_0 \qquad (III)$$

For hydroxylation only Fe(II)TA is important, therefore equations Ia and IIa are resolved with side condition (III) to one equation in x, which leads via rearrangement to equation (IV).

$$x^2 - \frac{x}{K_2 - K_1} \cdot \left(K_2 \cdot [Fe]_0 - K_1 \cdot [Fe]_0 + K_2 \cdot [TA^{2-}]_0 + K_1 \cdot [Ac^-]_0 - 1\right) - \frac{K_2 \cdot [Fe]_0 \cdot [TA^{2-}]_0}{K_2 - K_1} = 0 \qquad (IV)$$

with
$$-\frac{p}{2} = \frac{\left(K_2 \cdot [Fe]_0 - K_1 \cdot [Fe]_0 + K_2 \cdot [TA^{2-}]_0 + K_1 \cdot [Ac^-]_0 - 1\right)}{2 \cdot (K_2 - K_1)}$$

and
$$-q = \frac{K_2 \cdot [Fe]_0 \cdot [TA^{2-}]_0}{K_2 - K_1}$$

the equation can be solved with the p, q formula
$$x_{1,2} = -\frac{p}{2} \pm \sqrt{\frac{p^2}{4} - q}$$

When no iron is present ($[Fe]_0 = 0$) obviously no FeTA complex is formed and therefore x must be 0. It can be easily seen that this is only the case if the square root term is subtracted from -p/2, thus leaving only one chemical meaningful solution of the equation. By setting $[Ac]_0$ to the experimental concentration of 0.1 M the ratio of K_2/K_1 could be fitted with the experimental data. The resulting ratio of 50 (leading to a ΔpK of 1.70) is in good agreement with values found for similar systems [94]. The circles in Fig. 4.8 show the theoretical curve obtained when x is expressed in percentages of $[Fe]_0$ and plotted against different concentrations of TA^{2-}. The squares represent the experimental product ratios (1.0: 1.8: 3.0, using 250, 500 and 1000 μm TA^{2-}, respectively) multiplied with the relative FeTA concentration at 250 μM TA^{2-}. Plotting the experimental values against the theoretical ones (Fig. 4.8 inset) lead to a straight line through the origin with a slope of 1.01 and $R^2 > 0.9999$, demonstrating that the experimental data give an excellent agreement with the theory.
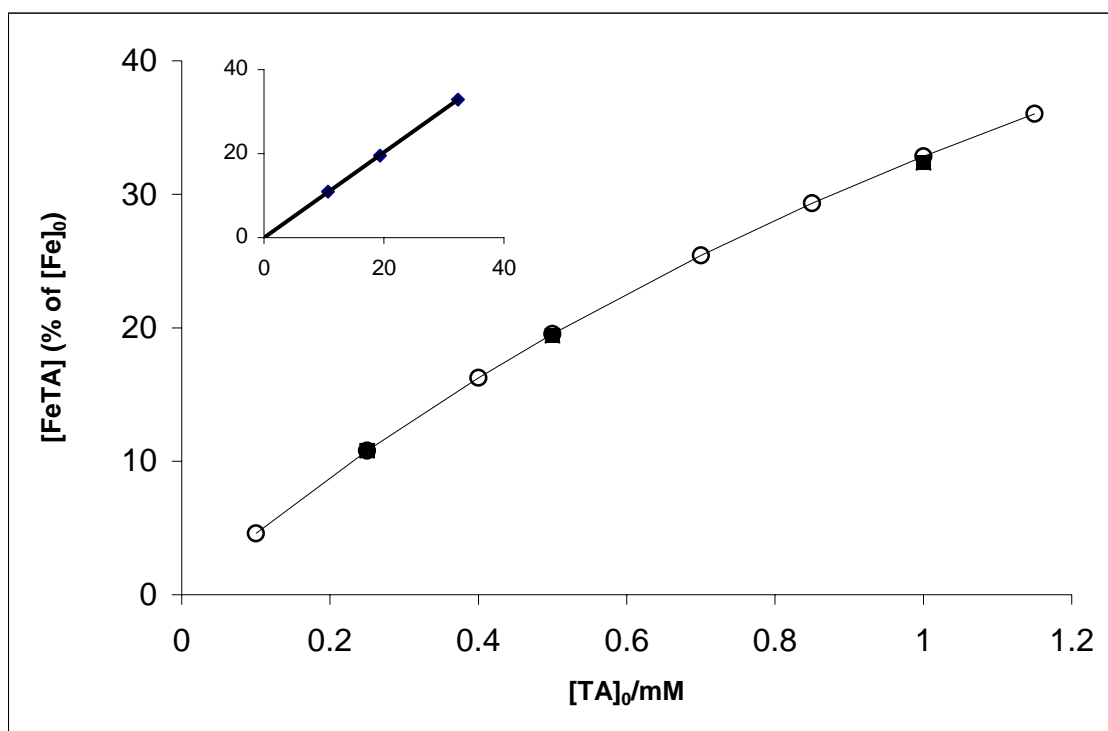
Figure 4.8. *Theoretical (circles) concentrations of FeTA and experimentally found (squares) vales of OH-TA normalized to $[TA]_0=250\mu M$. The inset shows the experimental values plotted against the theoretical one. Linear regression gave $k=1.01$ and $R>0.9999$.*

Thus, the formation of a Fe(II)TA complex, followed by an intra-molecular hydroxylation and electron transfer, provides a reasonable mechanism explaining the data (see scheme 4.2) of TA^{2-} hydroxylation in aCSF as well as in KAC. Intermediate (II) can be interpreted either as a "crypto" radical or as a Fe(IV) species, as discussed in the introduction [13-15]. Further support for the existence of a Fe(IV) oxo species rather than a free hydroxyl radical as the reactive intermediate comes from recent theoretical DFT studies on the Fenton reaction in water [95].
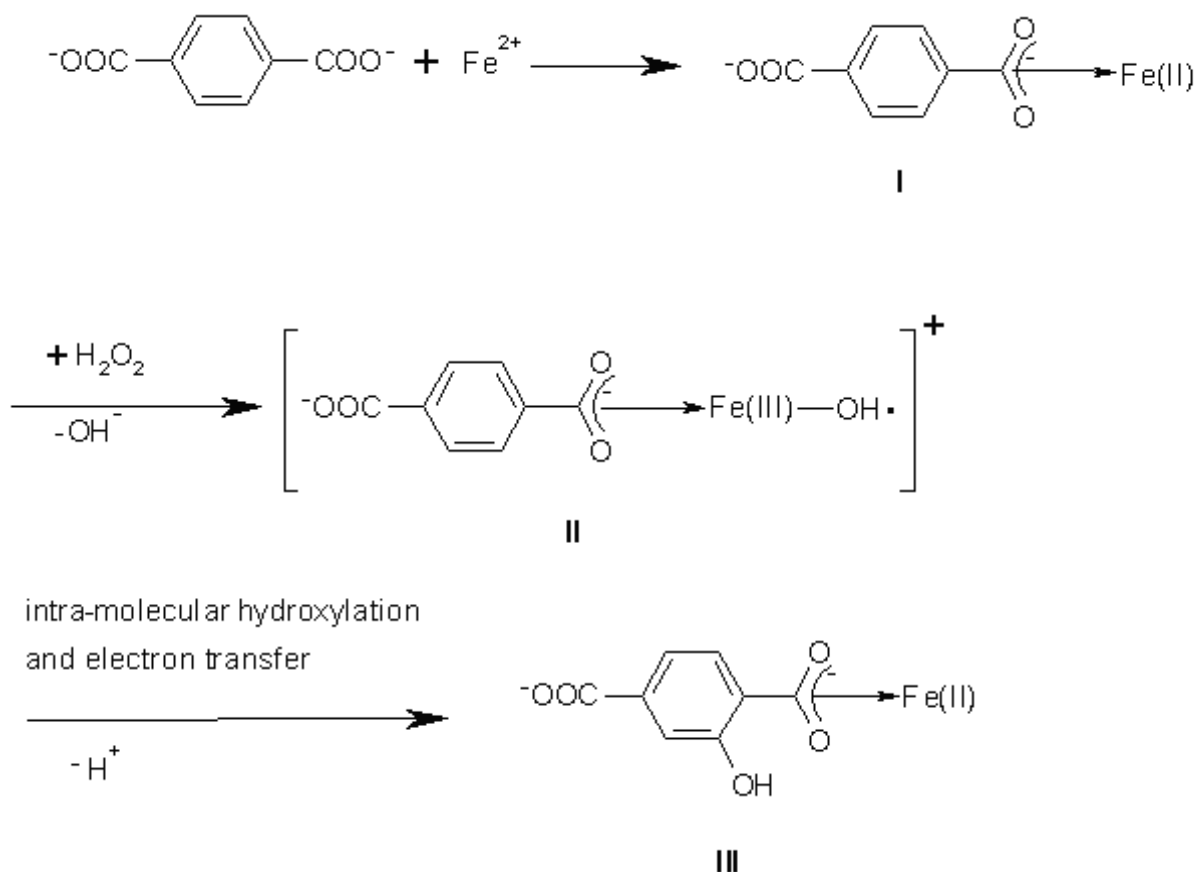
Scheme 4.2. *Proposed TA^{2-} Hydroxylation Mechanism. The arrows, from the carboxylate group to the iron centre, represent a coordinative bond.*

Nevertheless, for the EDTA experiments the results could not be interpreted that clearly, and both, an intra- as well as an inter-molecular mechanism could explain the experimental data.

However, comparing the composition of ECF to aCSF, there is no difference in the milli-molar concentration range but ECF contains additionally to aCSF high micro-molar amounts of amino-acids, and low micro-molar amounts of reactive species and (other) neurotransmitters e.g. amines like dopamine. As even high milli-molar concentrations of KAC could not force the hydroxylation reaction to an inter-molecular mechanism it is not expected that micro-molar concentration of amino acids or amines could do so. Since in ECF no significant amounts of non protein iron chelators, which might have the ability to change the hydroxylation mechanism, exist, it is concluded that at least in the cases, when iron, released from ferritin or transferrin, is responsible

for oxidative stress generation, the presented mechanism provides a reasonable model for the generation of oxidative stress *in vivo.*

The mechanism also allows an explanation of the problems arising when salicylic acid or phenylalanine are used for hROS quantitation. Therefore, in the following section these problems will be addressed from a mechanistical viewpoint and the advantageous properties of the TA^{2-} assay will be additionally described from the viewpoint of coordination chemistry.

The results clearly show the use of TA^{2-} for the detection of hROS in a physiological environment to be highly sensitive and not susceptible to the artefacts that may occur with the salicylic acid or the phenylalanine assays. Some of the particularly favourable properties of this system are listed below.

- Iron possesses 6 coordination sites, which in aCSF should be occupied by chloride ions and H_2O. Since one chloride ion, as well as H_2O, can be easily replaced by one TA^{2-}, the formation of the mono Fe(II)TA complex is not hindered in aCSF, which is consistent with the proposed mechanism .

- The complexes of amino acids and amines with iron (II) have stability constants (pK ~ 4) comparable to those of acetate [94]. The experiments described above demonstrate that acetate concentrations far above physiological levels are needed to significantly disturb the Fe-TA complex formation. Thus, it is evident that the amine and amino acid concentrations of the extracellular fluid do not significantly influence the Fe-TA complex formation providing a constant hydroxylation yield in ECF.

- As TA^{2-} is a mono-dentate ligand, only one complex species can be formed with Fe(II). Due to the symmetry of the TA^{2-} molecule the product distribution of the hydroxylation is independent of steric properties of intermediate (II). Therefore, the yield of the hydroxylation product should depend only on the redox potential of the intermediate, thus solely reflecting the Fenton activity.

- As even under cytotoxic conditions the concentration of transition metals is far below the used 250μM TA^{2-} concentration, the main amount of TA^{2-} is not complexed. Free hydroxyl radicals that might be produced by different chemical or biological processes, can be trapped by this non-bound TA^{2-}.

In the case of salicylic acid only one derivative (2,3 DHBA) can be used for the quantification of hROS *in vivo*. For that to be valid (as already mentioned above), it is essential for the three hROS hydroxylation products to be in a constant ratio. As already

shown in Tab. 1.1 and 1.2 in the introduction the product distribution of 2,3-DHBA and 2,5 -DHBA obtained in Fenton-like systems and in radiolysis experiments *in vitro* appears clearly to depend on the chemical environment as well as on the reaction time. This variable product ratio may result from salicylic acid being able to bind to the iron centre through its carboxyl as well as its OH group. This would give variable reaction intermediates with different electronic and steric properties. As these species might be in equilibrium, any change in the chemical environment could cause a transformation of one species into the other. Thus, since at least two different Fe(IV) or "crypto" radical intermediates are possible and a mixture of both could be present, the possibilities for the formation of each hydroxylation product are expected to be highly variable. This could result in significant changes in the product ratio occurring with changes in the chemical environment. As observed experimentally, the use of only the 2,3 DHBA derivative to quantify hROS formation can result in significant errors, thus raising serious doubts about the validity of the salicylic acid method for *in vivo* quantification of hROS formation. Similar arguments are also valid for the phenylalanine method, an alternative method reported in the literature see e.g. Ferger et al. [53].

4.5 Conclusions

The application of TA^{2-} for hROS detection yields robust and valid results for kinetical analyses as well as for HPLC quantitations. Moreover, this work provides a broad line of evidence that the reactive intermediate causing oxidative stress *in vivo*, is not a free hydroxyl radical, but a ferryl species or a "crypto" radical that can react more specific with other biomolecules, thus raising the question upon a specific role of hROS in the cell's apoptotic pathway. Since only ferryl species or crypto radicals are suitable candidates for a possible non pathological function of hROS, and furthermore hROS were always detected also in healthy and free moving animals, the role of hROS as possible messenger molecule e.g. as neurotransmitter warrants further investigations.

Part V

5   *In vivo* detection of the Fenton reaction

5.1   General Introduction

Although numerous authors claim, that the Fenton reaction is the key factor of hROS formation *in vivo*, this matter is still under discussion [88, 96]. Alternative explanations based on kinetical arguments which favour the formation of high valent iron compounds that can act without H_2O_2 as hROS generator are proposed by several authors [88]. However, based on our previous work [1-12], we could show *in vitro* that free iron(II) species may react in a Fenton type reaction with redox active compounds like H_2O_2 (which is a stoichiometric product of DA, adrenaline, etc. oxidation) to yield pathogenic species like 6-hydroxy dopamine (6-OH DA). Those in term are able to free Fe(II) from its storage protein Ferritin, producing an autocatalytic pathogenic cycle, schematically given in Fig. 5.1. Recently, Guy Jameson et al. [12], could demonstrate *in vitro* based on kinetical evidence a plausible mechanism of iron release from ferritin caused by 6-OHDA formation. One of the interesting results was an increase of iron levels due to addition of DA, which could be crucial for 6-OHDA formation in the DA rich region of the Substantia Nigra, which most possible plays an important role in the pathogenesis of PD. Also *in vivo* 6-OHDA has been shown to release iron in its ferrous (Fe^{2+}) form, from the iron-storage protein ferritin [12, 97-98], raising the question if the same mechanism found *in vitro* also occurs *in vivo*.

Iron release caused by 6-OHDA formation coupled with the observation that the iron chelator desferrioxamine could attenuate 6-OHDA neurotoxicity [99] implies that 6-OHDA mediates its neurotoxicity through release of iron. This iron can then induce the formation of hROS via the Fenton reaction. The observation that the total iron content of the substantia nigra is increased in 6-OHDA-lesioned rats [100], as well as in

Parkinson's disease (e.g., Dexter et al. [101]) may be a consequence of this iron mobilisation, or a secondary phenomenon related to attempted damage repair.
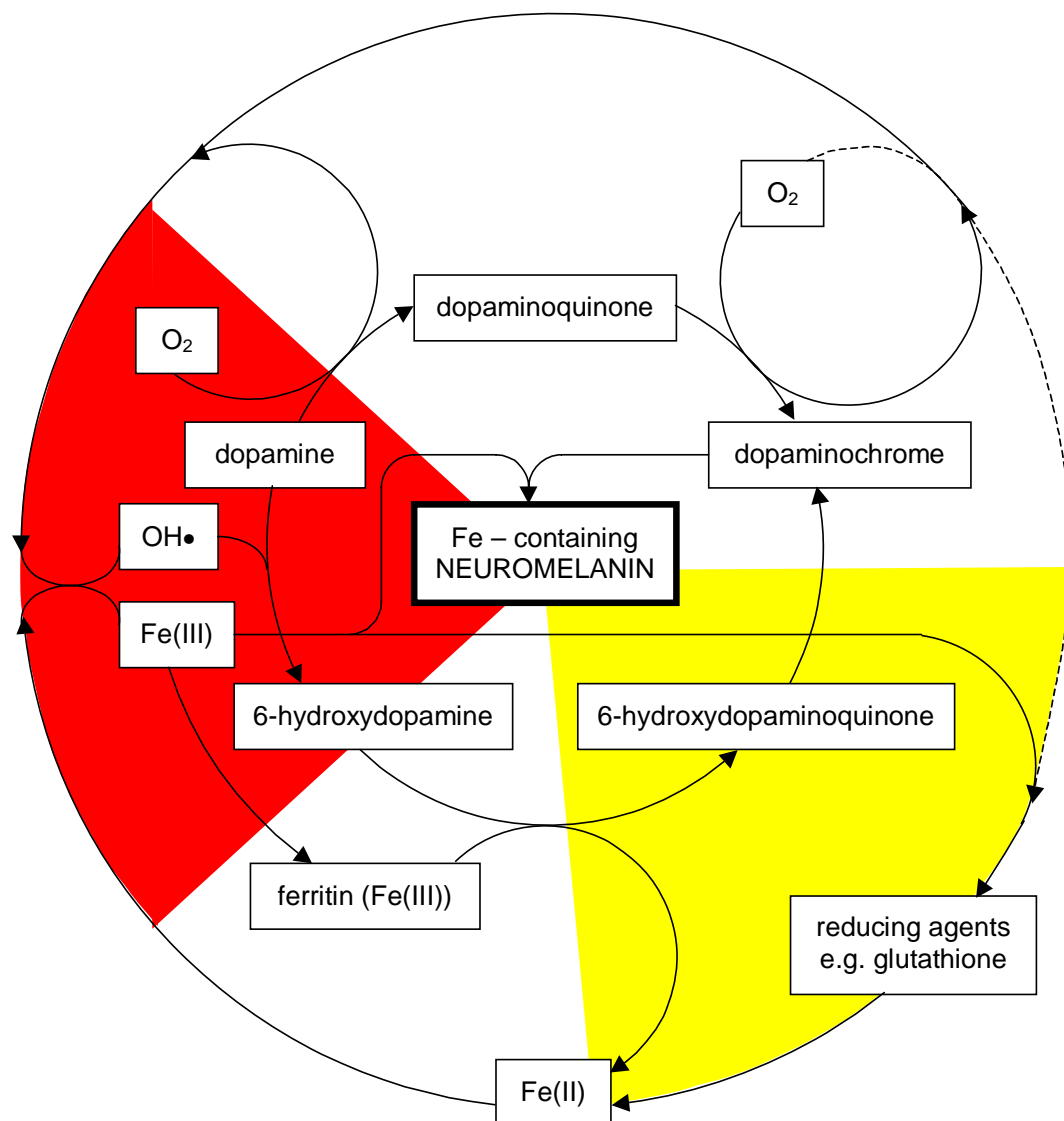
Figure 5.1. *A possible propagation of cytotoxins, based on the results obtained by in vitro kinetic experiments.*

As a consequence 6-OHDA stimulation may be considered a (simple) model of PD in mammalians.

Generally, for a detailed understanding of Fenton, or, if hROS formation would turn out to be independent of H_2O_2 formation, of high valent iron chemistry *in vivo,* it is necessary to monitor all relevant compounds involved in the Fenton reaction simultaneously. However, up to now no *in vivo* work was published measuring Fe(II), Fe(III), H_2O_2 and hROS at once, mainly because no practicable methods exist that allow an accurate quantitation with sample amounts of few micro-litres.

Therefore, before conducting microdialysis experiments using 6-OHDA stimulation, it was necessary to develop new methods for Fe(II), Fe(III) and H_2O_2 determination allowing a simultaneous measurement with hROS and neurotransmitters in a microdialysis sample. The next two sections (5.2 and 5.3) will describe in detail the *in vitro* work required for setting up the iron and H_2O_2 measurements, whereas section 5.4 will be dedicated to the *in vivo* application of the new methods giving new insights into iron as well as into hROS chemistry in the brain.

5.2 Iron determination by bathophenanthroline

5.2.1 Introduction

There exist numerous techniques for determining trace amounts of iron, but for our purpose only spectrophotometrical methods were of interest. Photometric determinations of Fe(II) are most commonly performed by using either ferrozine (see e.g. [102]) or bathophenanthroline. Since Ulf A. Nilsson et al. [103] recently published a procedure for microdialysis experiments using the disodium salt of sulfonated bathophenanthroline (BA), this substance (Fig. 5.2) was chosen for further investigations.

Both BA as well as ferrozine form stable and highly coloured complexes with non protein bound Fe(II), in the case of BA with an absorbance maximum at 535 nm. As visible bands in this area are most probable d-d transition bands they can normally be considered as selective bands of the iron complex allowing the amount of iron to be determined photometrically by simply using the law of Lambert Beer. However, it is not

possible, even if sensitive detection systems are used, to quantify iron in the low micro-molar range using sample amounts smaller than 50 µl [103], but on the other hand it would be possible by using the charge transfer band at 285 nm to reduce the required sample volume to ca. 2.5 µl. Since this band is not selective for the iron complex, HPLC separation is necessary for accurate iron quantification.

Therefore one aim of this work was to design and test an HPLC assay for iron determination with BA allowing an application in microdialysis experiments.

5.2.2 Experimental

The following chemicals were of the highest available purity and purchased from Sigma-Aldrich Chemical Company (Vienna, Austria): 4,7-diphenyl-1,10-phenantroline disulphonate (bathophenantroline disulphonate (BA)), ferrous ammonium sulphate $(NH_4)_2Fe(II)(SO_4)_2$, ferric sulphate $(Fe(III))_2(SO_4)_3$ x $6H_2O$, ascorbic acid (ASC), hydroxyl ammonium chloride ($HONH_3Cl$). Standard solutions of Fe(II) and Fe(III) were prepared as described in Part III and Part IV in the experimental section. 5mM BA stock solutions were prepared by dissolving the solid in H_2O and stored at 4 °C in a plastic beaker, since trace amounts of iron could be detected after approx. 1 week, when the stock solution was stored in normal laboratory call vessels. The stock solution was then diluted to 100 µM and added at least in a ratio of 4:1 to the Fe sample. It was necessary to use as little BA as possible, as in some cases iron impurities in the delivered chemical were found to be significant when BA was used in high (>100:1) excess. To reduce Fe(III) to Fe(II) in a convenient time a high concentration (100 mM) of $HONH_3Cl$ was necessary. Due to that reason $HONH_3Cl$ stock solutions were prepared by dissolving the solid in H_2O to give a final concentration of 1M, and stored at 4 °C. For Fe(III) determination the stock solution was added 10 min prior to BA addition in a ratio of 1:10 to the iron sample and kept at 80°C in a sandbath. For the *in vivo* Fe(II) determination 2.5 µl of microdialysate was diluted with 57.5 µl of 10 µM BA solution. Then, 50 µl of the sample was injected after at least 10 min into the HPLC system. It should be mentioned that it was important for a convenient reaction time to dilute the sample in the described manner, and to use only H_2O for dissolving and diluting BA. For the *in vivo* total iron (and Fe(III)) determination 2.5 µl of microdialysate was treated with 6µl 1M $HONH_3Cl$ solution at 80°C. To that the mixture was put for 10 min into a

sandbath, cooled to room-temperature, and then diluted with 51.5 µl of 10 µM BA solution. Then, 50 µl of the sample was injected after at least 10 min into the HPLC system. The same HPLC system as described in Part III was used for all measurements, whereby for detection a Perkin Elmer CC90 (Pelkin Elmer Milan, Italy) UV/VIS detector at 285nm was used. For gradient elution a mobile phase containing methanol and 1.5 mM HEPES buffer adjusted to pH 6.7 with the time program illustrated in Tab. 5.1 and a flow rate of 0.9 ml/min was utilised.

Table 5.1. Time program for HPLC gradient elution

Time (min)	Methanol (%)	1.5 mM HEPES buffer (%)
0.01	0	100
5	30	70
7	30	70
7.1	0	100
16	0	100

5.2.3 Results and discussion

The chemical structure of BA (Fig. 5.2) shows a bidentate ligand, coordinating to iron via the two nitrogen atoms in the phenanthroline ring system. Since iron usually accommodates six ligands, the binding stoichiometry will be three BA per Fe(II). The two sulphonate groups render the molecule hydrophilic, and there is practically no partition into lipophilic environments. Binding constants for Fe(II) are in the order of 10^{22} [104].
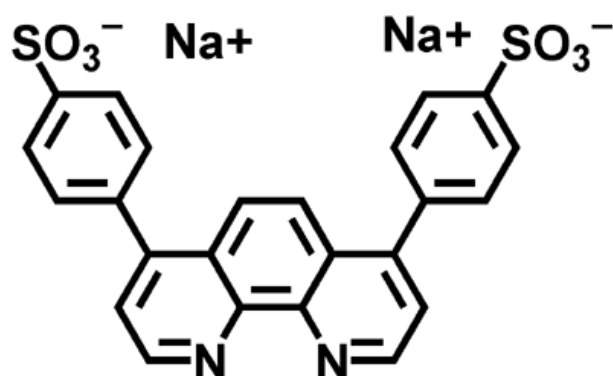
Figure 5.2. *Structural formula of BA*

Interestingly, the first attempts to elute $Fe(II)(BA)_3^{4-}$ with MeOH and KAC buffer resulted in a chromatogram containing three peaks (Fig. 5.3) with an uncomfortable high retention time, although the selective wavelength of the complex (535 nm) was used. Exchanging KAC to H_2O (data not shown) led to one peak short after the solvent front containing both the complex and the free ligand. As already mentioned in Part II low retention times like the ones measured by using H_2O is awaited for charged molecules like the $Fe(II)(BA)_3^{4-}$ complex, whereas for uncharged substances being able to interact with the C-18 ligands via strong hydrophobic interactions, retention times around the ones detected with KAC are expected. Since it can be excluded that KAC caused the complex to dissociate, an explanation of the chromatogram presented in Fig 5.3 must base on considerations related to the second coordination sphere or -in other words- the complex-solvent aggregate.
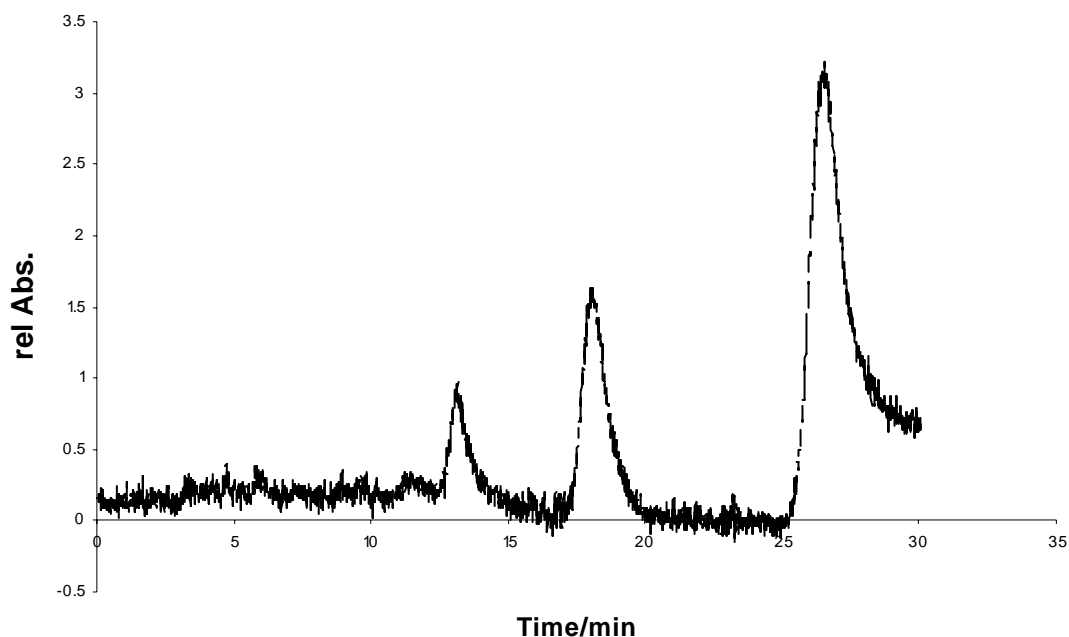
Figure 5.3. *Chromatogram of 1mM Fe(II) reacted with 10mM BA recorded at 535 nm. Isochratic elution with 25% MeOH and 75% 100mM KAC buffer adjusted to pH 5.48 was used.*

On the first sight it seemed to be unlikely that there exist three species of the Fe(II)(BA)$_3^{4-}$ complex, which can be separated by simple reverse phase chromatography. However, it can be seen in Fig. 5.4 that, indeed, three octahedral complexes differing in symmetry can be formed. The difference in the symmetry leads to three diverse distributions of the partial charge causing probably KAC to coordinate differently in the second coordination sphere. A diverse second coordination sphere can then induce for of each complex species different partial charges on the surface of the solvent-complex aggregate "seen" by the C-18 ligands of the column. The high retention times can be explained by assuming that for the C-18 particles the solvent-complex aggregate "looks" (nearly) neutral meaning that KAC shields the charge of the complex core, which then causes the hydrophobic interactions to dominate over the polarity. Taking these arguments together the found chromatogram can be entirely explained as neutral molecules showing strong hydrophobic interactions can be separated already by small differences of the partial charges "seen" by the C-18 ligands of the column, and, moreover, as described in the legend of Fig. 5.4, the probability of formation is not the same for the three complex species due to sterical and statistical

79

reasons which explains the observed difference of the peak areas. It is obvious that H_2O has not the ability for such a shielding and therefore in this case the charge is the determining factor for the retention time.
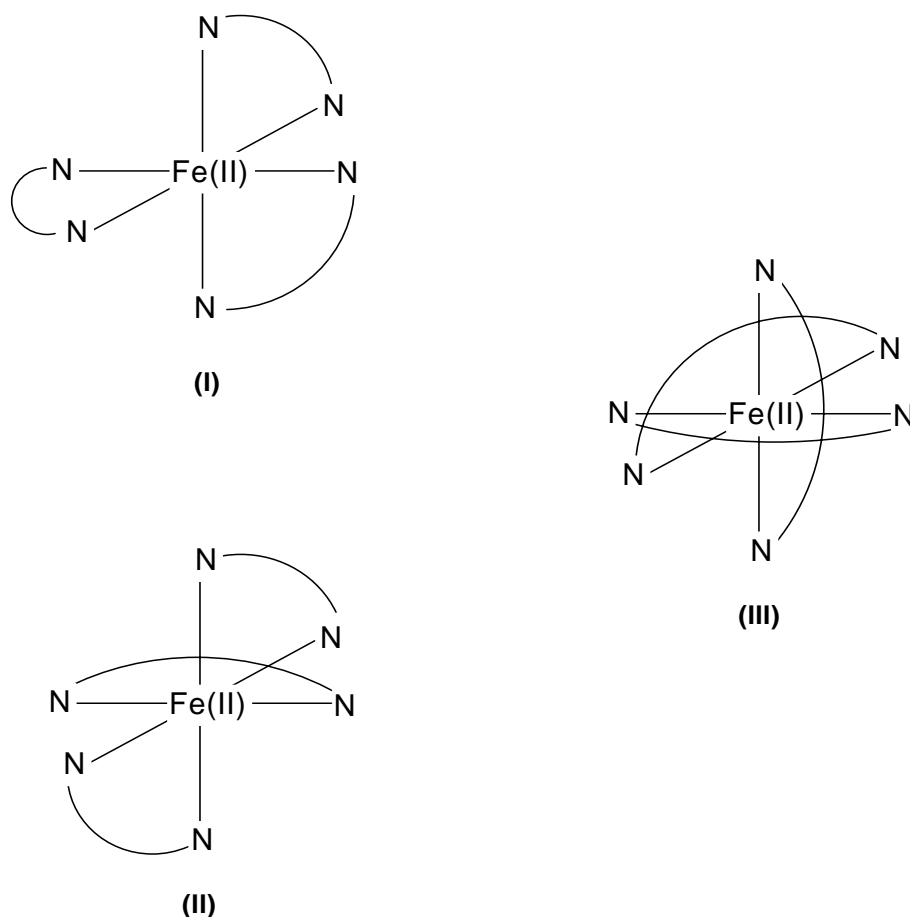
Figure 5.4. *The octahedral Fe(II) coordination sphere and the possibilities for BA to coordinate is schematically shown. As the iron centre bears two positive charges, whereas each ligand has two negative ones, the distribution of partial charge is different for each of the three species. The statistical probability of formation is three times higher for species (II) compared to species I and III. A different steric hindrance of complex formation is expected for each species, since the difference in coordination geometry will lead to variable repulsion energies among the rather big and rigid ligands. Both effects are likely to be responsible for the observed difference in the species' concentration.*

However, to maximize the sensitivity it was necessary to find suitable chromatographic conditions to unite the three $Fe(II)(BA)_3^{4-}$ peaks, but still keep them separate from the free ligand and other absorbing substances present in aCSF. It was found that the system was too sensitive to KAC, as varying the buffer concentration in the micro(!)-molar range already "switched" between the two described chromatograms, showing that already stoichiometric amounts of KAC can effectively shield the charge of the complex. Since it was not possible to find a suitable elution gradient using only water and MeOH, a quasi non coordinating buffer in the neutral pH area had to be found. It turned out that 1.5 mM HEPES buffer solution adjusted to a pH of 6.70 delivered the best results, even though the retention times were still sensitive to HEPES concentration, but in the easy manageable milli-molar concentration range. Fig. 5.5 shows a typical chromatogram obtained using the described conditions, whereby the retention time for the united $Fe(II)(BA)_3^{4-}$ peaks was around 9 min, sufficiently after the peaks of aCSF and substances like 6-OHDA, amino acids or catechol amines, and sufficiently before the free ligand peak. It needs to be mentioned that if both Fe(II) and BA were dissolved in aCSF the complex formation was partly hindered by phosphate coordination leading to an underestimation of the iron content. This problem could easily be resolved by using an aqueous BA solution and keeping a volume ratio to the aCSF containing Fe(II) sample of at least 10:1.
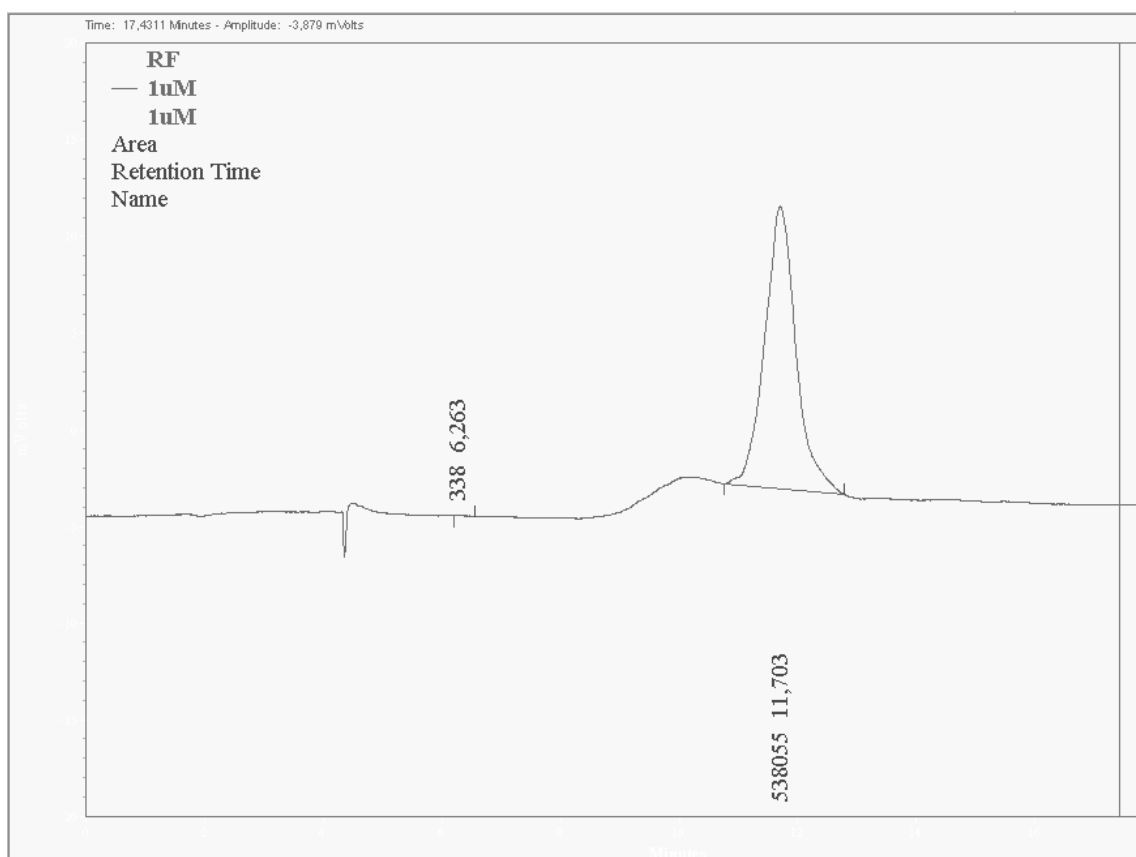
Figure 5.5. *Typical chromatogram obtained when 1 µM Fe(II) dissolved in aCSF was determined under the conditions described in the text.*

Plotting the peak areas against Fe(II) concentrations (Fig.5.6) resulted in a straight line with an intercept representing the iron impurities in aCSF and 10 µM BA solution. As the concentration range covers iron levels far below (Fig. 5.6 inset) that expected for non-pathological and far above that expected for pathological conditions, the data clearly demonstrate that Fe(II) determination with BA can be considered a robust and highly sensitive HPLC method for Fe(II) detection in an environment approximated to the *in vivo* chemistry of the ECF.

82
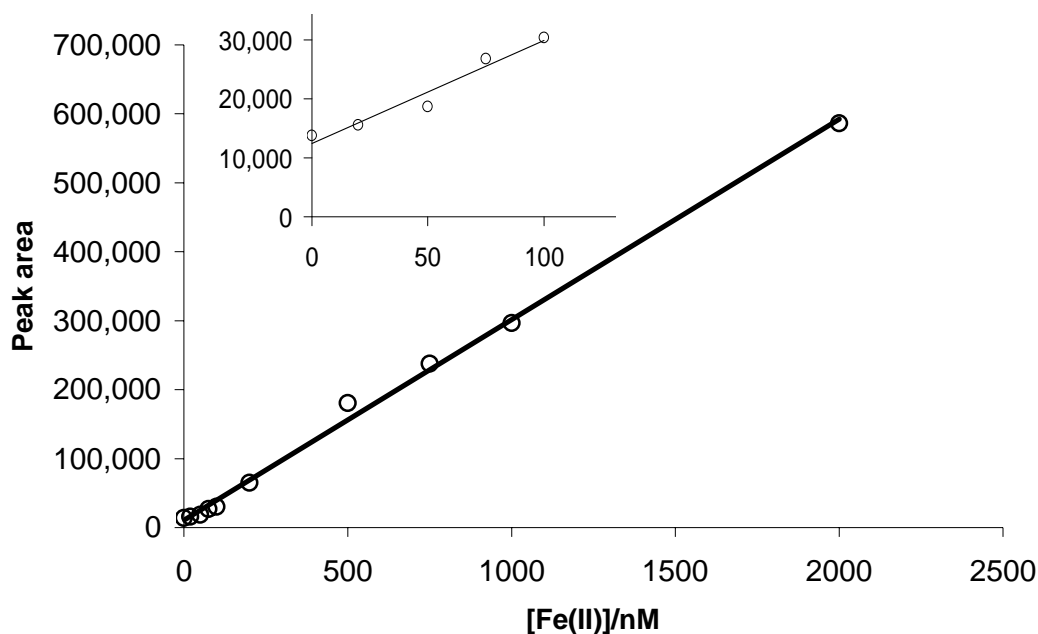
Figure 5.6. Peak area plotted versus nano-molar concentrations of Fe(II). Linear regression analysis gave a slope of 290.8, an intercept of 10,643 and an R^2 of 0.997

According to A. Nilson [103] it should have been possible to find a Fe(III)(BA)$_3^{3-}$ peak in the chromatogram using the described conditions, which could be used for Fe(III) determination. However, in contradiction to A. Nilsson et al. [103], but in agreement with Takagai et al. [105] no Fe(III) complex could be found, showing that under the conditions used, BA reacts selectively with Fe(II). Nevertheless it was possible to generate an unstable Fe(III)(BA)$_3^{3-}$ complex by oxidizing the Fe(II)(BA)$_3^{4-}$ complex with H_2O_2, but this procedure is obviously not applicable for Fe(III) detection.

Therefore, a direct measurement of Fe(III) was not possible and an indirect method, where Fe(III) is reduced prior to complexation with BA, had to be found.

Since it turned out that ASC was not able to reduce reproducibly Fe(III) and the reduction via 1mM HONH$_3$Cl at room temperature led to a reaction time of several days, it was required to carry out the reaction at 80°C, and use, as the rate of the reduction depends (pseudo) first order on the concentration of HONH$_3$Cl, at least 100 mM of the reductant. Fig. 5.7 shows the results obtained when Fe(III) was reduced via the described procedure and the resulting Fe(II) was determined with BA afterwards. By comparing Fig. 5.6 with Fig 5.7 it can be seen that the obtained slopes are -as required-

83

identical, but the intercept is significantly higher in the case of Fe(III) determination. This is, because the intercept represents in one case only the Fe(II) impurities, whereas in the other case it corresponds to the sum of the Fe(II) and Fe(III) contaminations. Overall, it could be shown that this method yields reliable results for Fe(III) detection. However, it should be pointed out that in samples containing both Fe(II) and Fe(III), this procedure measures the amount of total iron, and therefore for a complete determination of iron species two analyses are required, whereby the Fe(III) content can be easily achieved by subtracting the Fe(II) concentration from the one of total iron.
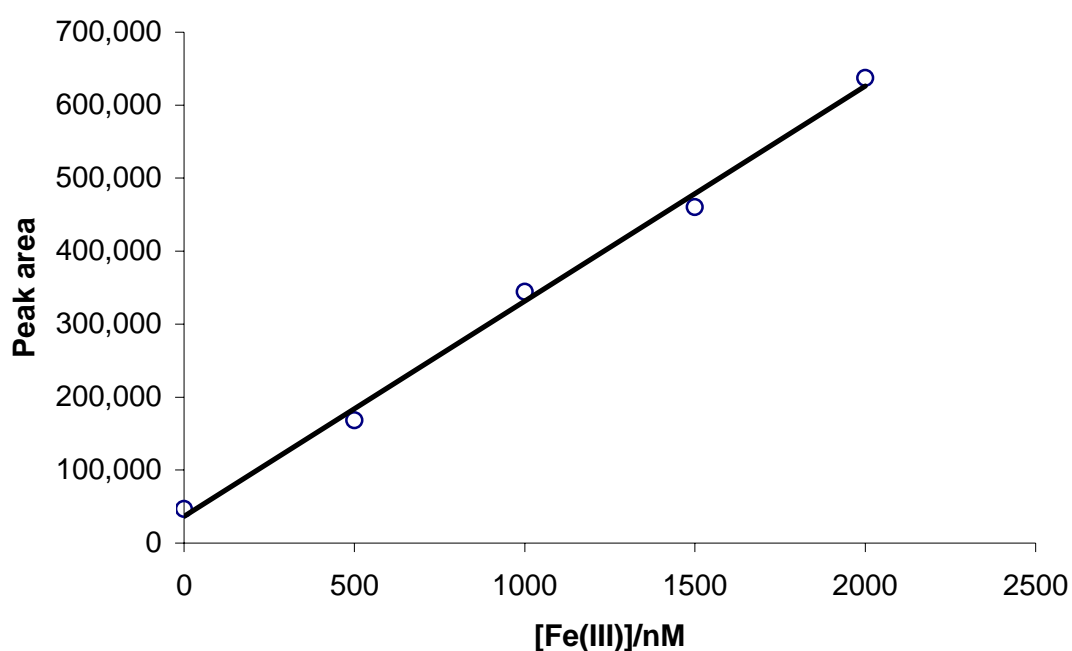

Figure 5.7. *Peak area plotted against nano-molar concentrations of Fe(III). Linear regression analysis gave a slope of 294.8, an intercept of 36,481 and an R of 0.997*

For reasons of presentation the iron results of the *in vivo* experiments using 6-OHDA stimulation will be presented below together with the *in vivo* data of hROS and H_2O_2.

5.3 The detection of H_2O_2 with Fe(II)EDTA and TA^{2-}

5.3.1 Introduction

As already described in Part I it is commonly believed that the formation of hROS goes along with a raise of H_2O_2. However, at least quantitatively this needs not to be case if iron is additionally or even solely the key factor of hROS formation. One of the tasks of this work was to investigate the relation of hROS and H_2O_2 formation. Although there exist a standard method of H_2O_2 detection in microdialysis experiments utilizing dichloro-fluorescine (DCSF) and horseradish peroxidase [106], for our purpose it was much more comfortable to develop a new method based on the hydroxylation of TA^{2-}, avoiding the technical and practical drawbacks of the standard procedure.

5.3.2 Experimental

All chemicals and experimental procedures regarding the Fenton reaction with non chelated iron are described in Part III (*in vitro* experimental section), whereas in Part IV (experimental section) the conditions of the Fenton reaction using EDTA as chelating agent are explained. The reactions were carried out in Florence, where no argon or nitrogen was available for degassing. To reach at least a partial removal of oxygen, the solvents were degassed by the use of an ultrasonic bath. The stock solution was prepared by dissolving 1mM Fe(II) in partly degassed 100mM KAC buffer (pH 4.50), chelated with 1.1 mM EDTA and stored at -20°C. The reagent was freshly prepared by diluting the stock solution with KAC buffer to 100μM. To 2μl of sample firstly 37 μl of buffer, secondly 6 μl of 10mM TA^{2-} and thirdly 15 μl of Fe(II)EDTA solution was added. The sample was mixed immediately after the addition of Fe(II)EDTA, and 10μl were injected after at least 15 min. into the HPLC, whereby an isochratic elution using 25% methanol and 75% 100mM KAC buffer (pH 5.48) was used.

The H_2O_2 stock solutions were stored at -20 °C, and titrated with $KMnO_4$ before usage.

5.3.3   Results and discussion

If some pitfalls, essentially described in Part IV, are borne in mind, the detection of H_2O_2 can be easily achieved via reversing the TA^{2-} method. The key to a reliable quantitation of H_2O_2 is to keep the Fenton activity constant, and to avoid a significant contribution of Fe(II) auto-oxidation to TA^{2-} hydroxylation. The first point demands a fixation of the Fe(II) coordination sphere and the pH, the second an exclusion or, if not possible, a reduction of the oxygen content of the sample. To fulfil these demands Fe(II) was dissolved in (partly) degassed 100mM KAC buffer (pH 4.50), and chelated with EDTA. To avoid a local concentration gradient the sample was mixed with buffer and TA^{2-} prior to the addition of Fe(II)EDTA solution and then again immediately mixed. The fluorescence of OH-TA was measured after at least 15 min by HPLC as already described in Part III. Fig. 5.8 shows the results, when the peak areas were plotted versus H_2O_2 concentrations.
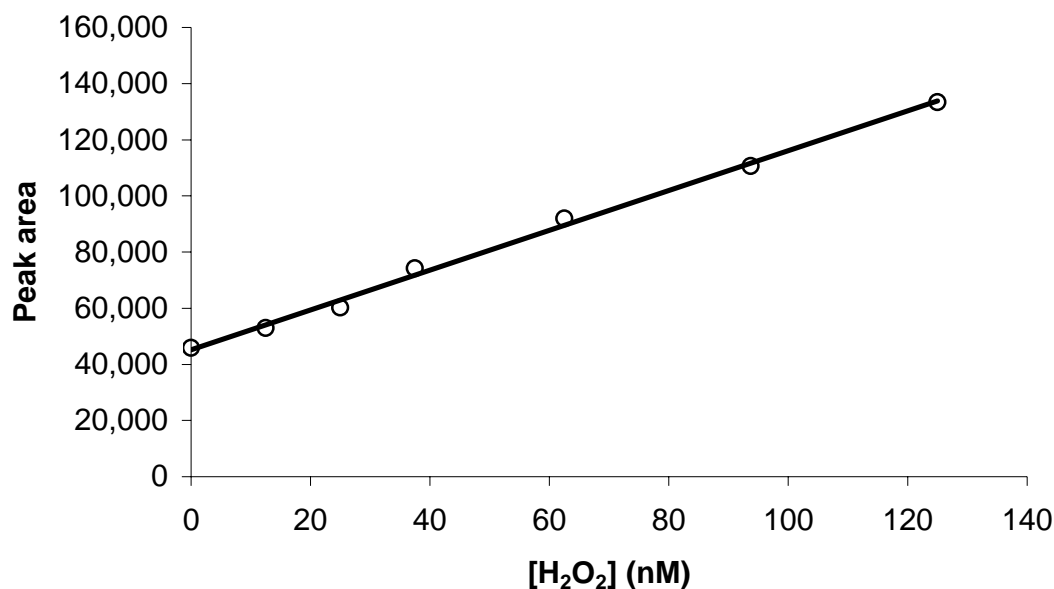
Figure 5.8. *Peak areas versus H_2O_2 concentration using the procedure described in the text. Linear regression analysis gave a slope of 708.7 an intercept of 45,233 and an R of 0.998*

The results show that the method yields precise and reliable results for H_2O_2 in a concentration area expected for pathological as well as for non-pathological conditions. As TA^{2-} is, on the contrary to DCSF, selective for hROS, and OH-TA formation due to hROS is of several orders of magnitude lower than that related to H_2O_2 determination, no blank samples containing catalase and reagent are needed for a reliable detection. When the solutions are stored at -20 °C they can be used for several weeks, facilitating the application in comparison to the DCSF assay.

5.4 *In vivo* measurements of Fe(II), Fe(III), H_2O_2 and hROS in a simple model of Parkinson's Disease

5.4.1 Introduction

As already stated above the stimulation with 6-OHDA can be considered a simple animal model of PD, therefore it seemed to be useful to apply all methods developed in this work to this model. It should be pointed out that only 7.5 µl of sample is needed for a complete (*ex vivo*) analysis of iron and H_2O_2 allowing a simultaneous measurement of hROS, catechol amines and amino acids. However, the focus of this part will be centred on Fenton chemistry, thus only the behaviour of iron, H_2O_2 and hROS will be shown. To get a better insight into the mechanisms of oxidative stress generation also experiments with selective Fe(III) chelators and additionally applied DA were performed.

The application of all methods developed in this work to a simple model of PD should also give an outlook to future possibilities of research in the field of neurodegeneration using these methods. Since with microdialysis also far more complex animal models of several neurodegenerative diseases can be investigated, the methods developed here can be utilised to get deeper insights into pathologic mechanisms possibly also playing a crucial role in human beings. It is dedicated to future work to show if an application to cell banks and other methodologies in animal research is also possible.

5.4.2   Experimental

5.4.2.1   General conditions

Animal housing, HPLC analysis of hROS and the microdialysis setup are described in Part III in the *in vivo* experimental section. Fe(II), total iron and H_2O_2 determination was performed identical to the *in vitro* experiments described above. Desferal (Desferrioxamine) and ICL-670, which is a ligand under development, were obtained from Sigma-Aldrich (Florence, Italy) and directly from the developers, respectively. The concentration of both chelators was 200 µM. Desferal was dissolved directly in aCSF, whereas ICL-670 had to be firstly dissolved in the minimum amount of 1M NaOH, followed by 1:10 dilution with aCSF and neutralisation with 0.1M HCl, to dilute it further to the desired concentration with aCSF.

5.4.2.2   The 6-OHDA protocol

As perfusate aCSF containing 250 µM TA^{2-} was used. After collecting at least 2 fractions to determine the basal levels of OH-TA, H_2O_2, Fe(II) and total iron, 200 µM of 6-OHDA dissolved in the perfusate with 0.05% ascorbic acid added, were applied through the probe to the neostriatum for one fraction. At least 3 more fractions were then collected perfusing again with the original perfusate. For the protection experiments, one fraction before and all fractions after the application of 6-OHDA, 200µM of either ICL-670 or Desferal were added to the perfusate. For studying the effect of additionally applied DA 200 µM DA was added to the 6-OHDA stimulus fraction.

5.4.3   Results and discussion

The *in vivo* results for Fe(II), total iron and H_2O_2 presented here must be considered preliminary, as up to now many results rely only on two animals. The author is well aware that the statistical considerations based on these data have to be treated with caution, and cannot be considered as "facts", as the usual variance between the animals in *in vivo* experiments typically demands at least a number of 4 animals. Further experiments will be needed to confirm especially the mechanistic considerations presented later in this part. Nevertheless it was decided to present these preliminary results, because they give an interesting overview about future possibilities to apply the methods developed in this work *in vivo*, and describe at least a mechanistic trend of 6-OHDA toxicity in the brain.

Before analysing the *in vivo* samples, it was checked if any substance in the microdialysate is disturbing Fe(II) or total iron detection, by injecting a sample without being treated with BA into the HPLC and analysing it under the same conditions used for iron detection. (data not shown) As no disturbing peak could be detected, the procedure was used without modifications for further measurements. Fig. 5.9 shows a typical chromatogram obtained during 6-OHDA stimulation, whereby the good visible iron peak is found at 8.74 min, whereas the sharp peak shortly after the solvent front is ascribed to ascorbate, the hardly visible peak around 6.5 min to 6-OHDA and the broad peak after the iron one to the free ligand.
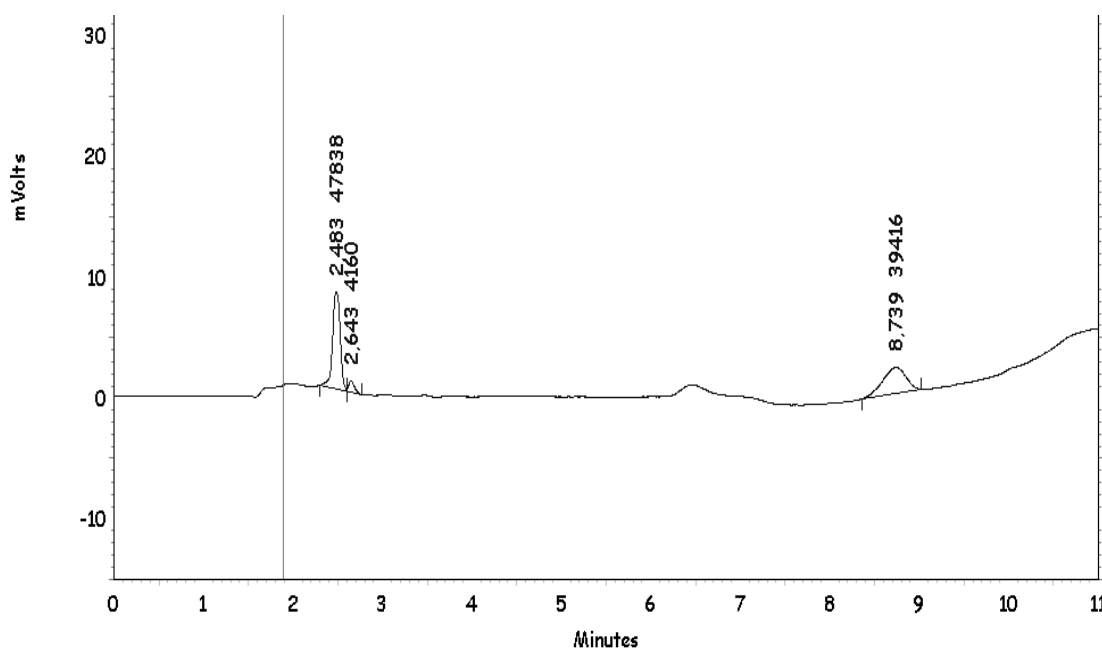
Figure 5.9. *Typical chromatogram for Fe (II) determination obtained during stimulation with 6-OHDA. The peaks are explained in the text.*

The results obtained for total iron (upper curve) and active (Fe(II) (middle curve) using 6-OHDA stimulation, plus the total iron levels of the control group where only ascorbate was added to the perfusate, can be seen in Fig. 5.10. It was possible to compare the results with the work of others only in the case of the detected basal levels, which are in good agreement with those reported by A. Nilson and others [103], as for iron levels after 6-OHDA stimulation no data exist in literature. The data clearly demonstrate that an iron release took place after, and solely due to the stimulation with 6-OHDA, which, however, did not last long after removement of the stimulus. By comparing the levels of Fe(II) and total iron it can be seen that the main iron species is Fe(III), which indicates that Fe(II) is quickly oxidized when released. If no other mechanisms than iron and/or Fenton chemistry are mainly responsible for hROS formation, it is reasonable to assume a redox cycling, since (see Tab. 5.2 and Fig. 5.10-5.12) the level of Fe(II) increases ca. 6 times, the one of total iron ca. 13 times and the one of H_2O_2 ca. 13 times, whereas the one of hROS increased ca. 80 times due to stimulation. Under these assumptions one released Fe(II) would cause the formation of ca. 6 units of hROS. Although 6-OHDA caused a significant relative increase of H_2O_2, the data clearly demonstrate that it is not possible to quantitatively predict hROS formation by simply measuring H_2O_2 as it is done by many authors.

90
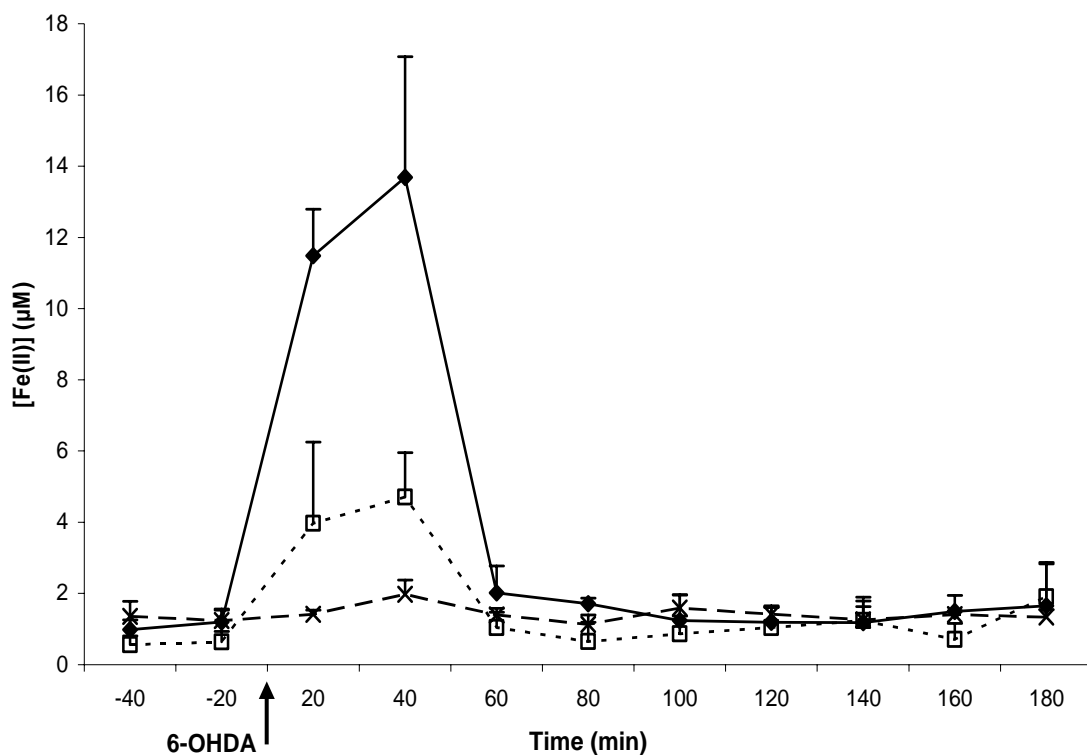
Figure 5.10. *Time course of* ———— *total iron and* ·-□-· *Fe(II) levels during 6-OHDA stimulation and* —✳— *total iron of the control group, where only ascorbate was infused. In the case of the control group, the points represent the mean values derived from 2 experiments, whereby the error bars representing the standard error give, as n=2, only qualitative information about the variance between the animals. The data of the Fe(II) time course rely on 4 and the data of the total iron one on 3 animals.*
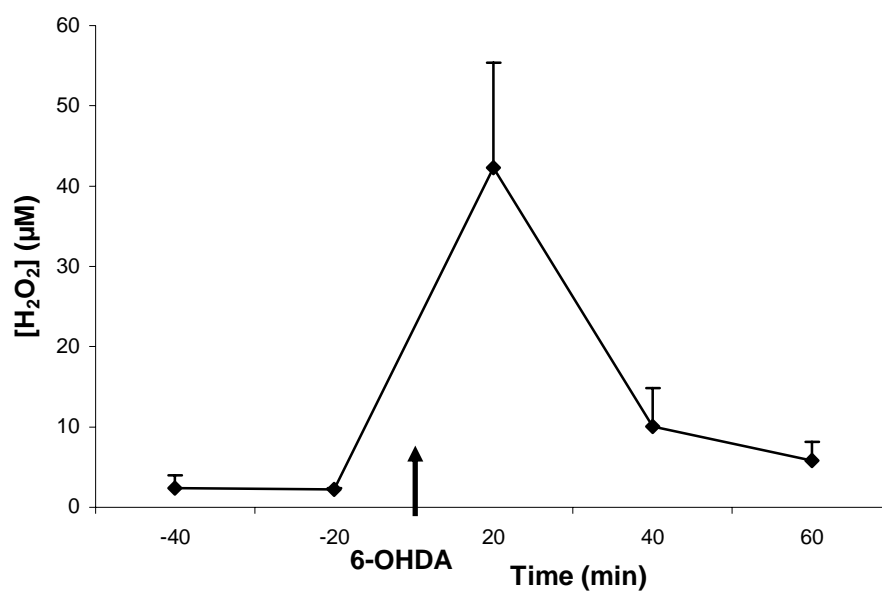
Figure 5.11. *Time course of* ⟶⟶ *H_2O_2 formation during 6-OHDA stimulation. The points represent the mean values derived from 2 experiments, whereby the error bars representing the standard error, give, as n=2, only qualitative information about the variance between the animals.*
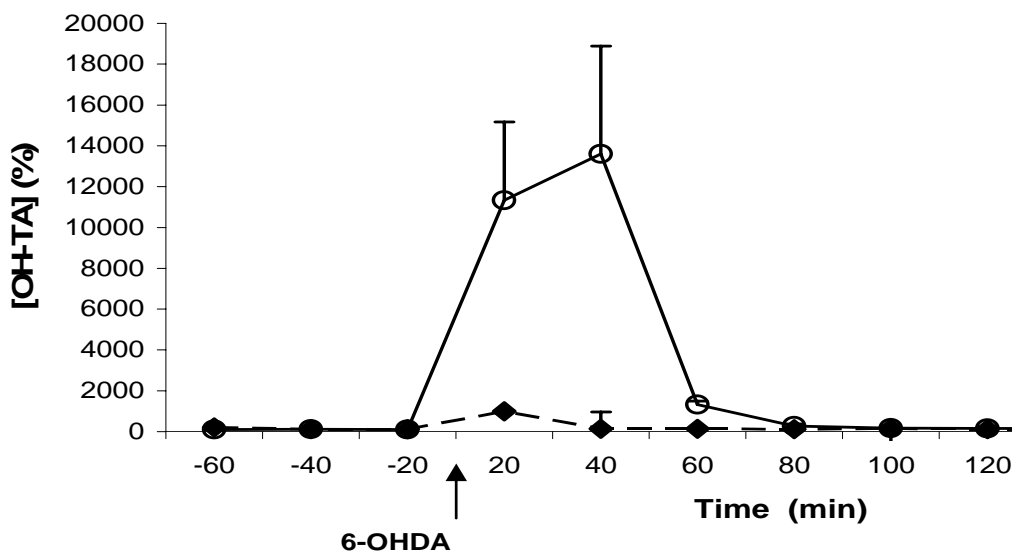
Figure 5.12. *Time course of* —o— *hROS formation during 6-OHDA stimulation and* — ◆ — *hROS formation of the control group, where only ascorbate was infused. The points represent the mean values in relative units related to the basal value ± SEM derived from 5 experiments for 6-OHDA stimulation, and for the control group they represent the mean values derived from 2 experiments, whereby the error bars representing the standard error, give, as n=2, only qualitative information about the variance between the animals.*

To investigate the influence of Fe(III) removal on the pattern of oxidative stress, before and after the stimulation the well known iron chelator Desferal (desferrioxamine) and the new ligand ICL-670 were added to the perfusate. As it can be seen in Fig. 5.13 both chelators completely prevented any formation of active Fe(II) in the ECF, whereby Desferal caused also a slight decrease in Fe(II) basal values. Since it was found *in vitro* that Fe(III) chelated by these ligands is completely released as Fe(II), when the Fe(III) complexes are treated with $OHNH_3Cl$, it made sense to analyse also the total iron content in the experiments done with ICL-670 and Desferal. In this case the data represent the chelated iron which is equivalent to the Fe(III) concentration in the perfusate. It can be seen in Fig. 5.14 that iron was released in significant amounts despite the addition of the chelators. From that, Tab. 5.2 and Fig. 5.16 it can be concluded that on one side 6-OHDA is the primary cause for iron release and on the

93

other side that during 6-OHDA stimulation approx. 75% of the iron was released because of a pathogenic cycle solely driven by hROS and active Fe(II). The hROS behaviour (Fig. 5.16) obviously correlates with Fe(II) but not with H_2O_2 (Fig. 5.15) formation, showing that iron redox chemistry plays the primary role in the occurrence of oxidative stress under these conditions. The difference in hROS formation between Desferal and ICL-670 might be caused by an additional Fe(II) chelation by Desferal, as the Fe(II) levels in the Desferal experiments were slightly below the ones of the ICL-670 experiments. A remarkable observation is the equal relative increase of total iron and H_2O_2 levels as they are presented in Tab. 5.2 for 6-OHDA stimulation without the chelators and the experiments carried out with ICL-670. A pure coincidence seems to be unlikely (a double sided t-test delivered p=0.03 for the normalized mean values to be different) as the data were observed in two independent series of experiments. However, more experiments will be needed to statistically proof or discard this hypothesis. In the case of the ICL-670 experiments also the relative increase of hROS is only slightly below the one of total iron and H_2O_2. However, the data of the Desferal experiments do not fit to these results, most likely –as already mentioned above- due to a partly chelation of Fe(II) by this chelator.

As the basal levels of Fe (II) were not influenced by the addition of ICL-670, it can be considered that the only action of this chelator is the removal of Fe(III), thus preventing any iron mediated redox cycling. As iron is released in its ferrous form from ferritin or transferrin it can induce a stoichiometric redox reaction before it is removed in its ferric form by ICL-670. A 1:1:1 stoichiometry of total iron, H_2O_2 and hROS can only be explained, when superoxide formation is considered the essential electron chain carrier, as it was already proposed by Gee and Davison [107]. Scheme 5.1 presents a possible system of equations which can explain the found stoichiometry.

$$\text{2 6-OHDA + 2 Fe}^{3+} \xrightarrow[\substack{\text{outer-sphere-oxidation} \\ -2\,H^+}]{} \text{2 Fe}^{2+} + \text{2 6-O-DA}^{\bullet} \qquad \text{(I)}$$

$$\text{2 6-O-DA}^{\bullet} + \text{2 O}_2 \xrightarrow[-2\,H^+]{} \text{2 6-O-DAQ} + \text{2 O}_2^{-\bullet} \qquad \text{(II)}$$

$$\text{2 O}_2^{-\bullet} + \text{6-OHDA} + \text{2 H}^+ \longrightarrow \text{6-O-DAQ} + \text{2 H}_2\text{O}_2 \qquad \text{(III)}$$

$$\text{2 Fe}^{2+} + \text{2 H}_2\text{O}_2 \longrightarrow \text{2 OH}^{\bullet} + \text{2 Fe}^{3+} + \text{2 OH}^- \qquad \text{(IV)}$$

$$\text{2 OH}^{\bullet} + \text{2 Ar-H} + \text{2 O}_2 \xrightarrow[-2\,H^+]{} \text{2 Ar-OH} + \text{2 O}_2^{-\bullet} \qquad \text{(V)}$$

$$\text{2 O}_2^{-\bullet} + \text{6-OHDA} + \text{2 H}^+ \longrightarrow \text{6-O-DAQ} + \text{2 H}_2\text{O}_2 \qquad \text{(VI)}$$
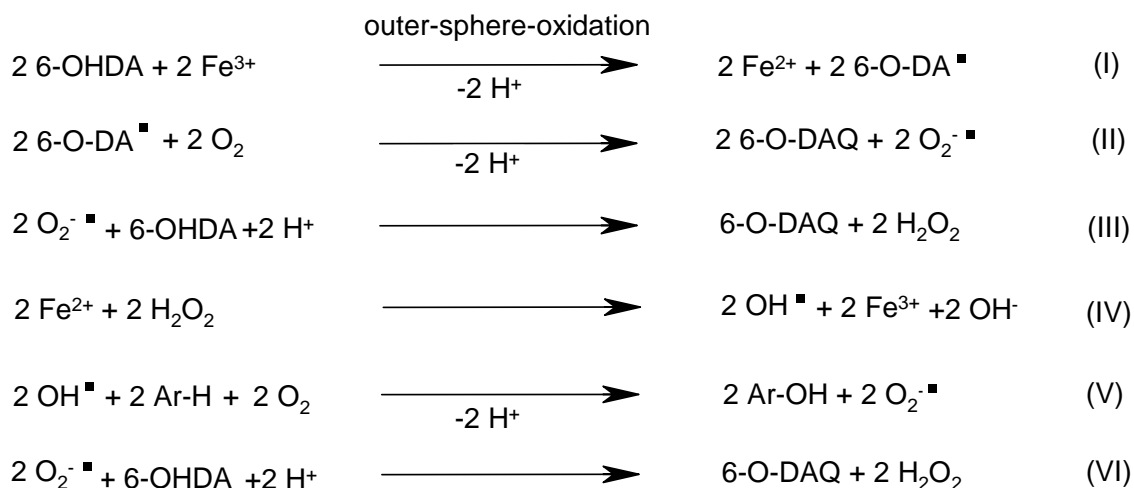
Scheme 5.1. *Reaction scheme explaining the preliminary found stoichiometry (1:1:1) of total iron, H_2O_2 and hROS. It is implied that 6-OHDA oxidation is more preferably performed by superoxide than by H_2O_2, which is in agreement with earlier results [107, 108]. For reasons of presentation hROS is stated as $OH^{\bullet}$ in equation (IV). 6-O-DA$^{\bullet}$ is written for the semi-chinone and 6-O-DAQ for the chinone, respectively. The Fe^{3+} in equation (I) comes from transferrin or ferritin, whereas the Fe^{3+} in equation (IV) is immediately removed by ICL-670. Fe^{2+}, which is released via reaction (I), reacts further in the Fenton reaction (IV) accompanied by a stoichiometric formation of hROS. Overall, 1 mol released Fe^{2+} causes the oxidation of 3 moles 6-OHDA and the formation of 1 mol H_2O_2 and hROS, respectively.*

It was already found [108] that in the presence of ascorbic acid transition metals are needed to initiate the oxidation from the catechol to the semichinone , which then can be continued (in the presence of dioxygen) to form the 6-hydroxydopamino-chinone accompanied by superoxide formation. Superoxide is able to reduce 6-OHDA and therefore can initiate an oxygen-driven redox cycling. As Fe(III) is removed by ICL-670 the maximum yield of superoxide which can be derived per released Fe(II) is two, leading to the oxidation of three moles 6-OHDA per released Fe(II) to the corresponding quinone, whereby one mole is oxidized by Fe^{2+} and dioxygen and the other two by superoxide. Equation (IV) involves (via the Fenton reaction) the formation of hROS which then react with aromatic compounds like TA^{2-} to the hydroxylated products and another superoxide allowing the production of an additional mole H_2O_2.

However, it should be mentioned that superoxide can also be regenerated by Fe(II) auto-oxidation, and therefore the involvement of this reaction cannot be excluded by comparing relative increases when a constant ratio between the Fenton reaction and iron auto-oxidation is assumed during the whole experiment. In this case only a constant percentage of Fe^{2+} and H_2O_2 would be converted to hROS. Nevertheless, it seems more likely that in this case the Fenton reaction is the predominant factor, because for a low ratio of Fe(II) to H_2O_2 a stoichiometry of Fe(II) to hROS close to 1:1 is expected [90]. The scheme could also be valid for the 6-OHDA experiments performed without a chelator with the difference that, as already mentioned earlier, iron mediated redox cycling can significantly contribute to hROS formation.
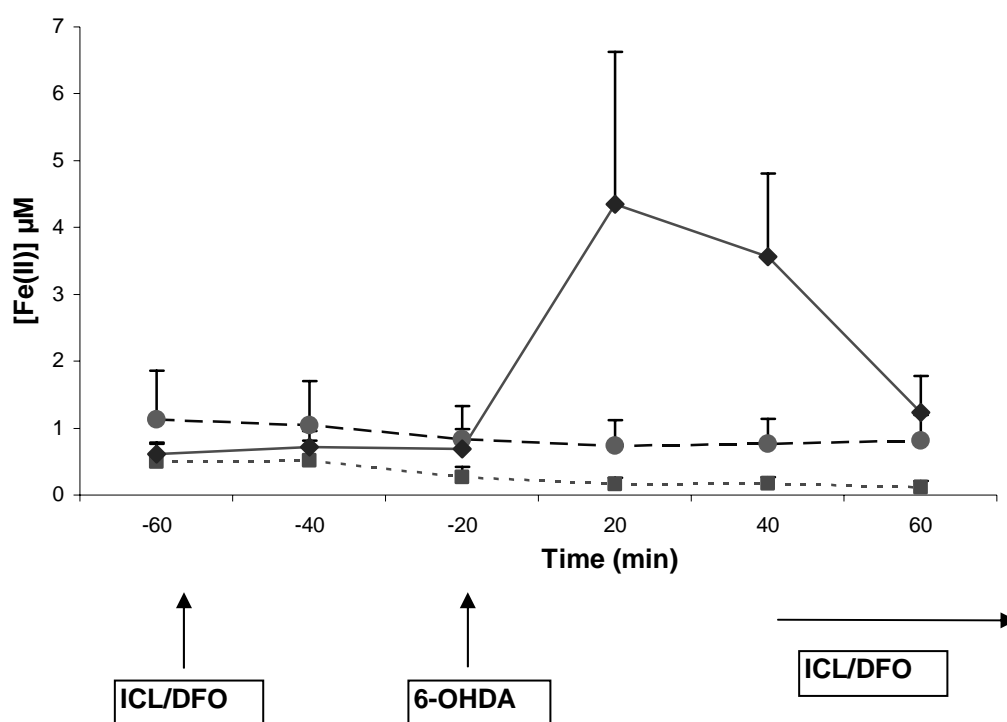
Figure 5.13. *The time course of Fe(II) formation without* ——•—— *and with the addition of* ⋯•⋯ *ICL-670 or* – –■– – *Desferal during 6-OHDA stimulation is shown. The points represent the mean values derived from 2 experiments, whereby the error bars representing the standard error, give, as n=2, only qualitative information about the variance between the animals.*
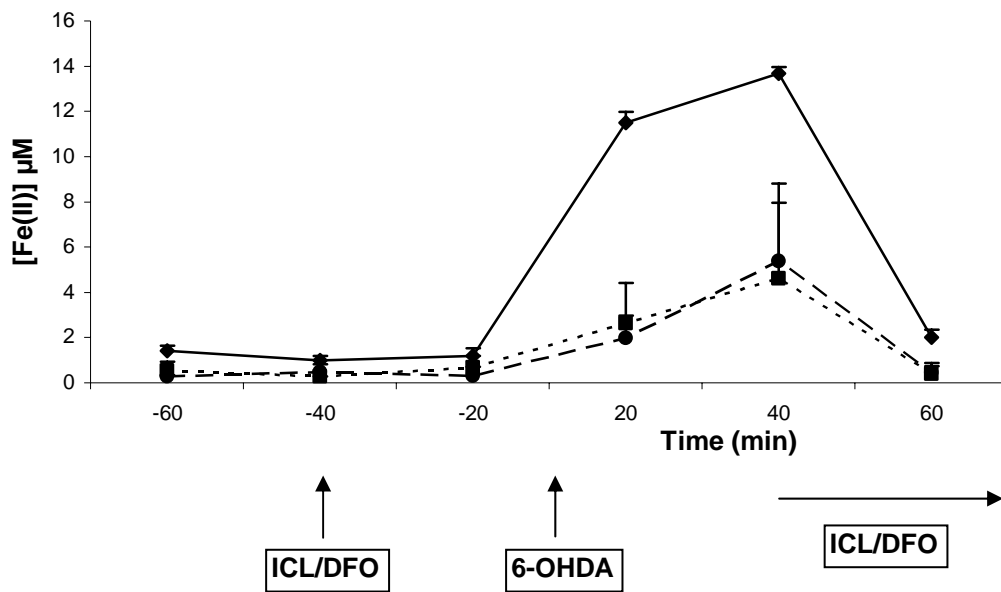
Figure 5.14. *The time course of total iron formation without* ⟶•⟶ *and with the addition of* ⋯•⋯ *ICL-670 or* — ■— *Desferal during 6-OHDA stimulation is shown. The points represent the mean values derived from 2 experiments, whereby the error bars representing the standard error, give, as n=2, only qualitative information about the variance between the animals. As only Fe(II) can be detected by BA the y-axis shows the detected amount of Fe(II) which is equivalent to total iron concentration in the sample.*
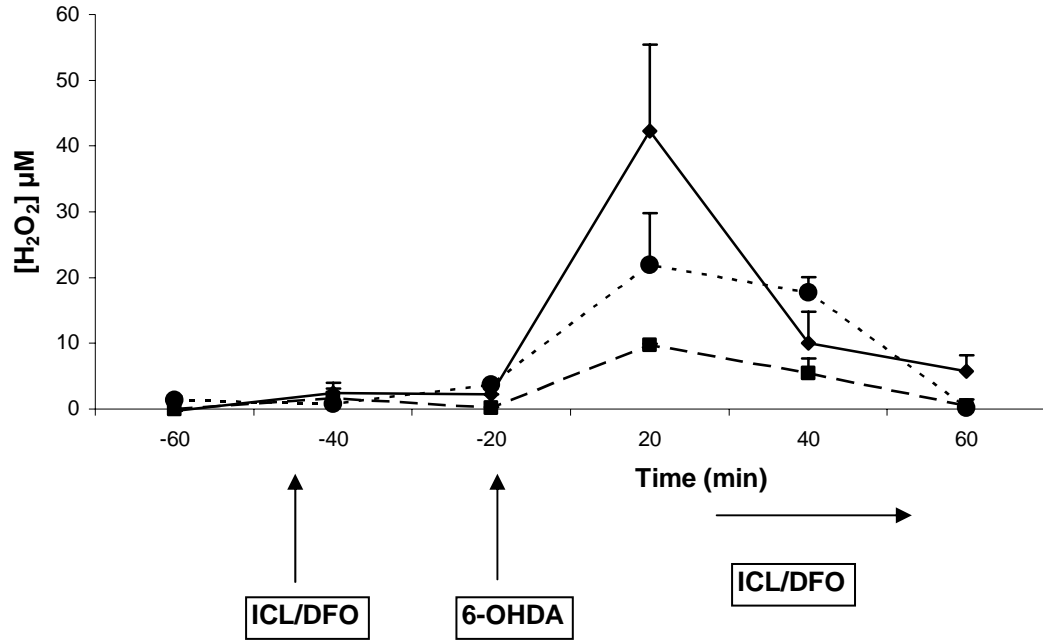
Figure 5.15. *The time course of H_2O_2 formation without ──◆── and with the addition of ┄┄◆┄┄ ICL-670 or ──■── Desferal during 6-OHDA stimulation is shown. The points represent the mean values derived from 2 experiments, whereby the error bars representing the standard error, give, as n=2, only qualitative information about the variance between the animals.*

Figure 5.16. *The time course of hROS formation without* —•— *and with the addition of* ···•··· *ICL-670 or* —■— *Desferal during 6-OHDA stimulation given in relative units related to the basal value is shown. The points of the Desferal and ICl-670 experiments are also shown in the inset and represent the mean values derived from 2 experiments, whereby the error bars representing the standard error, give, as n=2, only qua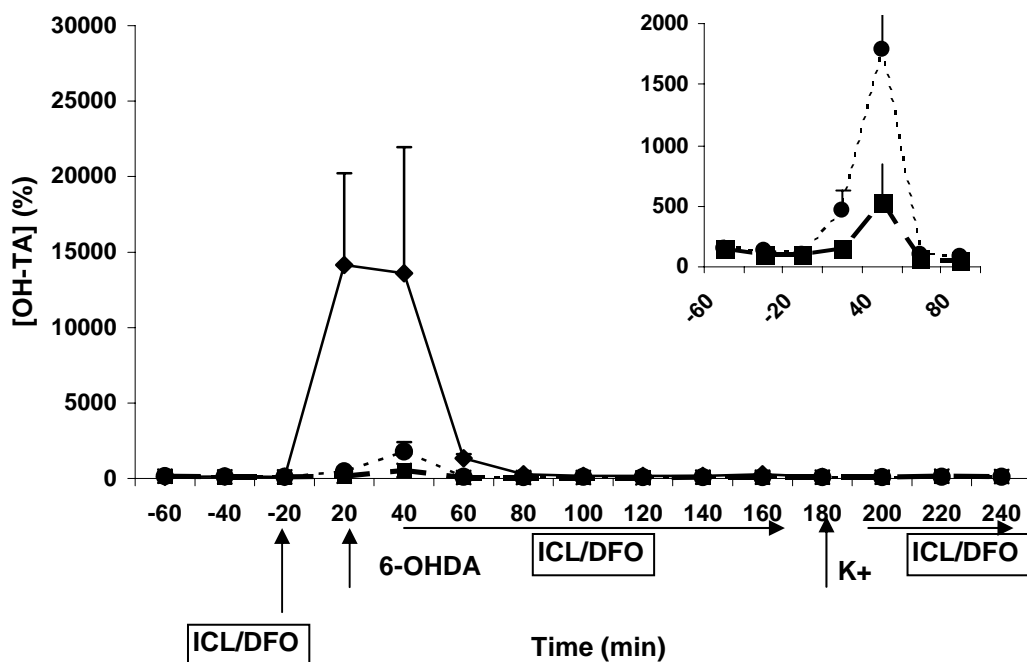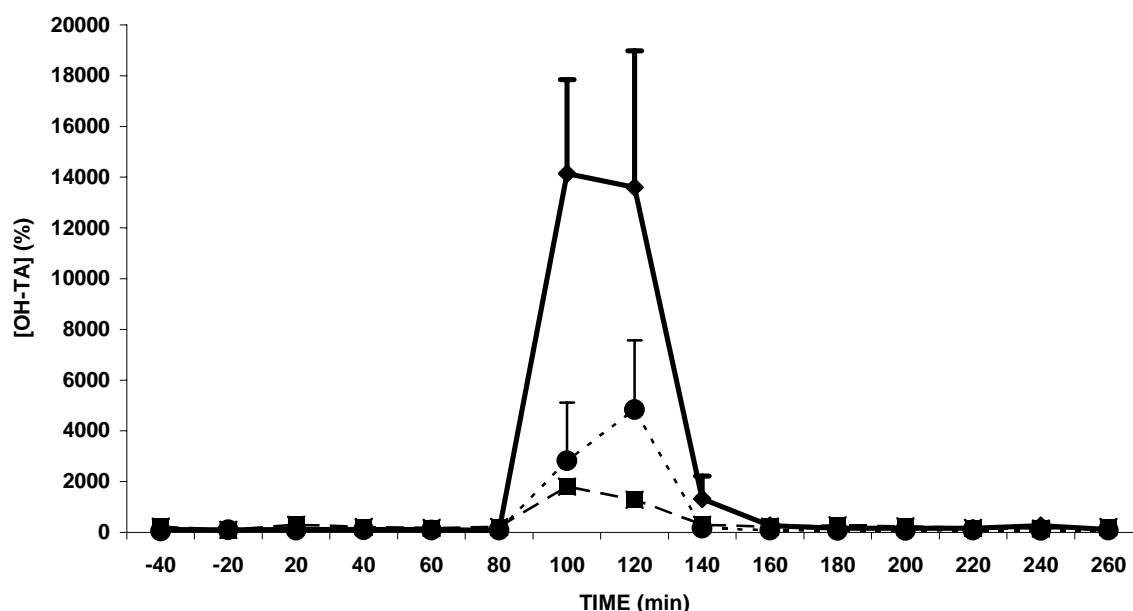litative information about the variance between the animals. The value for 6-OHDA stimulation without the addition of chelators represents the mean ± SEM derived from 5 experiments.*

Table 5.2. The "area under curve" values (AUC) from figures 5.12-5.15 are presented. Basal AUC values were taken from the 3 points before stimulation, whereas the stimulated AUC values were taken from the peaks 20 and 40 min after 6-OHDA stimulation plus half of the basal values before and after the stimulation. The data rely on 2 animals except the ones using 6-OHDA stimulation without the chelators which are based on 5 animals for hROS formation, 4 animals for the Fe(II) and 3 animals for the total iron release. For the hROS calculations the absolute values instead of the presented relative ones were used.

	6-OHDA + Asc			6-OHDA + ASC + Desferal		
	AUC Stim (μM)	AUC Bas (μM)	Relative Increase (%)	AUC Stim (μM)	AUC Bas (μM)	Relative Increase (%)
Fe(II)	9.51±3.44	1.58±0.60	600±217			
Fe(II)+Fe(III)	26.78±5.24	2.07±1.09	1295±253	7.76±0.37	1.480±0.16	524±25
H_2O_2	56.30±19.20	4.39±1.69	1283±437	15.55±2.49	1.88±1.61	825±132
hROS	$10^{-3}*$ 593±232	$10^{-3}*$ 7.34±0.74	8089±2142	$10^{-3}*$ 19.17±9.59	$10^{-3}*$ 8.81±3.63	217±108

	6-OHDA + Asc +ICL-670			Asc		
	AUC Stim (μM)	AUC Bas (μM)	Relative Increase (%)	AUC Stim (μM)	AUC Bas (μM)	Relative Increase (%)
Fe(II)				4.70±0.88	4.66±0.60	100±19
Fe(II)+Fe(III)	7.72±1.19	1.07±0.44	716±110	4.06±0.67	2.90±0.91	139±57
H_2O_2	41.54±10.41	5.81±0.63	714±179			
hROS	$10^{-3}*$ 50.59±17.32	$10^{-3}*$ 7.96±0.40	636±176	$10^{-3}*$ 20.29±14.48	$10^{-3}*$ 6.72±0.81	302±159

To test the hypothesis that DA can trigger iron release and particularly hROS formation 6-OHDA was applied together with the same amount of DA. On the contrary to the *in vitro* results it turned out (Fig: 5.17), that the addition of DA reduced and *not* enhanced hROS formation, showing a possible neuro-protective effect of this substance. A clear pronounced stoichiometry of iron, H_2O_2 and hROS, would be a strong argument for the ECF as the sole place of the reaction, which could explain the found discrepancy, as the *in vitro* experiments were performed using ferritin, which is not present in the ECF, whereas *in vivo* transferrin, which might show different properties in 6-OHDA cytotoxic mechanism, is the most likely source of the observed iron release.

Figure 5.17. *The time course of hROS formation without* ⟶•⟶ *and with the addition of* ⋯•⋯ *an equimolar amount of DA during 6-OHDA stimulation given in relative units related to the basal value is shown. The lower curve represents* ⎯■⎯ *hROS formation due to the perfusion of 200 μM DA. The points of the DA + 6-OHDA and DA experiments represent the mean values derived from 2 experiments, whereby the error bars representing the standard error, give, as n=2, only qualitative information about the variance between the animals. The value for 6-OHDA stimulation without the addition of DA represents the mean ± SEM derived from 5 experiments.*

5.4.4 Conclusion

The results, although preliminary, demonstrate that all methods developed in this work allow an *in vivo* application suitable for measurements of iron species, hROS and H_2O_2 in brain microdialysis or other applications were only micro-litre amounts of sample are available. They should be extremely helpful for all biological studies which intend to investigate the relation of oxidative stress with other neurological processes.

Further on, a preliminary *in vivo* mechanism for 6-OHDA cytotoxicity could be found that completely agrees with the pathogenic cycle established by our group *in vitro,* providing evidence that the scheme presented in the introduction of this part also describes *in vivo* the chemistry of oxidative stress caused by 6-OHDA formation.

6   Abbreviations and References

Abbreviations

aCSF	Artificial Cerebrospinal fluid
ASC	Ascorbic acid
BA	Bathophenanthroline, Sulfonated disodiumsalt
DHBA	Dihydroxy-benzoic acid
GABA	γ-aminobutyric acid
hROS	highly reactive oxygen species
KA	Kainate
OH-TA	2-Hydroxyterephthalate
PD	Parkinson's Disease
SA	Salicylic acid
TA^{2-}	Sodiumterephthalate

References

[1] Linert W., Jameson R. F., and Herlinger E.; Complex formation followed by internal electron transfer: the reaction between L-dopa and iron(III); *Inorg. Chim. Acta,* 187 (1991) 239-247.

[2] Linert W., Herlinger E., and Jameson R. F.; A kinetic study of the anaerobic reactions between adrenaline and iron(III); *J. Chem.Soc., Perkin Trans.2* (1993) 2435-2439

[3] El-Ayaan U., Herlinger E., Jameson R. F., and Linert W.; Anaerobic oxidation of dopamin by iron(III); *J. Chem. Soc., Dalton Trans.* (1997) 2813-2818

[4] El-Ayaan U., Jameson R. F., and Linert W.; A kinetic study of the reaction between noradrenaline and iron(III): an example of parallel inner- and outer-sphere electron transfer; *J. Chem. Soc. Dalton Trans.* (1998) 1315-1319.

[5] Herlinger E., Jameson R. F., Linert W.; Spontaneous Autoxidation of Dopamine; *J. Chem. Soc. Perkin Trans. 2* (1995) 259-263

[6] Kienzl E., Puchinger L., Jellinger K., Linert W., Stachelberger H., R. Jameson F.; The role of transition metals in the pathogenesis of Parkinson's Disease; *J. Neur. Sci.* (1995) 69-78

[7] Linert W., Herlinger E., Jameson R. F., Kienzl E., Jellinger K., Youdim M. B. H.; Dopamine, 6-hydroxydopamine, iron, and dioxygen - their mutual interactions and possible implication in the development of Parkinson's Disease; *Biochimica et Biophysica Acta, Molec. Basis of Disease,* 1316(3) (1996) 160-168

[8] Linert W., Bridge M. H., Huber M., Bjugstad K. B., Grossman S., Arendash G. W.; In vitro and in vivo studies investigating possible antioxidant actions of nicotine: relevance to Parkinson's and Alzheimer's diseases; *Biochimica et Biophysica Acta, Mol. Basis of Disease* 1454(2) (1999) 143-152.

[9] Jameson G. N. L., Linert W.; The oxidation of 6-hydroxydopamine in aqueous solution Part 3. Kinetics and mechanism of the oxidation with iron(III); *J. Chem. Soc., Perkin Trans.* 2 (4) (2001) 569-575

[10] Jameson G. N. L., Linert W.; The oxidation of 6-hydroxydopamine in aqueous solution. Part 2. Speciation and product distribution with iron(III) as oxidant; *J. Chem. Soc., Perkin Trans.* 2 (4) (2001) 563-568.

[11] Jameson G. N. L., Kudryavtsev A. B., Linert W.; The oxidation of 6-hydroxydopamine in aqueous solution. Part 1. The formation of three metastable quinones at low pH; *J. Chem. Soci., Perkin Trans.* 2 (4) (2001) 557-562.

[12] Jameson G. N. L., Jameson R. F., Linert W.; New insights into iron release from ferritin: direct observation of the neurotoxin 6-hydroxydopamine entering Ferritin and reaching redox equilibrium with the iron core; *Organ. Biomol. Chem.* 2(16) (2004) 2346-2351

[13] Rush J. D. and Koppenol W. H.; Reactions of Fe(II)NTA and Fe(II)EDDA with hydrogen peroxide; *J. Amer. Chem. Soc.* 110 (1988) 4957-4963

[14] Walling C.; Fenton's reagent revisited; *Acc. Chem. Res.* 8 (1975) 125-131

[15] Lloyd R. V.; The origin of the hydroxyl radical oxygen in the Fenton reaction; *Free Radic. Biol. Med.* 22 (1977) 885–888

[16] B. Halliwell; Role of free radicals in the neurodegenerative diseases: therapeutic implications for antioxidant treatment*; Drugs Aging* 18; (2001) 685–716

[17] J. Moskovitz, M. B. Yim, P. B. Chock; Free radicals and disease; *Arch. Biochem. Biophys.* 397 (2002) 354–359

[18] Pace GW, Leaf CD.; The role of oxidative stress in HIV disease. *Free Radic. Bio.l Med.* 19(4) (1995) 523-528

[19] Harman D.;Aging: a theory based on free radical and radiation chemistry. *J. Gerontol* 11 (3) (1956) 298-300

[20] Harman D. The aging process. *Proc. Nat. Acad. Sci. U S A* 78 (11) (1981) 7124-7128

[21] Beckman K. B., and Ames B. N.; The free radical theory of aging matures; *Physiol Rev* 78 (2) (1998) 547-581

[22] Orr W. C., and Sohal, R. S.; "Extension of life-span by overexpression of superoxide dismutase and catalase in Drosophila melanogaster; *Science* 263(5150) (1994) 1128-1130

[23] Orr W. C., Mockett R. J., Benes J. J., and Sohal R. S.; Effects of overexpression of copper-zinc and manganese superoxide dismutases, catalase, and thioredoxin reductase genes on longevity in Drosophila melanogaster; *J. Biol. Chem.* 278 (29) (2003) 26418-26422

[24] Parkes T. L., Elia A. J., Dickinson D., Hilliker A. J., Phillips J. P., and Boulianne G. L.; Extension of Drosophila lifespan by overexpression of human SOD1 in motorneurons; *Nat Genet* 19 (2) (1998) 171-174

[25] Sohal R. S., Mockett R. J., and Orr W. C.; Mechanisms of aging: an appraisal of the oxidative stress hypothesis; *Free Radic Biol Med* 33(5) (2002) 575-586

[26] de Magalhaes J. P., and Sandberg A.; Cognitive aging as an extension of brain development: A model linking learning, brain plasticity, and neurodegeneration; *Mech Ageing Dev* 126 (10) (2005) 1026-1033

[27] Schriner S. E., Linford N. J., Martin G. M., Treuting P., Ogburn C. E., Emond M., Coskun P. E., Ladiges W., Wolf, N., Van Remmen H., *et al.*; Extension of murine life span by overexpression of catalase targeted to mitochondria; *Science* 308 (5730) (2005) 1909-1911

[28] Schriner S.E., Ogburn E.C., Smith C.A., Newcomb G. T., Ladiges C.W., E. M. Dolle, J. Vijg, K. Fukuchi, G.M. Martin; evels of DNA damage are unaltered in mice overexpressing human catalase nuclei; *Free Radic. Biol. Med.* 29 (2000) 664-673.

[29] Pryor W. A. Oxy-radicals and related species: their formation, lifetimes, and reactions. *Ann. Rev. Physiol.* 48 (1986) 657–667

[30] Welch K. D., Davis T. Z., and Aust St. D; Iron Autoxidation and Free Radical Generation: Effects of Buffers, Ligands, and Chelators; *Arch. Biochem. a. Biophys.* 397 (2) (2002) 360–369

[31] Rush J. D., and Koppenol W. H.; Oxidizing Intermediates in the Reaction of Ferrous EDTA with Hydrogen Peroxide, J. Biol. Chem. 261 (15) (1986) 6730-733

[32] Duesterberg C. K., Cooper W.J., Waite T.; Fenton-Mediated Oxidation in the Presence and Absence of Oxygen; *Environ. Sci. Technol.* 39 (13) (2005) 5052 -5058,

[33] Burkitt, M.; J. ESR spin trapping studies into the nature of the oxidizing species in the Fenton reaction *Free Rad. Res. Commun.* 18 (1993) 43–57

[34] Koppenol W. H., Liebman J. F.; The Oxidizing Nature of the Hydroxyl Radical. A Comparison with the Ferryll Ion (FeO_2^+); J . Phys. Chem. 88 (1984) 99-101

[35] Linxiang L., Abe Y., Nagasawa Y., Kudo R., Usui N., Imai K., Mashino T., Mochizuki M., Miyata N.; An HPLC assay of hydroxyl radicals by the hydoxylation of terphthalic acid; *Biomedical Chromatography* 18 (2004) 470-474

[36] Blair J. A. and Pearson A. J.; Nonenzymic, tetrahydrobiopterin-mediated hydroxylation of phenylalanine; *J. Chem. Soc. Perkin Trans. 2* 3 (1975) 245-249.

[37] Mishin V. M. and Thomas P. E.; Characterization of hydroxyl radical formation by microsomal enzymes using a water-soluble trap, terephthalate; *Biochem. Pharmacol.* 68, (2004) 747–752

[38] Yan E. B., Langford S. J., Walker D. W., Yan J. K., Unthank M., Castillo-Melendez S. and Miller L.; A novel method for *in vivo* hydroxyl radical measurement by microdialysis in fetal sheep brain, in utero. *J. Appl. Physiol.* 98 (2005) 2304-2310

[39] Lang K., Wagnerova D. M. and Brodilova J.; The role of hydrogen peroxide in dioxygen induced hydroxylation of salicylic acid; *Collect. Czech. Chem. Commun.* 59 (1994) 2447-2453.

[40] Lunak S, Muzart J. and Brodilova J.; Photochemical hydroxylation of salicylic acid derivatives with hydrogen peroxide, catalyzed with Fe(III) and sensitised with methylene blue; *Collect. Czech. Chem. Commun.* 59 (1994) 905-912.

[41] Maskos Z., Rush J. D. and Koppenol W. H.; The hydroxylation of the salicylate anion by a Fenton reaction and γ-radiolysis: A consideration of the respective mechanisms; *Free Radic. Biol. Med.* 8 (1990) 153-162.

[42] Strolin Benedetti M., Brogin G., Bani M., Oesch F.and Hengstler J. G; Association of cytochrome P450 induction with oxidative stress *in vivo* as evidenced by 3-hydroxylation of salicylate; *Xenobiotica* 29 (1999) 1171–1180.

[43] Salzberg-Brenhouse H.C., Chen E.Y., Emerich D.F., Baldwin S., Hogeland K., Ranelli S., Lafreniere D., Perdomo B., Novak L., Kladis T., Fu K., Basile A.S.,

Kordower J.H., and Bartus R.T.; Inhibitors of cyclooxygenase-2, but not cyclooxygenase-1 provide structural and functional protection against quinolinic acid-induced neurodegeneration; *J Pharmacol. Exp. Ther.* 306 (2003) 218–228.

[44] Wang T, Qin L, Liu B, Liu Y, Wilson B, Eling TE, Langenbach R, Taniura S, and Hong JS. Role of reactive oxygen species in LPS-induced production of prostaglandin E2 in microglia.; J. Neurochem. 88 (2004) 939–947

[45] Catania A., Arnold J., Macaluso A., Hiltz M.E. and Lipton J.M. Inhibition of acute inflammation in the periphery by central action of salicylates. *Proc. Natl. Acad. Sci. USA* 88 (1991) 8544-8547.

[46] Dinis-Oliveira R.J., Sousa C., Remião F., Duarte J.A., Sánchez Navarro A., Bastos M.L. and Carvalho F.; Full survival of paraquat-exposed rats after treatment with sodium salicylate; *Free Radic. Biol. Med.* 42 (2007) 1017–1028.

[47] Grilli M., Pizzi M., Memo M. and Spano P.F. ; Neuroprotection by aspirin and sodium salicylate through blockade of NF-kappaB activation; *Science* 274 (1996) 1383-1385

[48] Themann C, Teismann P, Kuschinsky K, and Ferger B. Comparison of two independent aromatic hydroxylation assays in combination with intracerebral microdialysis to determine hydroxyl free radicals. J. Neurosci. Methods 108 (2001) 57–64

[49] Kaur H., B. Halliwell; Aromatic hydroxylation of phenylalanine as an assay for hydroxyl radicals; *Anal. Biochem.* 220 (1994) 11-15;

[50] Moreno S., Nardacci R., Cimini A., Ceru M.P.; Immunocytochemical localization of d-amino acid oxidase in rat brain; *J. Neurocytol.* 28 (1999) 169-18

[51] Sun, J.-Z., Kaur, H., Halliwell, B., Li, X.-Y., and Bolli, R. Use of aromatic hydroxylation of phenylalanine to measure production of hydroxyl radicals after myocardial ischemia in vivo. Direct evidence for a pathogenetic role of the hydroxyl radical in myocardial stunning *Circ. Res.* 73 (1993) 534–549

[52] Reddy S., Halliwell B., Jones A.D., and Longhurst J.C.; The use of phenylalanine to detect hydroxyl radical production in vivo: a cautionary note; *Free Radic. Biol. Med.* 27 (1999) 1465

[53] Ferger B., Themann C., Rose S., Halliwell B., and Jenner P.; 6-Hydroxydopamine increases the hydroxylation and nitration of phenylalanine in vivo: implication of peroxynitrite formation; *J. Neurochem.*; 78 (2001) 509-514

[54] Liu M, Liu, Peterson S.L, Miyake M., Liu K.J; On the application of 4-hydroxybenzoic acid as a trapping agent to study hydroxyl radical generation during cerebral ischemia and reperfusion Source; *Molec. A. Cellul. Biochem.* 234(1) (2002) 379-385

[55] Marklund N., Clausen F., Lewander T., Hillered L.; Monitoring of Reactive Oxygen Species Production after Traumatic Brain Injury in Rats with Microdialysis and the 4-Hydroxybenzoic Acid Trapping Method; *J. Neurotr.* 18(11) (2001) 1217-1227

[56] Matteoa V.D., Pieruccia M., Giovanni G.D., Santoa A. D., Poggia A., Benigno A., and Esposito E.; Aspirin protects striatal dopaminergic neurons from neurotoxin- induced degeneration: An in vivo microdialysis study; *Brain Res.* 1095 (1) (2006)167-177

[57] K. Setsukinai, Y. Urano, K. Kakinuma, H. J. Majima, T. Nagano; Development of Novel Fluorescence Probes That Can Reliably Detect Reactive Oxygen Species and Distinguish Specific Species; *J. Biolog. Chem.* 278(5) (2003) 3170–3175

[58] Schmid R., Sapunov V. N., „Non-Formal Kinetics", monographs in modern chemistry, Vol 14, Verlag Chemie, Weinheim, 1982

[59] compiled from http://en.wikipedia.org/wiki/High_performance_liquid_chromatography

[60] Plock N., Kloft C.; Microdialysis—theoretical background and recent implementation in applied life-sciences; *Europ. J. Pharmaceut.Sciences* 25 (2005) 1–24.

[61] Stiller C.-O., Taylor B. K., Linderoth B., Gustafsson H., Afrahc A. W., Brodinc E.; Microdialysis in pain research; *Advanced Drug Delivery Reviews* 55 (2003) 1065–1079

[62] Zhang M.-Y., Beyer C. E.; Measurement of neurotransmitters from extracellular fluid in brain by in vivo microdialysis and chromatography–mass spectrometry; *J. Pharmac. A. Biomed. Anal.* (2005) in the press (available online).

[63] Saran M., Summer K. H.; Assaying for hydroxyl radicals: hydroxylated terephthalate is a superior fluorescence marker than hydroxylated benzoate;. *Free Radic.Research* 31(5) (1999) 429-436.

[64] Fang X., Mark G., v. Sonntag C.; OH radical formation by ultrasound in aqueous solution Part I: the chemistry underlying the terephthalate dosimeter; *Ultrason. Sonochem.* 3 (1996) 57-63.

[65] X.-F. Yang, X.-Q. Guo; Fe(II)-EDTA chelate-induced aromatic hydroxylation of terephthalate as a new method for the evaluation of hydroxyl radical-scavenging ability; *Analyst* 126 (2001) 928-932.

[66] Matthews R. W.; The radiation chemistry of the terephthalate dosimeter; *Radiation Res.* (1980), 83(1), 27-41

[67] Price G. J., Duck F. A., Digby M., Holland W., Berryman T.; Measurement of radical production as a result of cavitation in medicalultrasound fields; *Ultrasonics Sonochem.* 4 (1997) 165-171.

[68] Samuni A., Goldstein S., Russo A., Mitchell J. B., Krishna M. C., Neta P.; Kinetics and Mechanism of Hydroxyl Radical and OH-Adduc. Radical Reactions with Nitroxides and with their Hydroxylamines; *J. Am. Chem. Soc.* 124 (2002) 8719-8724

[69] Huai Q., J. Li, Fang X.; Determination of •OH generated in copper ion catalyzed Fenton reaction by terephthalate; *J. Radiat. Res. Radiat. Process* 16(4) (1998) 193-197.

[70] Matthews R. W.; The radiation chemistry of aqueous sodium terephthalate solutions; *Aust. A. E. C.*, Res. Establ., [Rep.] AAEC/E (1980).

[71] Qu X., Kirschenbaum L. J., Borish E. T.; Hydroxyterephthalate as a fluorescent probe for hydroxyl radicals: application to hair melanin; *Photochem. a. Photobiol.* 71(3) (2000) 307-313.

[72] Vögtle H.R.; Organische Chemie 2.Aufl. Salle, Frankfurt/Main 1992

[73] Iida Y., Yasui K., Tuziuti T., Sivakumar M.; Sonochemistry and its dosimetry; *Microchemi. J.* 80(2) (2005) 159-164

[74] Field L. and Engelhardt P.R. Organic disulfides and related substances. XXX. Preparations and reactions of mercaptoterephthalic acids and derivatives. *J. Org. Chem.* 35 (1970) 3647-3655.

[75] Miura Y., Torres E., Panetta C. A. and Metzger R. M.; Electroactive organic materials. Preparation and properties of 2-(2'-hydroxyethoxy)-7,7,8,8-tetracyano-p-quinodimethane. *J. Org. Chem.* 53 (1988) 439-440.

[76] Tachiev G. Kinetics of hydrogen peroxide decomposition with complexed and "free" iron catalysts; *Int. J. Chem. Kin.* 32 (2000) 24-35

[77] Strliè M. A; Comparative Study of Several Transition Metals in Fenton-like Reaction Systems at Circum-Neutral pH. *Acta Chim. Slov.* 50 (2003) 619-632

[78] Benitez F. J.; The role of hydroxyl radicals for the decomposition of p-hydroxy phenylacetic acid in aqueous solutions; *Water Res.* 35 (2001) 1338-1343

[79] Muse W. T.; Anthony J. S., Bergmann J. D., Burnett D. C., Crouse C. L., Gaviola B. P. and Thomson S.; A; Chemical and toxicological evaluation of pyrotechnically disseminated terephthalic acid smoke; *Drug Chem. Toxicol.* 20. (1997) 293-302

[80] OECD SIDS (2001 *Terephthalic acid (TPA): Initial Assessment Report; For 12th SIAM* (Paris, France June 2001). United Nations Environment Programme (UNEP) Publications, Nairobi, Kenya.

[81] Paxinos G. and Watson C.; The Rat Brain in Stereotaxic Coordinates; *Academic Press*, Sidney (1986)

[82] Bianchi L., Della Corte L. and Tipton K. F. Simultaneous determination of basal and evoked output levels of aspartate, glutamate, taurine and 4-aminobutyric acid during microdialysis and from superfused brain slices. *J. Chromatogr. B* 723 (1999) 47–59

[83] Obata T., Inada T. and Yamanaka Y.; Intracranial microdialysis of salicylic acid to detect hydroxyl radical generation by antidepressant drugs in the rat; *Neurosci. Res. Commun.* 21 (1997) 223-229

[84] Camarero J., Sanchez V., O'Shea E., Green A.R. and Colado M.I.; Studies, using in vivo microdialysis, on the effect of the dopamine uptake inhibitor GBR 12909 on 3,4-methylenedioxymethamphetamine ('ecstasy')-induced dopamine release and free radical formation in the mouse striatum; *J. Neurochem.* 81 (2002) 961-972.

[85] Montgomery J., Ste-Marie L., Boismenu D. and Vachon L. Hydroxylation of aromatic compounds as indices of hydroxyl radical production: a cautionary note revisited; *Free Radic. Biol. Med.* 19 (1995) 927-933

[86] Clapp-Lilly K.L., Roberts R.C., Duffy L.K., Irons K.P., Hu Y. and Drew K.L.; An ultrastructural analysis of tissue surrounding a microdialysis probe; *J. Neurosci. Methods* 90 (1999) 129-142

[87] Wang O., Yu S., Simonyi A., Sun G. Y. and Sun A. Y.; Kainic acid-mediated excitotoxicity as a model for neurodegeneration; *Mol. Neurobiol.* 31 (2005) 3-16.

[88] Saran M., Michel C., Stettmaier K. and Bors W., Arguments Against the Significance of the Fenton Reaction Contributing to Signal Pathways Under *in vivo* Conditions; *Free Rad. Res.,* 33 (2000) 567-579

[89] Burkitt, M. J.; ESR spin trapping studies into the nature of the oxidizing species in the Fenton reaction; *Free Rad. Res. Commun.* 18 (1993) 43–57

[90] Yamazaki I. and Piette L. H.; ESR Spin-trapping Studies on the Reaction of Fe^{2+} Ions with H_2O_2-reactive Species in Oxygen Toxicity in Biology; *J. Biol. Chem.* 265 (23) (1990) 13589-13594

[91] Gutterride J. M. C.;Ferrous-salt-promoted damage to deoxyribose and benzoate The increased effectiveness of hydroxyl-radical scavangers in the presence of EDTA; *Biochem. J.* 243 (1987) 709-714;

[92] Maskos Z., Rush J. D., and Koppenol W. H; The Hydroxylation of Phenylalanine and Tyrosine: A Comparison with Salicylate and Tryptophan; *Arch. Biochem. Biophys*; 296 (2) (1992) 521-529

[93] Sherif F. G. ;Heavy metal terephthalates; *Ind. Eng. Chem. Prod. Res. Develop.* 9 (1970) 408-412.

[94] Buda F., Ensing B., Gribnau M. C. M., and Baerends E. J.; DFT Study of the Active Intermediate in the Fenton Reaction; *Chemistry - A European Journal* (2001) 2775 – 2783

[95] Perrin D.D. *Stability Constants of Metal-ion complexes: Part B Organic Ligands* International Union of Pure and Applied Chemistry, (1979) Pergamon Press, Oxford

[96] Koppenol W. H.;Facts and Fiction in Free Radical Biochemistry: The Haber-Weiss Cycle; Oxygen Society Annual Meeting, San Diego, CA Nov 17 -20, 2000

[97] Double K. L., Maywald M., Schmittel M., Riederer P.,Gerlach M.; In vitro studies of ferritin iron release and neurotoxicity; *J. Neurochem.* 70 (1998) 2492–2499

[98] Jellinger K., Linert W., Kienzl E., Herlinger E., Youdim M. B. H.; Chemical evidence for 6-hydroxydopamine to be an endogenous toxic factor in the pathogenesis of Parkinson's disease; *J. Neural Transm.*6 (suppl.) (1995) 297–314

[99] Ben-Shachar D., Eshel G., Finberg J. P., Youdim M. B.; The iron chelator desferrioxamine (Desferal) retards 6-hydroxydopamine-induced degeneration of nigrostriatal dopamine neurons; *J. Neurochem.* 56 (1991) 1441–1444

[100] Oestreicher F., Sengstock G. J., Riederer P., Olanow C., Dunn W., Arendash A. J.;Degeneration of nigrostriatial dopaminergic neurons increases iron within the substantia nigra: A histochemical and neurochemical study; *Brain Res.* 660 (1994) 8 –18

[101] Dexter D. T., Carayon A., Javoy-Agid F., Agid Y., Wells F. R.; Levels of iron, ferritin and other trace elements in Parkinson's disease and in other neurodegenerative diseases affecting the basal ganglia; *Brain* 114 (1991) 1953–1975

[102] Berlett B. S., Levine R. L., Chock P. B., Chevion M., and Stadtman E. R.; Antioxidant activity of Ferrozine–iron–amino acid complexes; *PNAS* 2001;98;451-456

[103] Nilson U. A., Basssen M., Savmann K. and Kjellmer I.; A Simple and Rapid Method for the Determination of "free"Iron in Biological Fluids; *Free Radic. Res.* 36 (6) 2002 677–684

[104] Perrin, D.D., (comp.), Stability constants of metal-ion complexes Part B: Organic Ligands. IUPAC chemical data series—No. 22, Pergamon Press, Oxford

[105] Y. Takagai and S. Igarashi; Simultaneous detection of Fe(II) and Fe(III) by micellar electrokinetic chromatography using an off-line selective complexing reaction, *Anal. Science* 19 (2003) 1207-1209

[106] B. Lei, N. Adachi, T. Arai, Measurement of the extracellular H_2O_2 in the brain by microdialysis; *Brain Res. Prot.* 3 (1998) 33–36

[107] Gee and Davison, P. Gee and A.J. Davison, Intermediates in the aerobic autoxidation of 6-hydroxydopamine: relative importance under different reaction conditions, *Free Radical Biol. Med.* 6 (1989) 271–284.

[108] Tyurina Y. Y. , Kapralov A. A., Jiang J., B. Grigory G., Potapovich A. I., Sorokin A., Kochanek P. M., Graham St. H., Schor N. F. and Kagan V. E.; Oxidation and cytotoxicity of 6-OHDA are mediated by reactive intermediates of COX-2 overexpressed in PC12 cells; *Brain Research* 1093 (1) (2006) 71-82

7 Curriculum vitae

Personal Data

Name:	Wolfhardt Freinbichler
Date of birth:	27th of May 1973
Place of birth:	Salzburg
Marital status:	Live partnership, father of one daughter
Nationality:	Austria

Education and Qualification

1980 – 1984	Primary school in Salzburg
1984 – 1992	High school "Akademisches Gymnasium" in Salzburg (with emphasis on humanistic subjects)
June 1992	Final high school exam
October 1992	Begin of studies in "Technische Chemie" and "Technische Physik" at the Vienna University of Technology.
October 1992-June 1996	Several activities in the "Österreichische Hochschülerschaft" (student union) at the University of Vienna and the University of Technology
July 1998 - October 1999	Community services in Vilnius (Lithuania) in the Vilna Gaon Jewish State Museum. Activities: Among other things project coordination of the travelling exhibition "Anne Frank- a History for today" in cooperation with the "Anne Frank House" in Amsterdam; Archive works in the former KGB archives in Moscow.
October 2002 – October 2003	Tutor at the Institute for Applied Synthetic Chemistry at the Vienna University of Technology.
October 2003	Graduation of studies in "Technische Chemie" Title of the diploma thesis: "The Kinetic of the system copper (II) and 3-methoxy-saliciliden-2-aminothiophenol"

September 2002 – February 2004	Computer trainer on the adult evening school of Vienna
Since November 2003	Scientific staff member ("wissenschaftlicher Mitarbeiter in Ausbildung") at the Institute for Applied Synthetic Chemistry at the Vienna University of Technology and start of PhD study
March 2004	Lecture at the „3. Workshop Anorg. Chemie in Österreich" (3. WACÖ)
April - May 2004	Research month at the university of Strassburg (F) in the lab of Prof. Annemarie Albrecht-Gary (Laboratory for bioinorganic und Physical chemistry (among others lecture about autocatalytic reaction kinetics)
June 2005, October 2005	Research stays at the University of Florence. Initial experiments for setting up a new fluorescent standard to measure hydroxyl radicals with terephthalic acid by microdialysis were performed
April 2006, September 2006	Research stays in Florence finishing the work for the TA^{2-} method
November 2006, February 2007	Setting up methods for iron and H_2O_2 detection; first *in vivo* experiments using 6-OHDA stimulation.

Further Activities

November 1999 - November 2000	Member of the executive committee of the Holocaust education association "Verein Gedenkdienst"
1993-2004	Extra-professional activities as a teacher of chemistry, mathematics, physics and English
1999-2005	Extra-professional activities as a computer advisor for Linux and Windows
Foreign Languages:	English (fluent) Lithuanian (advanced) Russian (basic) Spanish (basic) Latin (school) Ancient Greek (school)
Hobbies	Electronics, Ninjutsu